Alma Mater Studiorum – Università di Bologna

DOTTORATO DI RICERCA IN

SCIENZE BIOMEDICHE E NEUROMOTORIE

Ciclo XXXIII

Settore Concorsuale: 05/E1

Settore Scientifico Disciplinare: BIO/10

Modulation of cancer energy metabolism: the role of the ATPase inhibitor factor 1 (IF_1) in the bioenergetics of cancer cells experiencing oxygen deprivation

Presentata da: Dott.ssa Francesca Liuzzi

Coordinatore Dottorato

Chiar.mo Prof. Pietro Cortelli

Supervisore

Chiar.ma Prof.ssa Alessandra Baracca

Co-Supervisori

Prof.ssa Paola Taddei

Dott. Gianluca Sgarbi

Esame finale anno 2020

THESIS ABSTRACT

Cancer cells experience a great variety of metabolic changes during carcinogenesis to adapt to the bioenergetic stresses occurring in the tumour microenvironment, including lack of nutrients and oxygen deprivation. Therefore, given the pivotal role of metabolic reprogramming in tumour development, many studies currently aim to characterize the bioenergetic profile of tumours to selectively target their energy metabolism. Several efforts are thus focused on identifying and targeting cancer-specific metabolism by exploiting the differences in protein expression profile between normal and transformed tissues.

In this regard, among the proteins involved in the energy metabolism, particular attention has been addressed to IF_1, the endogenous inhibitor protein of mitochondrial F_1F_o-ATPase, as an upregulated protein in solid tumours compared to normal tissues. Physiologically, IF_1 is ubiquitously expressed in mammalian tissues where it protects cells from energy depletion by partially inhibiting the ATP hydrolytic activity of ATP synthase triggered by mitochondrial depolarization caused by oxygen deficiency as it occurs during ischemic episodes.

Considering both the physiological function of IF_1 and that cancer cells in solid tumour are frequently exposed to oxygen deprivation, we hypothesized that IF_1 overexpression represents a strategy that cancer cells develop to protect themselves from energy depletion under conditions of low oxygen availability.

To assess this, after identifying the oxygen tension needed to induce the reversal of ATP synthase and activate the IF_1 inhibitory role, we assayed the bioenergetic changes in 143B and HCT116 cancer cells with different metabolic features following stable silencing of IF_1. Interestingly, we found that in both cell lines exposed to oxygen deprivation conditions the presence of IF_1 limits the energy dissipation due to the activation of the ATP hydrolytic activity of ATP synthase. Furthermore, the analyses of cellular growth and viability under the same experimental conditions revealed that the IF_1 silencing inhibited proliferation in the highly glycolytic 143B cells, while it induced more than 50% of cellular death in HCT116 OXPHOS-dependent cells,

indicating that the energetic advantage conferred by IF_1 is essential for cancer cell proliferation or survival depending on the energy metabolism of each cell line.

Furthermore, under mitochondrial depolarization conditions, both mitophagy and mitochondrial biogenesis markers were found up-regulated in IF_1-expressing cells only. Indeed, the presence of IF_1 promoted a continuous renewal and preservation of the mitochondrial mass. Taken together, our results sustain the idea that IF_1 overexpression supports cancer cell adaptation to hypoxic or anoxic conditions also favoring the proliferation of re-oxygenated cells by promptly providing functional mitochondria.

Index

LIST OF ABBREVIATIONS

2DG; 2-deoxyglucose

3BP; 3-bromopyruvate

3PG; 3-phosphoglycerate

Acetyl CoA; acetyl coenzyme A

ADP; adenosine diphosphate

AMPK; 5' AMP-activated protein kinase

ATP; adenosine triphosphate

BCL-2; B-cell lymphoma 2

BNIP3; BCL2 and adenovirus E1B 19 kDa-interacting protein 3

BSA; bovine serum albumin

CI; complex I or NADH dehydrogenase

CII; complex II or succinate dehydrogenase

CIII; complex III or cytochrome bc1

CIV; complex IV or cytochrome c oxidase

CO_2; carbon dioxide

CoA-SH; reduced acetyl coenzyme A

CoQ; coenzyme Q or ubiquinone

COX; cytochrome c oxidase

CV; complex V or ATP synthase

Cyt c; cytochrome c

DHAP; dihydroxyacetone phosphate

DMEM; Dulbecco's Modified Eagle Medium

DTNB; 5'-dithio-bis-2-nitrobenzoic acid

ETC; electron transport chain

F_1F_o-ATPase; ATP synthase

$FADH_2$; reduced flavin adenine dinucleotide

FBS; fetal bovine serum

FCCP; Carbonyl cyanide-4-(trifluoromethoxy)phenylhydrazone

G6P; glucose 6-phosphate

GFP; green fluorescence protein

HBSS; Hanks' balanced salt solution

HIF-1α; hypoxia-inducible transcription factor 1α

HKII; hexokinase II

IF_1; ATPase inhibitor factor 1

IMM; inner mitochondial membrane

IMS; mitochondrial intermembrane space

LC3; microtubule-associated protein 1A/1B-light chain 3

LDHA; lactate dehydrogenase A

MCT; monocarboxilate transporter

MOMP; mitochondrial outer membrane permeabilization

mtDNA; mitochondrial DNA

mtRFP; mitochondria-targeted red fluorescent protein

NAD^+; nicotinamide adenine dinucleotide

NADH; reduced nicotinamide adenine dinucleotide

O_2; oxygen

OCR; oxygen consumption rate

OXPHOS; oxidative phosphorylation

PBS; phosphate-buffered saline

PEI; polyethylenimine

PGC-1α; peroxisome proliferator-activated receptor gamma coactivator 1-alpha

P_i; inorganic phosphate

PI3K; phosphoinositide 3-kinase

PINK1; PTEN-induced kinase 1

PKA; cAMP-dependent protein kinase A

PMSF; phenylmethylsulfonyl fluoride

ROS; reactive osygen species

SDS-PAGE; sodium dodecyl sulphate–polyacrylamide gel electrophoresis

shRNA; short hairpin RNA

SIRT1; sirtuin 1

SOC medium; super optimal broth with catabolite repression medium

TCA; tricarboxylix acid cycle

TMRM; tetramethylrhodamine methyl ester

TNB; 5-thio-2-nitrobenzoic acid

TOMM20; translocase of outer mitochondrial membrane 20

VDAC1; voltage dependent anion channel 1

YFP; yellow fluorescence protein

$\Delta\Psi_m$; mitochondrial membrane potential, transmembrane potential

1. INTRODUCTION

1.1 Metabolic reprogramming: a major hallmark of cancer

Cancer is one of the leading causes of death in the world. It is a complex and multifactorial disease characterized by uncontrolled cellular growth and proliferation whose aetiology involves genetic and environmental factors.

The development of cancer is the result of a multistep process whose steps reflect genetic alterations that drive the progressive transformation of a normal cell into a malignant one. These genetic alterations involve a large number of genes responsible for the acquisition of malignant proprieties in cells, including oncogenes and tumour suppressor genes affecting the regulation of cell proliferation and differentiation, cell cycle progression, and apoptosis.

In 2000, Hanahan and Weinberg described the cancer cell atypical phenotype defining the common biological capabilities acquired by cancer cells during the malignant progression. These acquired capabilities, the hallmarks of cancer, included the capability to sustain growth signals, the escape from anti-growth signals, the ability to invade surrounding tissue and metastasize, the induction of angiogenesis, the resistance to apoptotic cell death, and the unlimited potential for cellular proliferation [1].

In the following years, the concept of cancer hallmarks has been extended and cancer metabolic reprogramming has been recognized as a major hallmark implicated in cancer development and malignant progression [2].

Indeed, it is well established that mutations in oncogenes and tumour suppressor genes promote the metabolic rewiring in cancer cells to sustain the high demand for macromolecules and energy production, necessary to support uncontrolled proliferation and continuous growth [3].

Moreover, emerging evidence reveals that the altered metabolic phenotype of tumours is also induced by the interaction between cancer cells and tumour microenvironment [4, 5]. Indeed, tumour microenvironment can be characterized by adverse conditions, such as hypoxia, nutrient deprivation, and acidification leading cancer cells to

modulate their metabolic activity in order to develop efficient strategies to survive and keep proliferating. Therefore, depending on microenvironment modifications and because of their metabolic plasticity, cancer cells can rely on different fuel sources besides glucose, such as amino acids (e.g. glutamine and serine), lactate, and fatty acids [6].

1.1.1 Warburg effect and glycolytic pathway

The notion that cancer cells exhibit different metabolic phenotypes in comparison to normal cells is not a new concept but it dates back to almost 100 years ago with the pivotal observation by Sir Otto Warburg about the altered glucose metabolism.

Indeed, Warburg first observed that cancer tissues displayed an increase in glucose consumption and in lactate production compared to normal tissues, regardless of oxygen availability [7, 8, 9].

In normal cells, glucose is catabolized into pyruvate (glycolysis) that enters mitochondria to be fully oxidized in the Krebs cycle producing energy in the form of adenosine triphosphate (ATP) via oxidative phosphorylation (OXPHOS). This process is known as aerobic respiration and is the most effective energetic pathway under normoxic conditions since it generates up to 36 ATP molecules through the complete oxidation of one molecule of glucose, mainly thanks to mitochondrial respiration.

Only in the absence of oxygen, glucose is catabolized to lactate in the cytosols and glycolysis becomes the main energy production pathway producing only 2 ATP molecules for each glucose molecule metabolized.

In contrast, cancer cells preferentially use glycolysis to metabolize glucose converting pyruvate into lactate even in the presence of oxygen [10, 11, 12]. Therefore, the high glucose consumption and lactate production are due to the upregulation of glycolytic flux, which is required to compensate for the lower glycolysis efficacy in energy generation compared to aerobic respiration. This phenomenon is thus called “aerobic glycolysis” or “Warburg effect” to differentiate it from the aerobic glycolysis occurring in normal cells [13].

At that time, Warburg suggested that the switch from mitochondrial respiration to glycolysis was due to permanent mitochondrial damage responsible for the impairment

of mitochondrial respiration activity [14, 15]. However, this hypothesis was challenged since subsequent studies showed that mitochondrial function is preserved in most cancer cells. Indeed, although aerobic glycolysis is frequently found in cancer cells, OXPHOS still contributes to the energy production and may represent the main energy production pathway in several cancers [16]. Nevertheless, the aerobic glycolysis remains one of the best-investigated metabolic pathways.

Today, it is clear that glycolytic phenotype is promoted by oncogenes and tumour suppressors genes, such as p53, Myc, and hypoxia-inducible transcription factor 1α (HIF-1α), that modulate the expression or activity of transporters, enzymes and cofactors. These transcription factors promote the upregulation of glucose transporters (Glut1, Glut2, Glut3 and Glut 4) to uptake more glucose as well as the expression of key enzymes and isoforms responsible for the increase of glycolytic flux, such as hexokinase II (HKII), phosphofructokinase-1, triosephosphate isomerase 1, and lactate dehydrogenase A (LDHA) [17].

In particular, LDHA is the enzyme catalysing the conversion of pyruvate to lactate, which is the end product of aerobic glycolysis. This reaction is essential in cancer cells as it regenerates nicotinamide adenine dinucleotide (NAD^+) from reduced nicotinamide adenine dinucleotide (NADH) allowing glycolysis to continue.

Then, lactate is released into extracellular microenvironment via monocarboxylate transporter (MCT) 4 inducing acidification of tumour microenvironment that promotes the metalloproteinase activity for the extracellular matrix destruction, thus favouring cancer invasion and metastasis. Moreover, lactate released in the tumour microenvironment can be uptaken by oxidative cancer cells through MCT1 and used as an alternative metabolic substrate to fuel the tricarboxylic acid cycle (TCA cycle) [18].

Importantly, the increased glycolytic rate in tumour cells is needed not only to fulfil the energy demand but also to provide glycolytic metabolites required for the biosynthesis of macromolecules, which is essential for sustaining the cancer cells' high growth rate.

The biosynthetic activity of proliferating cancer cells needs high rates of nucleotide synthesis, amino acid synthesis, and lipogenesis. Therefore, several glycolytic intermediates, such as glucose 6-phosphate (G6P), dihydroxyacetone phosphate (DHAP), and 3-phosphoglycerate (3PG) are diverted into other metabolic pathways. In

particular, G6P is often consumed by the pentose phosphate pathway to produce both pentose phosphate for nucleotide synthesis and the reduced form of nicotinamide dinucleotide phosphate for anti-oxidant defences. Whereas DHAP can be used for lipid synthesis and 3PG can be converted into serine, providing the building blocks for the anabolic metabolism (Fig.1) [10, 12, 19].

1.2 Mitochondria and cancer

Mitochondria are complex organelles with a central role in the physiology of eukaryotic cells. They contain their own DNA, the mitochondrial DNA (mtDNA), and are involved in several vital processes. Notably, mitochondria play a key role in cell metabolism providing both the bulk of cellular energy by means of oxidative phosphorylation and metabolic intermediates for biosynthetic reactions.

Given the central metabolic function of mitochondria, it is not surprising that their activity is implicated in the wide range of metabolic changes observed in cancer cells [20]. Nonetheless, it has long been believed that metabolic reprogramming in cancer cells was independent of mitochondrial activity and that the transition of cellular metabolism to aerobic glycolysis was due to a mitochondrial damage in cancer cells.

Currently, in contrast with these obsolete theories, it is well documented that mitochondrial activity is intact in most cancer cells and supports both energy

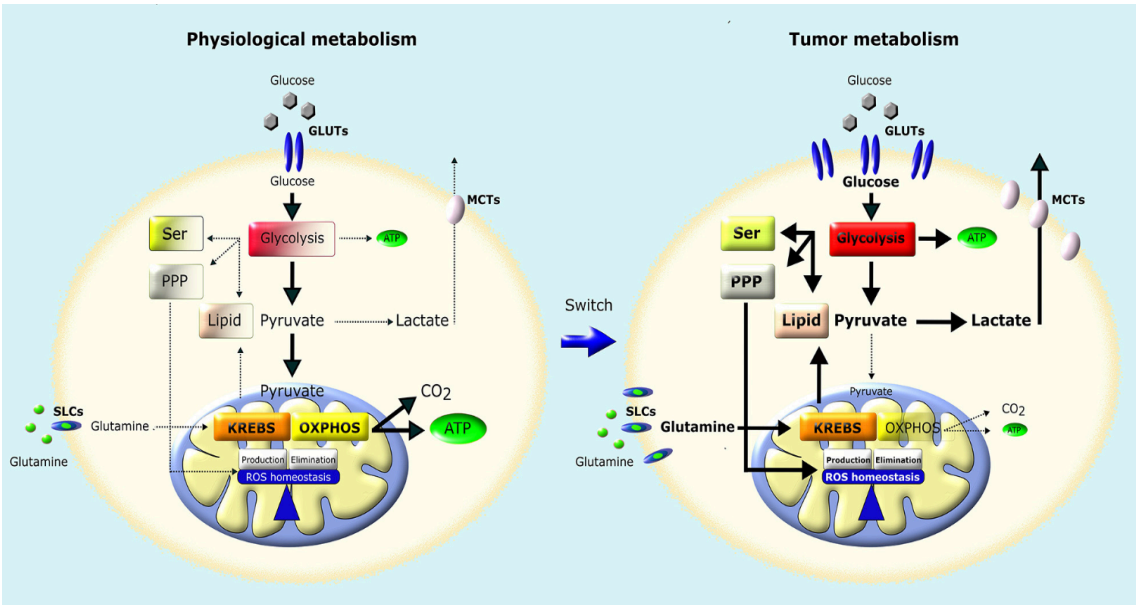

Fig. 1. Cancer cells metabolic remodelling.

production and biosynthetic pathways together with aerobic glycolysis [21].
A demonstration that mitochondria are still active in many tumours is that glucose is not the only fuel for cancer cells, but they can use different growth substrates that are metabolized in mitochondria [22, 23]. As already mentioned, depending on substrate availability in the tumour microenvironment, amino acids, fatty acids, and lactate can supply substrates to Krebs cycle in mitochondria.
For instance, high glutamine consumption has been observed in several tumours overexpressing glutamine transporters such as SLC1A5 (Fig.1). In particular, glutamine is metabolized to glutamate that is converted to alpha-ketoglutarate to fuel the Krebs cycle. Then, the intermediates of Krebs cycle can be used for the synthesis of amino acids, lipids, cholesterol, and other metabolites. In addition, Krebs cycle produces NADH and $FADH_2$ (reduced flavin adenine dinucleotide) that provide electrons for mitochondrial electron transport chain (ETC) to generate ATP. Thus, just like glucose, glutamine supplies cancer cells with not only energy but also essential precursors for the continuous biosynthesis and the enhanced proliferation [10, 12].

In addition to the above-mentioned role as key organelles of cell metabolism, mitochondria play many other roles in cell physiology, contributing to cancer development and progression in different ways. Indeed, mitochondria functions include the generation of reactive oxygen species (ROS) and the regulation of both cell signalling and apoptotic cell death [24]. Furthermore, the mitochondrial DNA has been proposed to be involved in carcinogenesis because of the high mutation rate and the limited DNA repair mechanisms compared to nuclear DNA. Indeed, mtDNA mutations affecting various components of electron transport chain have been found in several tumours and have been recognized to have an important role in cancer pathogenesis [25, 26, 27, 28].
The mitochondrial electron transport chain represents the major source of intracellular ROS, which act as second messengers in redox signalling from the organelle to the cytosol and nucleus. However, under pathophysiological conditions, the ROS ability in regulating different signalling pathways can also contribute to cancer progression. For instance, mitochondrial ROS seem to regulate the phosphoinositide 3-kinase (PI3K) pathway, well known for promoting cell survival and proliferation, and promote the stabilization of HIF-1α, one of the most important factor involved in

tumour cell adaptation to hypoxic condition. Also, the increased mitochondrial ROS production in tumour can promote oxidative damage to DNA, contributing to the initiation of nuclear and mitochondria DNA mutations inducing the malignant transformation [29].

Notably, since resistance to cell death is one of the main common features of all tumours, another mechanism by which mitochondria are involved in malignant transformation is related to their pivotal role in the activation of caspases, the proteases responsible for the apoptotic cellular death [30].

Physiologically, apoptosis is a fundamental process that controls proliferation and tissue homeostasis by involving mitochondria through different mechanisms. In particular, apoptotic signals converge on mitochondria inducing the mitochondrial outer membrane permeabilization (MOMP), thus promoting the release into the cytosol of mitochondrial effectors including cytochrome c that activates cytosolic caspases [31, 32]. However, this process is frequently altered in cancer cells where alterations in factors involved in the mitochondrial apoptotic pathway, such as the inhibition of MOMP and the overexpression of mitochondrial anti-apoptotic BCL-2 (B-cell lymphoma 2) genes, contribute to confer apoptotic resistance and promote malignant progression [33, 34].

1.2.1 OXPHOS activity and cancer

As previously stated, it has become clear that not all tumours depend solely on glycolysis for their energy supply and that mitochondrial ATP generation via OXPHOS helps tumours progression contributing to cancer cell energy production [35].

During oxidative phosphorylation, mitochondria convert the energy of chemical bonds of food molecules into ATP, the energy-carrying molecule used by cells. The energy conversion takes place at the level of “respiratory chain” or electron transport chain located in mitochondrial cristae, invaginations of the inner mitochondrial membrane extending into the mitochondrial matrix [36]. Indeed, mitochondria are surrounded by a double-membrane system consisting of inner and outer mitochondrial membranes separated by the intermembrane space. The space within the inner membrane is known

as the mitochondrial matrix and contains the enzymes involved in the oxidation of carbohydrates and fatty acids.

The high-energy electrons deriving from oxidable substrates via catabolic pathways (glycolysis, Krebs cycle, and fatty acid β-oxidation) are carried to ETC by electron carriers NADH and $FADH_2$.

The ETC is composed of 4 protein complexes and 2 electron carriers containing redox centres involved in redox reactions that transfer electrons from NADH and $FADH_2$ up to molecular oxygen (O_2), the final acceptor of the chain.

Interestingly, structural and biochemical studies showed that the respiratory complexes in the inner mitochondrial membrane are organized into supramolecular structures known as supercomplexes [37]. The presence of these supramolecular organizations has been long studied and seems to stabilize the structural integrity of each complex increasing the efficiency of electron transport through the respiratory chain [38, 39].

In more detail, Complex I (CI or NADH dehydrogenase) and Complex II (CII or succinate dehydrogenase) receive electrons from NADH and $FADH_2$ respectively. Then, the electrons are transferred from CI and CII via the mobile electrons carrier ubiquinone (or coenzyme Q; CoQ) to Complex III (CIII or cytochrome bc1).

Afterwards, another mobile electron carrier, the cytochrome c (cyt c), transports

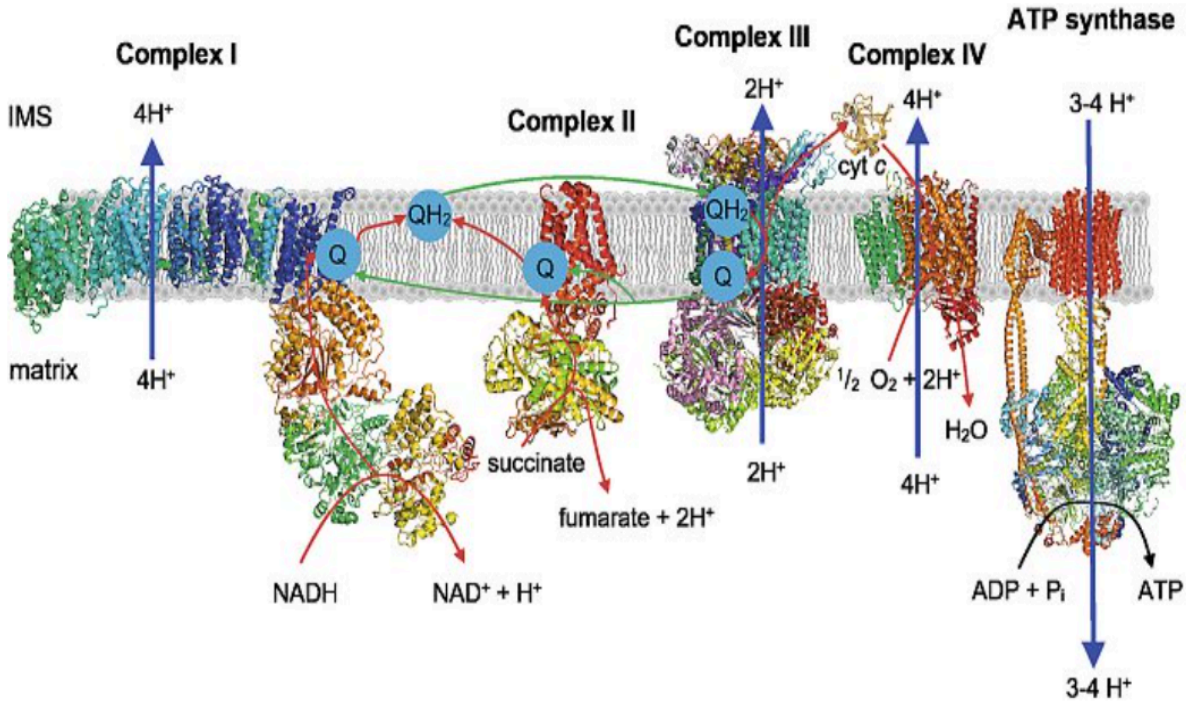

Fig. 2. Representation of oxidative phosphorylation system and proton gradient.

electrons from CIII to Complex IV (CIV or cytochrome c oxidase; COX), the terminal electron transfer enzyme that moves electrons to molecular oxygen.

All the redox reactions catalysed by respiratory complexes are highly exergonic and provide CI, CIII and CIV with the energy needed to pump protons (H^+) against a concentration gradient from the mitochondrial matrix to the intermembrane space across the inner mitochondrial membrane. This proton movement creates an electrochemical proton gradient ($\Delta\mu_{H^+}$) or "proton motive force (corresponding to approximately -180 mV, negative in the matrix) produced by the distribution of both electric charges (electrical gradient; $\Delta\psi$) and chemical species (chemical gradient; ΔpH) across the inner mitochondrial membrane (IMM) [40].

This proton motive force triggers protons from the inner intermembrane space back into the matrix through the ATP synthase (or Complex V, CV) driving the phosphorylation of ADP (adenosine diphosphate) to ATP, coupling ATP synthesis to substrate oxidation (Fig.2). This process, in which potential energy from the proton gradient is used by ATP synthase to synthetize ATP, is called chemiosmosis and it was first proposed by Sir Peter Mitchell in 1961 [41].

Several recent studies demonstrated that OXPHOS is not commonly downregulated in cancer cells and that a functional oxidative phosphorylation can be required for tumorigenesis [42, 43].

The downregulation of OXPHOS activity has been often associated with mitochondrial DNA mutations and reduced mtDNA content as mtDNA encodes for proteins and RNAs that are essential for the oxidative phosphorylation system.

However, it has been shown that mtDNA mutations do not always induce impairment in OXPHOS activity, but they can also promote the cancer cell bioenergetic adaptation to changes occurring in the tumour microenvironment. Indeed, several types of cancer cells acquire a hybrid glycolysis/OXPHOS phenotype that allows them to switch between these bioenergetic pathways favouring their survival under harsh conditions [44].

Interestingly, the role of OXPHOS system in tumour initiation and progression has also been demonstrated by the fact that depriving cancer cells of their OXPHOS capacity may prevent them from generating tumours. In fact, cancer cells defective in OXPHOS due to mtDNA depletion are not able to form tumours after implantation

into mice, unless they recover OXPHOS capacity reacquiring mtDNA from the host [45].

The role of OXPHOS in tumorigenesis is not only linked to the energy production, but other aspects of OXPHOS activity were reported to be essential for tumour growth and formation, such as the role of mitochondrial respiration in de novo pyrimidine synthesis. Notably, it has been demonstrated that a functional OXPHOS system is necessary for the activity of the dihydroorotate dehydrogenase, a crucial mitochondrial enzyme of pyrimidine biosynthetic pathway catalysing the oxidation of dihydroorotate. Indeed, this enzyme relies on a functional respiratory chain for its activity as it requires ubiquinone as electron acceptor [46].

In the same way, other studies proved that functional ETC is essential to provide oxidizing power to synthetize aspartate, which is also needed for the same biosynthetic pathway [47].

1.3 Bioenergetics of cancer: interplay between glycolysis and OXPHOS

Cancer cells exhibit great metabolic plasticity that enables them to switch their bioenergetic phenotype between glycolysis and oxidative phosphorylation during carcinogenesis and cancer progression [48].

Smolkova et al. proposed 4 waves of gene expression reprogramming that promote different bioenergetic phenotypes during malignant transformation. In the first wave an oncogene-mediated signalling leads to a partial glycolytic Warburg phenotype, where the pyruvate is still partially oxidized into mitochondria. This phenotype allows a high proliferation rate promoting tumour formation. Then, the high proliferation and the impaired vascularization induce hypoxic regions within tumour mass. Hypoxia thus promotes the second wave of metabolic reprogramming involving the hypoxia-induced factor 1. The activation of the HIF signalling pathway allows cancer cells to adapt to the new tumour microenvironment favouring the classical Warburg phenotype and the mitochondrial biogenesis inhibition.

However, the great energy demand due to the high rate of proliferation results in the lack of nutrients and aglycemia. Subsequently, the third wave of gene reprogramming

promotes the myc-mediated glutaminolysis and restores the OXPHOS function, favouring the use of glutamine as alterative energy substrate. In particular this wave involves the liver kinase B1/5' AMP-activated protein kinase (AMPK)/p53 pathway and the PI3K/Akt/mammalian target of rapamycin pathway.

Finally, the fourth wave of the carcinogenic process promotes mitochondrial biogenesis through the peroxisome proliferator-activated receptor gamma coactivator (PGC)-1α-dependent pathways and the complete recovery of mitochondrial oxidative capacity, which is essential to meet the high-energy demand and sustain the invasive growth of malignant tumours [49].

Therefore, cancer cells may experience a large variety of metabolic changes and phenotypes to be adaptable to bioenergetic stresses occurring in the tumour microenvironment. In this regard, some recent studies focused on understanding how cancer cells orchestrate the interplay between glycolysis and OXPHOS [50].

Computational modeling studies based on a system biology approach proposed that the interplay between the two bioenergetic pathways is coordinated by a regulatory circuit composed of AMPK, HIF-1, and ROS, where AMPK and HIF-1 are respectively the master regulators of glycolysis and OXPHOS, whereas both mitochondrial and cytosolic ROS play a critical role in mediating the interaction between these regulatory factors. Oncogenic signalling pathways such as Myc, Ras, and proto-oncogene tyrosine-protein kinase Src then modulate the main regulatory circuit.

According to this model, cancer cells can acquire three bioenergetic phenotypes, a glycolysis phenotype associated with high HIF-1 activity and low AMPK activity, an OXPHOS phenotype with low HIF-1 activity and high AMPK activity, and a hybrid glycolysis/OXPHOS phenotype characterized by high activity of both HIF-1 and AMPK. This latter metabolic phenotype has been described in several cancer cell lines including melanoma B16-M4b cells, human SUM-159 and MDA-MB-231 TNBC cells and human cervix squamous carcinoma SiHa-F3 cells. Interestingly, it seems provides significant advantages for cancer cells in favouring their survival, proliferation, and metastasis compared to phenotypes using only glycolysis or OXPHOS. Indeed, the hybrid glycolysis/OXPHOS state endows cancer cells with metabolic plasticity to adapt to changing microenvironments including hypoxia or acidic condition and to use all the available substrates to produce energy. Furthermore,

cancer cells in the hybrid metabolic phenotype can produce energy via both glycolysis and OXPHOS and at the same time to use lactate and pyruvate from glycolysis to generate biomass for cell proliferation. In addition, these cells can efficiently modulate ROS levels avoiding the detrimental effects of excessive oxidative stress, thus taking advantage of ROS mediated signalling to promote metastasis [51, 52].

1.3.1 Hypoxia modulates cancer cell bioenergetics

It is well established that the tumour microenvironment has a crucial role in shaping the metabolic phenotype of cancer cells. In particular, hypoxia is one of the main environmental factors affecting the interplay between energy pathways.

Hypoxia is due to an imbalance between the consumption and the supply of oxygen within tumour mass. In many solid tumours, this imbalance is caused by the high proliferative rate of cancer cells in combination with the abnormal angiogenesis and disordered vascularization. Therefore, cancer cells in a solid tumour experience a large variability of oxygen concentrations, from normoxia (2-5% oxygen tension) to severe hypoxia or anoxia (<0.1% oxygen tension), depending on their distance from the blood vessel (Fig.3). For instance, cells at a distance of 200 μm from the vessel are exposed to a condition of severe hypoxia with an oxygen concentration of 0.1-0.2% [53].

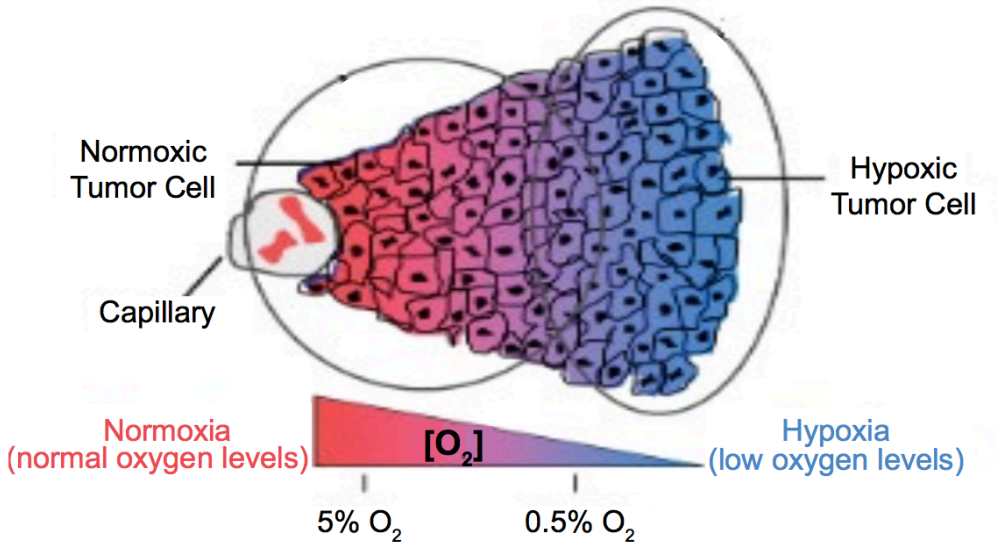

Fig. 3. Oxygen concentrations in tumour mass.

A key event occurring under hypoxia is the stabilization of HIF-1α, which is a subunit of the heterodimeric transcription factor HIF-1, the master regulator of cellular response to low oxygen concentration.

Under normoxic conditions, the cytoplasmic HIF-1α subunit is continuously degraded via the ubiquitin-proteasome system. Instead, under hypoxia, HIF-1α enters the nucleus and binds the HIF-1β subunit to form the transcriptionally active heterodimer that induces the expression of many genes required for adaptation to changes in O_2 availability. These genes include those stimulating angiogenesis (vascular endothelial growth factor, inducible nitric oxide synthase), cell survival and proliferation (epidermal growth factor, insulin-like growth factor 1), and metabolic adaptation by increasing glycolytic flux. Notably, HIF-1 activity upregulates glucose transporters and glycolytic enzymes including LDHA, limiting the oxidative mitochondrial metabolism by favouring pyruvate conversion into lactate. Therefore, glycolysis becomes the main energy production pathway since the low oxygen availability limits the activity of both OXPHOS and Krebs cycle.

However, the oxygen deprivation in the tumour microenvironment not always reaches oxygen concentrations low enough to inhibit the mitochondrial electron transport chain [54]. Indeed, it has been observed that OXPHOS may be not compromised in the presence of oxygen concentrations higher than 1 μm (0.1% O_2) because the Michaelis-Menten constant for O_2 of cytochrome c oxidase is usually between 0.1- 0.8 μm. Furthermore, it has been observed that HIF-1 can mediate the expression of CIV subunits with high affinity for oxygen, optimizing COX activity [55]. Therefore, the oxygen concentrations, although severe, could be still sufficient to saturate the COX enzyme in certain solid tumours maintaining the mitochondrial membrane potential functionally active, thereby allowing the ATP synthesis via ATP-synthase [56]. However, the contribution of the OXPHOS system to energy production seems to be negligible under hypoxic conditions and the enhanced glycolysis is considered the main ATP supplier.

1.4 Energy metabolism as a therapeutic target

Given the essential role of metabolic reprogramming in carcinogenesis and cancer development, targeting cancer metabolism is a hot topic for anti-cancer drug discovery.

For a long time, the scientific interest focused on metabolic pathways involved in biomass production since cancer cells depend on biosynthetic processes to sustain rapid growth and proliferation. Therefore, blocking the cancer source of biomolecules constituted a widely pursued anti-cancer therapeutic strategy [57].

Besides abundant biomolecules, cancer growth requires a lot of energy and, therefore, targeting cellular ATP supply represents another promising approach. Indeed, almost all cellular processes require ATP, including biomolecules synthesis and kinase-mediated growth signalling. Also, a severe ATP depletion is incompatible with the preservation of basal metabolism and the activity of membrane transports [58]. Consequently, modulating the ATP availability may be an efficient strategy to prevent tumour progression and to promote an energy deprivation-induced cell death.

As already reported, all cancer cells rely on glycolysis and/or oxidative phosphorylation for ATP supply. Indeed, although the glycolytic pathway is upregulated in cancer cells compared to normal cells, its contribution to cellular ATP supply usually does not exceed 50-60% and oxidative phosphorylation widely contributes to satisfying cancer energy demand. Therefore, several drugs have been developed to selectively inhibit enzymes involved in both energy pathways [59].

Some of these compounds showed successful results and are currently at various stages of the clinical trial process. Therefore, it is expected that drugs targeting energy metabolism will play a significant role in the future clinical oncology.

For instance, interesting results have been obtained inhibiting glycolytic energy production by employing inhibitors of lactate production (such as dichloroacetate and FX11) or inhibitors targeting glycolytic enzymes. Among the latter ones, 2-deoxyglucose (2DG), lonidamide, and 3-bromopyruvate (3BP) seem to be the most promising drugs.

In particular, 2DG and lonidamide, which selectively block glycolysis inhibiting the hexokinase enzyme, are the most advanced drugs in clinical trials with a good safety profile and a moderate increase in patient survival [10, 60].

There is also increasing interest in alkylating agent 3-bromopyruvate as it displayed satisfying antitumor effects and high tumour selectivity. Preclinical studies in vivo showed that this compound selectively targets cancer cells with a high glycolytic phenotype, significantly reducing tumour mass without notably side effects [61, 62]. Indeed, 3BP enters cancer cells via lactate transporter MCT1, mainly overexpressed in tumour cells, and its main target is the glycolytic enzyme HK-II, the key hexokinase isoenzyme selectively expressed in tumours. Therefore, these aspects guarantee the high selectivity of 3BP for tumour cells and make it a promising candidate for clinical studies.

In addition to inhibiting glycolysis, targeting energy metabolism is also attempted by blocking energy production via OXPHOS. Indeed, there is growing interest in developing drugs to target OXPHOS complexes.

Interestingly, emerging data showed that some drugs used in the clinic for non-oncologic indications, such as metformin, atovaquone, and arsenic trioxide, have an antitumor effect due to their capability to inhibit OXPHOS complexes. In particular, the anticancer effect of metformin is related to the inhibition of Complex I that induces a decrease in ATP production [63]. Preclinical in vivo studies showed promising results about the efficacy of metformin in reducing tumour growth. Therefore, clinical trials are currently ongoing to test the impact of metformin on cancer patients with promising initial data regarding patient survival and the improvement of clinical outcomes.

Other interesting drugs targeting OXPHOS complexes are BAY87-2243, an inhibitor of CI, and VLX60, which inhibits CI, CII, and CIV [64, 65]. Indeed, both compounds induced tumour regression in preclinical models and are now under clinical trials.

Moreover, particular attention is recently paid to BAM 15, a novel type of mitochondrial uncoupler that has attracted interest because it depolarizes mitochondria without affecting plasma membrane potential [66]. Therefore, BAM15 may selectively disrupt oxidative phosphorylation by dissociating the ATP-synthesis from the mitochondrial respiration without off-target effects, thus representing an attractive compound to target energy metabolism in cancer studies [35,42,58].

However, a crucial factor to be considered in the development of a therapeutic approach targeting energy metabolism is the metabolic plasticity. As previously discussed, due to their different origin and differentiation, cancer tissues show great

variability in the use of energy substrates and therefore in bioenergetics phenotype. In addition, cancer cells can display a hybrid bioenergetic phenotype relying on both glycolysis and oxidative phosphorylation, depending on microenvironment conditions and nutrient availability. These features may enable tumours to bypass the inhibitory action of therapeutic agents, thereby making the treatment ineffective. In keeping with these considerations, therapies targeting energy metabolism should be selected according to the metabolic dependency of each tumour. Additionally, the simultaneous inhibition of both ATP-generating pathways may represent a more efficient strategy to elude cancer metabolic plasticity, thus improving anticancer therapeutic effects [67].

1.5 The ATPase inhibitor factor 1 (IF_1): a potential therapeutic target for anticancer therapies

Energy metabolism attracts considerable attention as a target for the development of novel anticancer therapies. However, selectively targeting the bioenergetics of cancer cells is no easy, as the host cells also rely on the same pathways for ATP supply. Therefore, several efforts are being performed to identify cancer-specific targets by determining the most significant differences in the energy metabolism between tumour cells and normal host cells. Thus, target-identification studies were mainly carried out by comparing between tumours and normal tissues the differential expression/activation of genes or proteins involved in the modulation of tumour metabolism.

Among proteins overexpressed in cancer tissues, particular interest has been addressed to a mitochondrial protein called IF_1, the endogenous inhibitor protein of mitochondrial F_1F_o-ATPase (ATP synthase).

Physiologically, IF_1 is ubiquitously expressed in mammalian tissues where it preserves cellular ATP levels preventing the ATP hydrolysis, which is promoted by the reverse activity of ATP synthase under conditions inducing mitochondrial depolarization such as lack of oxygen [68, 69]. Despite its ubiquitous expression, IF_1 levels widely vary in human tissues, with the highest expression in tissues having a very-high metabolic demand such as heart, liver, and kidney and a negligible expression in other tissues including breast, colon, ovary, and lung. Notably, IF_1 expression significantly

increases in several solid tumours including the human breast, colon, ovary, and lung carcinomas whose healthy tissues normally express very low IF_1 levels [70].

Therefore, the mechanism promoting IF_1 overexpression as well as the role played by IF_1 in tumours has become subject of cancer studies. In particular, some studies demonstrated that IF_1 overexpression is regulated at post-transcriptional levels and it has been suggested that the high expression of the protein in tumours is promoted by an increase in translation of IF_1 mRNA, promoted by gene mutations or signals from tumour microenvironment [71].

The Oncomine database analyses also report increased IF_1 mRNA levels in the bladder, parathyroid, cervix, pancreas carcinomas and in myeloma and melanoma compared to normal tissues, indicating that the high IF_1 levels in these cancers are promoted by an increased gene expression rate [72].

Interestingly, recent findings showed that the high IF_1 expression in carcinomas of the lung, liver, bladder, and stomach and in gliomas is associated with both advanced clinical stage of tumour and reduced patient survival. This clinical evidence highlights the relevance of IF_1 as a predictive marker of clinical outcome, pointing out its promising potential as a therapeutic target [73, 74, 75, 76, 77].

In this context, several studies are ongoing to clarify the involvement of IF_1 in tumours and investigate the mechanisms by which IF_1 regulates the energy metabolism and the activity of its physiological target, the ATP synthase, in cancer cells.

1.5.1 The ATP synthase: structure and ATP generation

The mitochondrial ATP synthase, also known as Complex V or F_1F_o-ATPase, is the engine of OXPHOS pathway. It is an enzymatic complex located in the inner mitochondrial membrane, at the level of the cristae compartment, that catalyses the ATP synthesis from ADP and inorganic phosphate (P_i) using energy stored in the proton gradient across the inner mitochondrial membrane. Cryogenic electron microscopy and X-ray crystallography studies showed that the ATP synthase forms dimers organized into rows on tightly curved edges of the cristae. These dimers seem to be required for proper cristae formation, promoting the cristae membrane curvature in the best way to favour the ATP synthesis [78].

Human ATP synthase complex consists of 28 subunits of 17 types with a total molecular mass of 592 kDa. These subunits are organized in two domains, a membrane-extrinsic F_1 domain and a transmembrane F_o domain, linked together by a central stalk and a peripheral stalk.

F_1 is composed of five globular proteins, α, β, γ, δ, and ε with 3:3:1:1:1 stoichiometry. The three α-subunits and the three β-subunits are arranged alternately forming a hexameric ring around the γ subunit. The γ-subunit protrudes from the hexameric ring and is associated with the δ and ε subunits forming together "the central stalk", which interacts with the "c-ring" of transmembrane domain F_o [79].

The F_o domain, embedded in the inner mitochondrial membrane, is composed by a ring of eight hydrophobic c-subunits and the ATP6 subunit, which is associated with single copies of supernumerary subunits ATP8, e, f, g, DAPIT, 6.8PL that are not present in the well-characterized bacterial enzyme and whose role in mammalian ATP synthase is contributing to the enzyme dimerization [80].

The ATP6 and the associated subunits are in contact with the peripheral stalk, which connects the ATP6 subunit of the F_o domain to the F_1 catalytic domain and consists of single copies of OSCP (oligomycin -sensitivity conferring protein), b, d and F6 subunits.

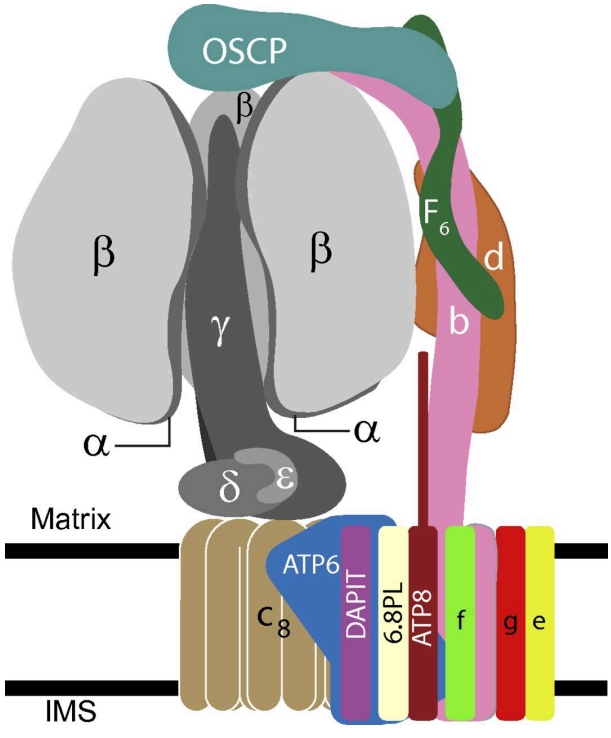

Fig.4. Schematic representation of ATP synthase in mammalian mitochondria.

Functionally, three main sectors are identified in the ATP synthase structure, a catalytic core, a rotor and a stator.

F_1 is the catalytic core of the enzyme that includes the β-subunits containing the catalytic nucleotide-binding site, where the ADP phosphorylation takes place to form ATP. The c-ring of F_o domain represents the rotor of the enzyme as it generates rotation using the energy stored in the proton gradient. The rotational energy is then transferred to the catalytic domain by another rotary element, the central stalk. Otherwise, the peripheral stalk acts as a stator holding the catalytic $\alpha_3\beta_3$ subcomplex and the ATP6 subunit in a fixed position, counteracting the rotation tendency triggered by the rotor movement [81].

The mechanism underlying the ATP synthesis driven by proton flux is "the binding change mechanism" or "rotary catalysis model", first proposed by Paul Delos Boyer [82]. According to this model, the nucleotide-binding sites on the β subunits catalyse the ATP synthesis cyclically assuming three inconvertible conformations with different affinity for nucleotides, the β_E or "O" conformation (Open site), unable to bind ATP, the β_{TP} or "T" conformation (Tight site), which tightly binds ATP, and the β_{DP} or "L" conformation (Loose Site), which binds ADP and Pi (Fig. 5).

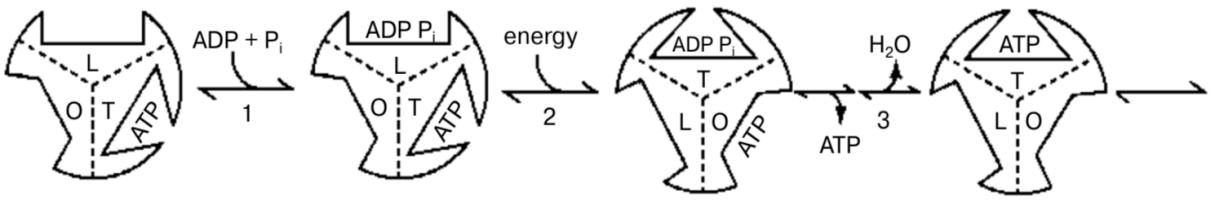

Fig.5. The binding-change mechanism for ATP synthesis.

The β-subunit conformational changes are induced by the clockwise rotation of γ-subunit of the central stalk. Every 120° rotation, γ-subunit interacts with a different β-subunit promoting the interconversion of nucleotide-binding site [83].

During a catalytic cycle, ADP and P_i bound to β-subunit in "L" conformation are converted to ATP when the same β-subunit reaches the "T" conformation. The newly

formed ATP is then released by the β-subunit, once the subunit assumed the "O" conformation. Therefore, each 360° rotation leads to the formation of three ATP molecule, one from each of the three β-subunits [84].

The γ-subunit rotation triggering ATP synthesis is powered by the proton flux crossing the Fo domain. In particular, the generation of rotational mechanism involves the ATP6 subunit, corresponding to the a-subunit in bacterial ATP synthase, and the hydrophobic c-ring of transmembrane domain [85].

The a-subunit contains two proton channels, an inlet half-channel opening to the intermembrane space and an outlet half-channel opening to the matrix. Protons flowing from the intermembrane space through the inlet half-channel protonate a negative carboxyl residue of c-subunit, which is exposed on the outer surface of the c-ring in contact with the a-subunit surface.

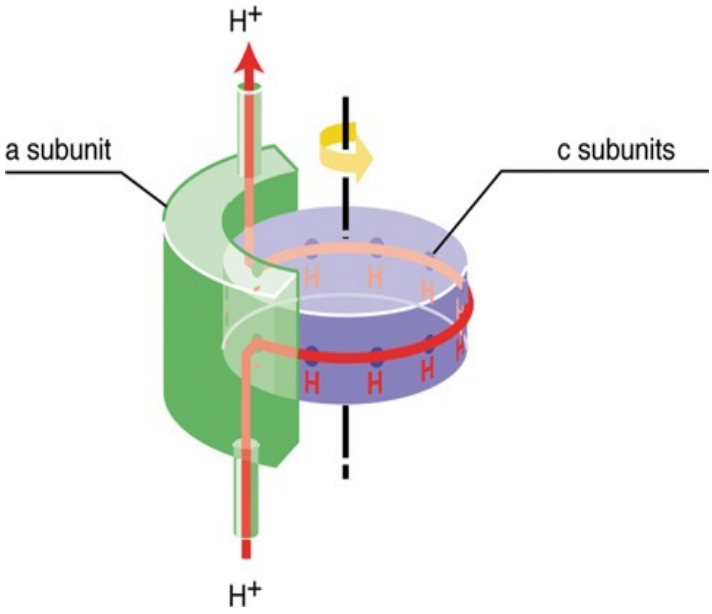

Fig. 6 Generation of rotational mechanism in the Fo domain of ATP synthase.

Once neutralized, the protonated residue moves through the hydrophobic membrane generating a rotational step of the c-ring. This rotation exposes another negatively charged residue to the interface with the inlet half-channel of a-subunit, allowing another residue to be protonated, thus generating another rotational step. These rotational steps allow protons carried by the neutralized carboxyl groups to reach the

outlet channel where another site in contact with the a-subunit reionizes the carboxy group releasing the proton into the matrix.

The number of protons necessary to generate a 360° rotation of the c-ring corresponds to the number of c-subunits present in the ring (8 in mammalians).

Notably, the γ-subunit is strictly associated with the c-ring and each 360° rotation of the rotor provides the energy needed to generate 3 ATP molecules in the catalytic domain [81].

1.5.2 Reversal of the ATP synthase activity and regulation of mitochondrial membrane potential.

Physiologically, the ATP synthase catalyzes ATP synthesis by using the energy stored in mitochondrial membrane potential to power the rotational catalysis mechanism.

However, the ATP synthase, as a reversible nanomotor, is also able to perform the reverse reaction. Indeed, under conditions inducing the collapse of mitochondrial membrane potential, this nanomotor can hydrolyze ATP obtaining the energy needed to translocate protons from the matrix to intermembrane space in order to restore the proton motive force.

Conditions triggering the ATP hydrolysis by ATP synthase occur every time

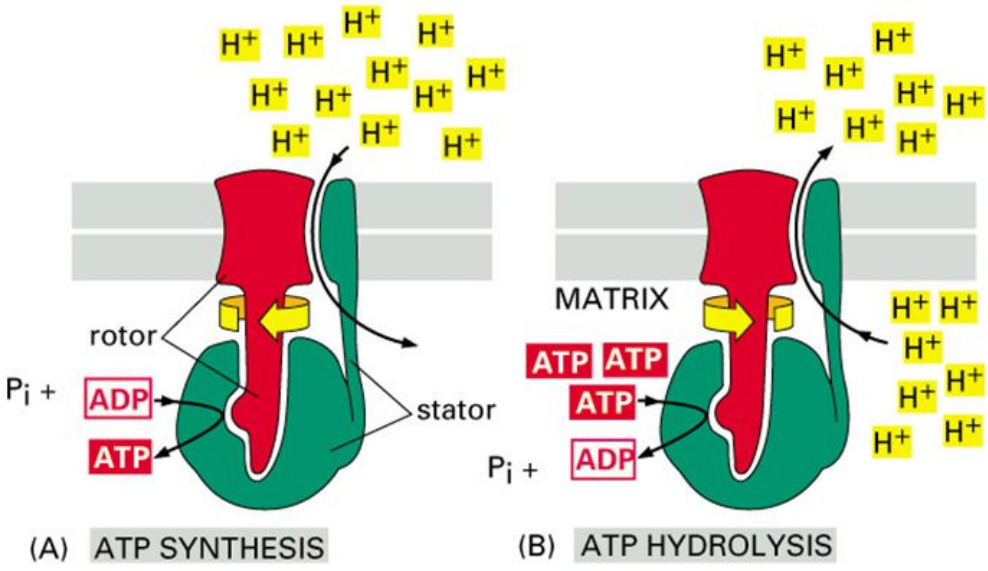

Fig. 7. Mechanism of synthesis (A) and hydrolysis (B) of ATP by the mitochondrial ATP synthase complex.

respiration is impaired. Mitochondrial respiration impairment may result from alterations of the structural integrity of the inner membrane or defects in the activity of respiratory complexes, as it occurs in mitochondrial inherited diseases and neurodegenerative conditions. Otherwise, respiration impairment may be also due to oxidative stress or environmental factors such as the absence of oxygen [86]. Cells may experience hypoxia under pathological conditions such as ischemia, but transient hypoxic episodes may also physiologically occur in healthy tissues, where the absence of the final electron acceptor leads to a temporary impairment of mitochondrial respiration and consequently to the collapse of the transmembrane proton gradient.

Concerning the ATP hydrolysis process, it occurs in the β-subunits of catalytic F_1 domain of the ATP synthase complex through the rotational catalysis mechanism, just like the ATP synthesis. Every 360° rotation drives each β-subunit through the three catalytic states hydrolysing three ATP molecules.

During ATP hydrolysis, an Mg-ATP molecule from the cytosol enters the empty β_E-subunit inducing a 120° counterclockwise rotation of the γ-subunit and promoting the conversion of β_E-subunit in β_{TP}-subunit. An additional 120° rotation induces the transition to β_{DP} –conformation, where the nucleophilic attack of a water molecule at the γ-phosphate of ATP occurs, releasing the energy required for inducing the rotational movement to pump protons into the intermembrane space. Finally, a further counterclockwise rotation completes the 360° rotary cycle, releasing the products of ATP hydrolysis (phosphate, ADP and the magnesium ion) [87].

The reversal activity of the ATP synthase, which allows the maintenance of the mitochondrial membrane potential ($\Delta\Psi_m$), is a crucial mechanism for the regulation of cellular homeostasis. Indeed, the $\Delta\Psi_m$ is not only the driving force for ATP synthesis, but it is involved in several non-energetic functions.

For this reason, even under hypoxic conditions, where the ATP production through oxidative phosphorylation is prevented, mitochondria maintain their transmembrane potential at the expense of cytosolic ATP, thus highlighting the importance of $\Delta\Psi_m$ for other cellular functions. These functions include the regulation of ion homeostasis, protein import, ROS production, mitophagy, and cellular death [88, 89].

In this regard, the negative mitochondrial matrix charge conferred by $\Delta\Psi_m$ is crucial to drive the transport of cations and positively charged proteins from cytosol into

mitochondria. This property of transmembrane potential allows mitochondria to accumulate the essential cofactors for mitochondrial reactions, such as Ca^{2+} and Fe^{2+}, and the necessary proteins for mitochondrial functioning [90, 91].

Furthermore, it has been demonstrated that the mitochondrial respiratory chain becomes a considerable ROS producer in the presence of a high $\Delta\Psi_m$. Indeed, a high mitochondrial membrane potential, which is usually associated to a decrease of ATP synthesis rate via OXPHOS, induces a decrease of electron transport rate through redox centres of ETC, favouring the leak of electrons from the respiratory complex to the oxygen and increasing the production of mitochondrial ROS [92].

Notably, the loss of mitochondrial membrane potential is a common feature of dysfunctional mitochondria and may be a signal to induce mitochondrial-dependent apoptotic death or, on the contrary, an event triggering autophagic degradation of dysfunctional mitochondria in order to escape apoptosis. Indeed, since mitochondrial damage is detrimental to cell survival, damaged depolarized mitochondria need to be removed by mitophagy. However, depending on the severity of the mitochondrial damage, a prolonged mitochondrial depolarization may alternatively trigger the mitochondria-mediated apoptotic pathway, thus leading to apoptotic death [93, 94].

Hence, the crucial role of mitochondrial membrane potential in cellular homeostasis justifies its maintenance at the expense of cellular ATP. However, although cells can physiologically experience oscillation in intracellular ATP concentrations, the ATP levels need to be maintained within a certain range in order to preserve cellular homeostasis [95].

During reversal of ATP synthase activity, depletion of cellular ATP can be more or less severe. In particular, in organs with high ATP request like brain and skeletal muscle, or in case of an increased energy demand, a prolonged ATP consumption may seriously compromise cell viability.

Therefore, cells evolved a mechanism to prevent the excessive ATP depletion consisting of the ATPase inhibitory factor 1 (IF_1). This inhibitory protein interacts with F1 portion of the ATP synthase hindering the counterclockwise rotation of the enzymatic rotor, thus inhibiting the ATP hydrolysis and protecting cells from cellular death due to ATP depletion [96].

1.5.3 IF_1: structure and inhibitory function

The inhibitory factor 1 was first purified in 1963 from bovine heart mitochondria by Pullman and Monroy. They described IF_1 as a low molecular weight protein (10 kDa) specifically inhibiting, through a non-competitive mechanism, the ATP-hydrolytic activity of the ATP synthase, without interfering with its ATP-synthetic activity [97].
IF_1 is located in the mitochondrial matrix, although evidence reported its presence in the cytosol and on the plasma membrane of endothelial cells, which present ectopic expression of ATP synthase on the cellular membrane [98].
It is encoded by nuclear DNA and is highly conserved among species, ranging from yeast to mammals. The high degree of sequence conservation confers IF_1 from one species the ability to inhibit the ATP synthase from another.
The human mature protein, encoded by nuclear gene ATP1 in chromosome 1, is composed of 81 amino acids and presents a high sequence homology of about 75% with the well-defined bovine protein of 84 amino acids [99].

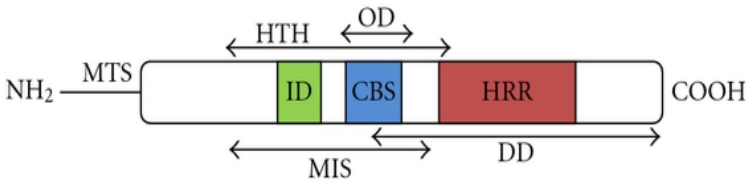

Fig. 8. Schematic representation of bovine IF_1 structure.

Both human and bovine proteins are translated as precursor proteins with an N-terminal sequence of 25 amino acids (mitochondria targeting sequence, MTS), necessary for the protein import into the mitochondrial matrix [100].
IF_1-conserved protein regions have been first identified in the well-characterized bovine structure. In particular, the N-terminal region with a helix-turn-helix structure (HTH) comprises the inhibitory domain (ID), which includes the minimal inhibitory sequence (MIS) necessary for the interaction with the F_1 portion of the ATP synthase, a calmodulin binding site (CBS), whose role seems to be involved in the regulation of the import of IF_1 into mitochondria, and the oligomerization domain (OD) [101]. Whereas, the C-terminal region includes the dimerization domain (DD) containing a histidine-rich region (HRR) involved in the pH-sensing mechanism.

The dimerization domain is involved in the formation of IF_1 homodimer, which is the active form of the protein. Two α-helical monomers form an antiparallel double-stranded coiled-coil by establishing hydrophobic interactions between the two C-terminal regions of the helices. The dimer so formed presents protruding N-terminal minimal inhibitory sequences that can simultaneously bind two F_1 catalytic domains.

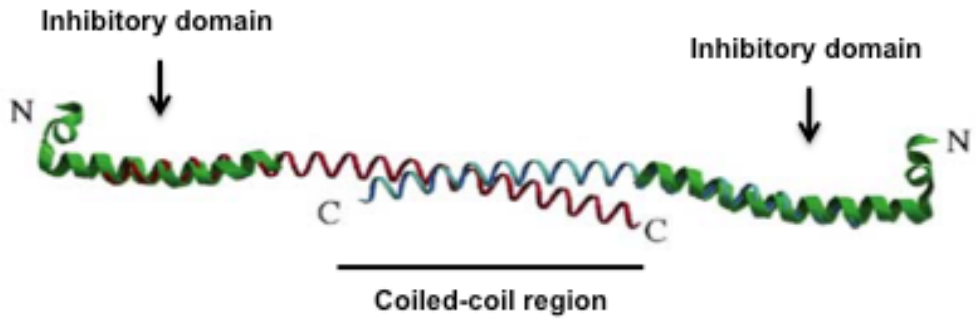

Fig. 9. Ribbon representation of the IF_1 dimer.

This active dimeric state is favoured by pH values below 7, whereas at pH above neutrality the IF_1 dimers aggregate in oligomers by forming antiparallel coiled-coils in the N-terminal regions, occluding the inhibitory sites of the dimers and rendering the inhibitor inactive and unable to bind the ATP synthase [102].

Therefore, IF_1 may exist in two states, the inactive oligomeric state and the active dimeric state, depending on a pH-sensitive mechanism. In particular, the pH-dependent switch between inactive oligomers and active dimers involves the deprotonation or protonation of five highly conserved histidines in the C-terminal region [103]. This has been demonstrated in vitro by deleting histidine 49, whose absence removes the IF_1-capacity to dimerize, thereby producing a pH-insensitive monomeric inhibitor, which is active even at basic pH [104].

Consistently, the $\Delta\Psi_m$ collapse occurring under hypoxic/ischemic conditions in vivo causes matrix acidification as a result of H^+ increase in the matrix. Consequently, the fall in pH promotes the formation of active dimers that bind the F_1 domains of two ATP synthase, inhibiting the ATP hydrolysis [105, 106].

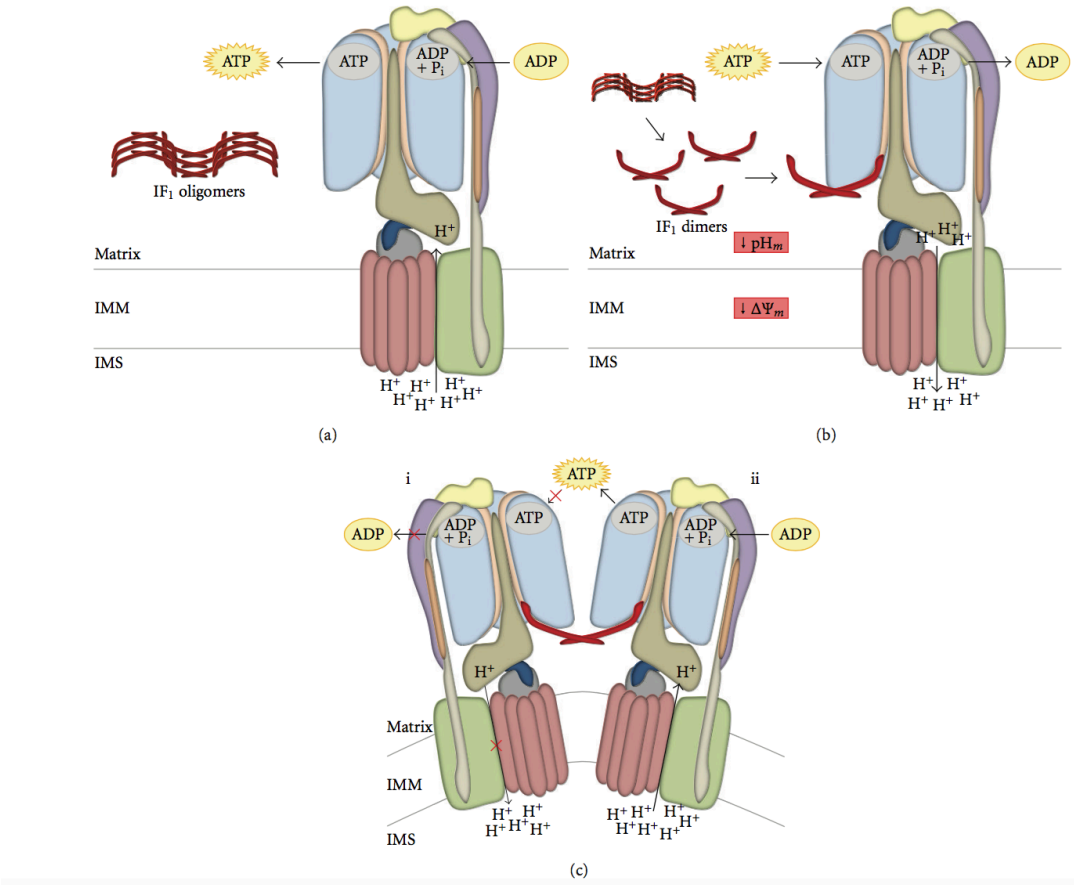

Fig. 10. Interaction of IF_1 with the ATP synthase*. In physiological conditions IF_1 is mainly in its inactive oligomeric form (a). Under conditions inducing the collapse of mitochondrial membrane potential, the decrease in matrix pH favours the disaggregation of oligomers into dimers (b). Free IF_1 dimers are thus able to bind an ATP synthase dimer inhibiting the ATP hydrolytic activity (c).*

The mechanism of inhibition of ATP synthase by IF_1 has been studied in detail by Walker and co-workers. According to their model, the formation of the inhibited complex and the consequent arrest of the catalytic cycle by IF_1 require the hydrolysis of two ATP molecules and two 120° rotations of the γ-subunit. In particular, the initial interaction between IF_1 and the F_1 domain takes places in a site on the empty β_E-subunit at the α_E-β_E-interface [107, 108]. After the hydrolysis of the first ATP molecule, the anticlockwise 120° rotation of γ-subunit converts the α_E-β_E-interface to the α_{TP}-β_{TP}-interface, allowing further interactions to take place between IF_1 and the enzyme. At the next step, a second ATP molecule is hydrolysed inducing a second 120° rotation that converts the α_{TP}-β_{TP}-interface to the fully closed α_{DP}-β_{DP}-interface, with IF_1 strictly bound to the enzyme. In the final inhibited state the long α-helix of IF_1

appears well-inserted into the core of the enzyme by also interacting with the γ-subunit and the α_E-subunit.

Thus, the presence of IF_1, strictly bound to the enzyme, inhibits the rotational catalysis responsible for the hydrolysis of ATP via two possible mechanisms. According to the first proposed mechanism, IF_1 bound to the β_{DP}-subunit blocks the release of ADP after the ATP hydrolysis, so that the further ATP binding to the empty B_E-subunit is no longer able to generate the rotation of γ-subunit. Alternatively, a more likely inhibition model states that the presence of IF_1 prevents the hydrolysis of ATP bound to the β_{DP} –subunit, thereby avoiding the next rotational step [109, 110].

In contrast to the well-investigated mechanism of IF_1 inhibition, the mechanism of the reversal of the IF_1 inhibition in response to the restore of a proton motive force is not still defined. However, the inversion of direction of rotation occurring during the restore of ATP synthesis seems to induce the disruption of the IF_1 inhibitory binding by destabilizing the interactions between IF_1 and F_1 domain, leading the protein ejection from its binding site in the catalytic interface [111].

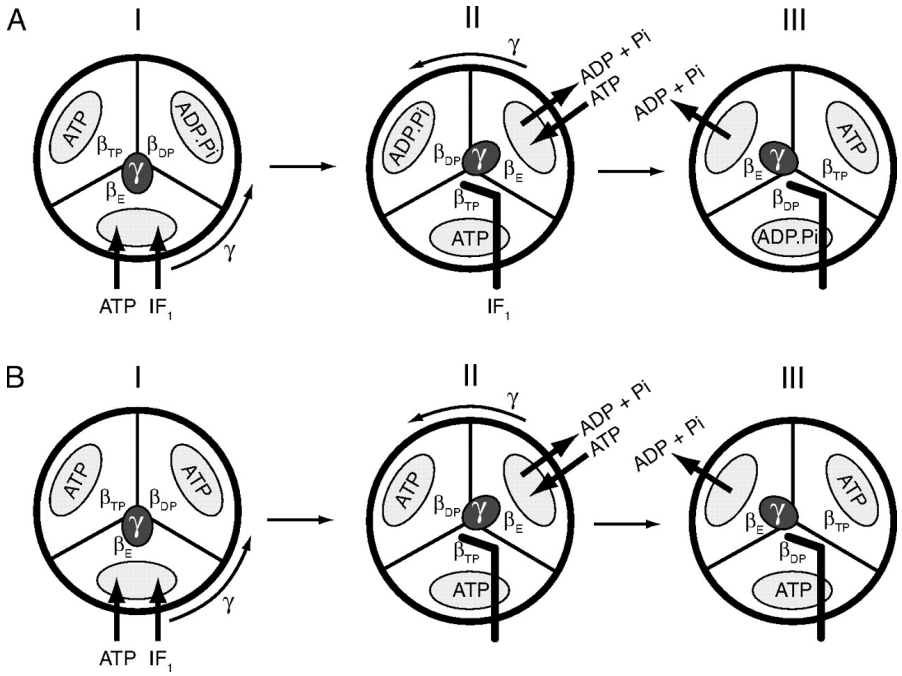

Fig. 11. Mechanisms of inhibition of ATP synthase by IF_1.
For simplicity, only the β catalytic subunits are shown.

The above-described inhibitory role of IF_1 has been deeply investigated in ischemic disease, in which the loss of blood supply induces a reduction of oxygen availability

abolishing mitochondrial respiration. In particular, in myocardial tissue, where the ATP synthase contributes 90% of the ATP required and glycolysis is unable to satisfy the high-energy demand, IF_1 becomes essential to prevent the irreversible necrotic damage during the ischemic episodes [112, 113].

In addition to the well-investigated function as inhibitor of the ATP synthase hydrolytic activity under ischemic conditions, IF_1 is now examined for other possible roles, with a large attention to its contribution in pathophysiological conditions such as cancer. Notably, several research groups recently investigated on the tumour IF_1 overexpression, prompting various speculations about the role of IF_1 in cancer metabolism. Indeed, the protein overexpression has been related to an increase of tumour malignancy by increasing tumour capability to escape apoptosis, survive in adverse conditions, invade, and metastasize.

1.5.4 IF_1 and cancer studies

As widely described, IF_1 is directly involved in the regulation of cellular energy balance by modulating the ATP hydrolytic activity of the ATP synthase. In this regard, considering its primary biological role and the rediscovery of the importance of energy metabolism in cancer biology, IF_1 has been proposed to contribute to the onset of the metabolic plasticity characterizing the peculiar cancer energy metabolism.

In particular, because of the central role of ATP synthase as a master regulator of energy metabolism, the role played by IF_1 in regulating the mitochondrial ATP synthase activity represents an interesting matter of debate in cancer studies.

In normal tissues, IF_1 is reported to inhibit the ATP hydrolytic activity of ATP synthase, without affecting its ATP synthetic activity. However, recent studies sustain that the overexpression of IF_1 observed in cancer cells is responsible for the inhibition of the ATP synthesis by the ATP synthase complex [114]. Indeed, consistent with these studies, the inhibitory activity of IF_1 involves both hydrolyse and synthase activities of the enzyme and depends on IF_1 phosphorylation. Specifically, the phosphorylation of serine 39 seems to prevent the interaction of IF_1 with the ATP synthase, abolishing its inhibitory activity [115]. In vivo, the phosphorylation is

mediated by a mitochondrial cAMP-dependent protein kinase (PKA), which is also involved in the regulation of other mitochondrial proteins [116]. Consistently, it has been demonstrated that the dephosphorylation of IF_1, promoted by treatments with PKA inhibitors, induces the inhibitory binding to the ATP synthase. However, the mechanisms responsible for IF_1 dephosphorilation in vivo are unknown and it has been suggested that the pool of active dephospho-IF_1 may rapidly be reestablish by the high turnover of the protein.

Importantly, a large fraction of active dephosphorylated IF_1 has been found in human carcinomas and has been associated with the inhibition of ATP synthesis via OXPHOS and the metabolic switch towards the Warburg phenotype [117, 118].

In this scenario, the inhibition of the ATP synthase activity by IF_1 overexpression blocks the backflow of H^+ into the matrix, triggering mitochondrial hyperpolarization. Under these conditions, mitochondria increase the production of radical oxygen species, which act as secondary messengers mediating the activation of signalling pathways. These pathways include the NFkB (nuclear factor kappa-light-chain-enhancer of activated B cells) pathway, known to promote the acquisition of tumour features such as enhanced proliferation rate, protection against cell death via Bcl-xL (B-cell lymphoma-extra large) overexpression and upregulation of angiogenesis by VEGF (vascular endothelial growth factor) [119].

However, additional experimental evidence contradicted the above results reporting opposite data over the role of IF_1 in the ATP synthase inhibition, transmembrane potential modulation, and ROS production.

These latter studies, performed on stable IF_1 silenced cells, questioned the reliability of the previous ones, which were performed by transient modulation of IF_1 expression and therefore in a model that could not properly represent a steady-state metabolic condition.

These experimental data sustain that IF_1 inhibits the ATP synthase activity in cancer cells only under conditions inducing the collapse of mitochondrial membrane potential and, therefore, when the enzyme hydrolyses ATP. Importantly, under these conditions, IF_1 has been reported to modulate the cancer bioenergetics preserving the cellular energy [120, 121, 122, 123].

Conversely, under normal condition, when mitochondrial respiration is not compromised and ATP synthase is synthesizing ATP, IF_1 overexpression seems to promote OXPHOS activity in cancer cells. Indeed, studies from different research groups report that cancer cells expressing IF_1 show a reduced mitochondrial membrane potential compared to cells in which IF_1 expression was suppressed, indicating a more efficient OXPHOS system [120, 123, 124]. In support of this, the IF_1 expression has also been associated with an increased ADP-induced respiration rate, suggesting that IF_1 modulates the proton flux by enhancing the ATP synthesis rate via OXPHOS [123].

It has been proposed that the positive modulation of OXPHOS by IF_1 may be due to the direct interaction of the protein with the ATP synthase. Indeed, the association of IF_1 with the dimeric form of the ATP synthase complex has been observed even under normal growing conditions. Therefore, it has been suggested that the binding of IF_1 to the ATP synthase may increase the OXPHOS rate either directly, by increasing the ATP synthase catalytic activity, or indirectly, by improving the structure of mitochondrial cristae stabilizing the dimeric form of the enzyme.

As regards the last point, the high cristae curvature promoted by ATP synthase dimerization favours the charge accumulation in the proximity of the enzyme, increasing the proton flux through ATP synthase and, consequently, the rate of ADP phosphorylation [125]. Therefore, IF_1 may improve the efficiency of ATP synthesis by promoting ATP synthase dimerization. Consistently, cancer cells overexpressing IF_1 showed an increase in the number of cristae per mitochondrion compared to cells with reduced protein expression.

However, the role of IF_1 in the oligomeric organization of the ATP synthase is still under debated. In particular, according to some investigators the presence of IF_1 is directly involved in the formation of dimers as its lack decreases the dimer/monomer ATP synthase ratio [124, 126]. Conversely, other studies demonstrated the ATP synthase dimeric organization is not influenced by the binding of the protein, since the distribution of ATP synthase between the dimeric and monomeric forms was found to be similar in the presence and in the absence of IF_1 [127, 123]. Nevertheless, these latter observations do not exclude the possibility that the presence of IF_1 could still improve the ATP synthesis efficiency stabilizing the enzymatic structure and modelling the mitochondrial cristae.

Another controversy concerns the involvement of IF_1 in the control of ROS generation in cancer cells. Indeed, according to the data previously reported, the presence of IF_1 seems to favour the increase of mitochondrial production of reactive oxygen species, which act as second messengers activating pathways implicated in cellular growth and proliferation [119]. In contrast, evidence from different research groups indicates that IF_1 has a protective role against ROS production, reporting a lower content of ROS in IF_1 expressing cells, probably related to the lower transmembrane potential and the proposed high OXPHOS efficiency in the presence of the protein [128, 129]. Notably, by preventing excessive ROS production, IF_1 could protect cancer cells from macromolecular damage and ROS-mediated apoptosis.

Furthermore, since IF_1 expressing cells exhibited a better tolerance to pro-apoptotic stimuli, the role of the protein in relation to the apoptotic process was also investigated. Indeed, several experimental data suggested that IF_1 may limit the apoptotic cell death signalling in response to an apoptotic stimulus by favouring cristae stabilization and the preservation of mitochondrial ultrastructure, limiting the release of Cyt c and, consequently, the signalling cascade that culminates in apoptosis [130, 131].

The conflicting views emerging from the reported data indicate that direct biochemical evidence is needed to confirm the speculative models proposed to explain the regulation of ATP synthase activity by IF_1 in cancer cells. Therefore, the scientific interest is still focusing on the mechanism of action of this protein to define how and in which tumour microenvironment conditions IF_1 contributes to cancer cell survival and tumour progression.

2. AIM OF THE STUDY

Over the last two decades, cancer studies showed a renewed interest in the metabolic reprogramming occurring in cancer cells during tumorigenesis. Notably, metabolic reprogramming results in a flexible and heterogeneous energy metabolism that provides cancer cells with the energy needed to survive and proliferate under the adverse conditions of tumour microenvironments.

Given the pivotal role of energy metabolism for cancer development and spread, ongoing studies aim to characterize cancer bioenergetic profile with the purpose to identify therapeutic strategies selectively targeting the energy metabolism of each single tumour.

In this regard, studies are focusing on the identification of possible therapeutic targets by comparing the protein expression profile of tumours and surrounding healthy tissues. Among the upregulated proteins observed in cancer tissues, particular attention has been paid to the mitochondrial protein IF_1, the endogenous inhibitor of the mitochondrial ATP synthase [70]. In several solid tumours, the overexpression of this mitochondrial protein has been associated with an advanced cancer stage and reduced patient survival, highlighting its relevance as a potential therapeutic target [73-77].

The canonical role of IF_1 has been deeply addressed in studies on ischemia, where its function as an inhibitor of the ATP hydrolytic activity of the ATP synthase has been well defined. In ischemia, due to lack of oxygen, mitochondrial respiration is compromised and, consequently, the electrochemical proton gradient across the inner mitochondrial membrane falls. Under these conditions, the ATP synthase is pushed to work in reverse hydrolysing cytosolic ATP to restore the transmembrane potential, which is essential for many cell functions. However, if ATP hydrolysis keeps progressing out of control, the excessive ATP consumption would compromise cell survival and lead to cellular death. The regulation of ATP hydrolysis by IF_1 thus becomes critical to limit energy dissipation and protect ischemic cells from death.

Therefore, given its physiological function in preserving cellular energy balance, IF_1 has been proposed to play a crucial role in cancer cell bioenergetics and different

research groups have been studying its involvement in tumorigenesis. In particular, an interesting matter of debate is the function played by IF_1 in regulating the mitochondrial ATP synthase activity of cancer cells. In this context, Cuezva J.M and co-workers proposed that IF_1 overexpression might promote tumour development favouring the switch toward aerobic glycolysis by inhibiting the ATP synthesis activity of the ATP synthase [115]. However, data from different research groups contradicted this view, questioning the lack of biochemical evidence demonstrating the inhibition of ATP synthesis by IF_1 and defining the Cuezva's model as speculative [120-123]. In this regard, our previous studies demonstrated, by directly measuring both the activities of ATP synthase in both IF_1-epxressing and IF_1-silenced cells, that IF_1 inhibits the ATP synthase in cancer cells only when the enzyme hydrolyses ATP following mitochondrial depolarization, as it occurs in mammalian cells during ischemic episodes [121].

Based on our evidence, we thus proposed that cancer cells might overexpress IF_1 to preserve the energy needed to survive and promote tumour growth under low oxygen availability, a condition that cells frequently experience within the tumour mass.

To assess this hypothesis, the role of IF_1 in promoting cancer cell survival and proliferation under severe hypoxic and anoxic conditions will be evaluated by assessing mitochondrial function and bioenergetics of 143B and HCT116 cells, both derived from solid tumours as osteosarcoma and colon cancer, respectively. Notably, considering that in non-transformed ischemic tissues IF_1 shows a pro-survival function mainly in those ones showing the highest protein expression and an OXPHOS-dependent metabolism [122, 124, 132], the possible protective role of IF_1 will be investigated and discussed in relation to the bioenergetic phenotype of the two cell lines used as cancer cellular models and their IF_1 expression level.

It is also noteworthy that IF_1 exerts its protective role by preserving cellular energy at the expense of losing the mitochondrial membrane potential. However, the prolonged loss of $\Delta\psi m$ is a detrimental event for the cells that may represent a signal either for mitochondria-dependent apoptotic death or for the selective degradation of dysfunctional mitochondria to escape apoptosis. Taking these observations into account, the effects of the prolonged mitochondrial depolarization on both mitochondrial content and quality control system including mitophagy and mitochondrial biogenesis will be also assessed. Notably, all the investigations will be

carried out in control cells and stable IF_1-silenced clones produced in our laboratory and will be then extended to various mutant cell lines expressing altered forms of IF_1 produced in collaboration with Professor Walker from University of Cambridge, who previously identified and characterized the mutant forms of IF_1. These investigations aim to further explore the role of IF_1 as a molecular target by deepening the mechanisms by which IF_1 modulates the ATP synthase activity, hopefully providing useful information for the development of potential antitumor strategies.

3. MATERIALS AND METHODS

3.1 Cell culture

The study was performed in human osteosarcoma 143B and human colon cancer HCT116 cells and their derived IF_1-silenced clones.

IF_1-silenced GFP-negative clones were obtained via RNA-interference by infecting parental cells with retroviral vectors. Stable clones expressing a red fluorescence protein targeted to mitochondria (mtRFP) were previously obtained from 143B parental cell line as reported by Costanzini *et al* [133].

The parental cell lines and all clones used were maintained at 37°C with 5% carbon dioxide (CO_2) in Dulbecco's Modified Eagle Medium (DMEM) containing 10% FBS (Fetal Bovine Serum), 100 U/ml penicillin, 100 μg/ml streptomycin and 0.25 μg/ml amphotericin B. The culture medium was supplemented with growth substrates according to the ATCC (American Type Culture Collection) guidelines: 25 mM glucose, 4 mM glutamine and 1 mM pyruvate or 16.7 mM glucose and 2 mM glutamine for 143B and HCT116 cells, respectively.

Cell culture reagents were purchased from Gibco (ThermoFisher), except for glucose, glutamine and pyruvate, which were provided by Sigma Aldrich.

All the experiments were performed seeding cells in complete medium containing saturating amounts of energy substrates (25 mM glucose, 4 mM glutamine and 1 mM pyruvate) two days before the experiment. On the day of the assay, growth medium was replaced with fresh medium and cells were exposed to hypoxic/anoxic conditions, or to anoxia mimicking conditions by supplementing the medium with the uncoupler FCCP (carbonyl cyanide-4-trifluoromethoxy-phenylhydrazone), a weak acid that dissipates the proton gradient by transporting H^+ across the inner mitochondrial membrane into the matrix.

The hypoxic condition was obtained culturing cells in the hypoxic workstation Ruskin INVIVO200 equipped with the gas mixer Q to maintain oxygen levels at 0.1% and carbon dioxide at 5%.

To provide the anoxic environment, cells were placed in a tightly sealed glass jar in the presence of an oxygen absorber (FMT1000-ATCO). In addition, to avoid any possible oxygen contamination, the device was maintained in the INVIVO200 chamber set at 0.1% oxygen tension. An oxygen indicator was placed into the glass jar with cells to reveal the absence of oxygen by changing colour (Fig. 12).

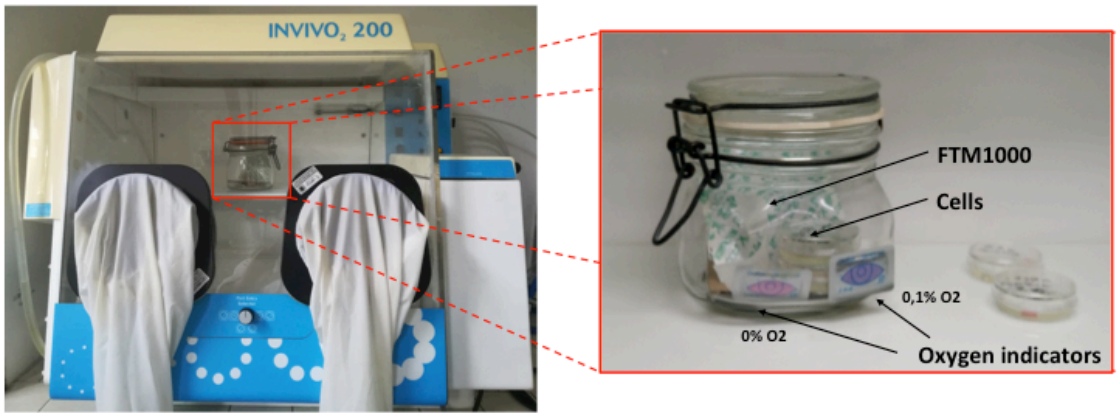

Fig. 12. Generation of anoxic condition.

3.2 Production of stably IF_1-silenced GFP-negative clones

Osteosarcoma and colon carcinoma GFP-negative clones were produced via RNA interference by infecting parental cells with retrovirus packaged with either scrambled or short hairpin RNA (shRNA) directed to IF_1 as described below.

3.2.1 Bacterial transformation and plasmid purification

To obtain the plasmid of interest in amounts suitable for the following manipulation, competent DH5α E. coli cells (Invitrogen-ThermoFisher) were transformed with plasmid DNA by the heat shock method. In brief, after adding plasmid DNA to bacterial cell suspension, the mixture was gently shacked and incubated on ice for 30 minutes. The heat shock was performed by placing the mixture at 42° C for 30 seconds

and subsequently cooling for 2 minutes on ice. Hence, transformed bacteria were incubated at 37°C for 1 hour in SOC (Super Optimal broth with Catabolite repression) medium (Sigma-Aldrich) under shaking conditions. Bacteria were then seeded onto pre-warmed plates containing solidified Luria-Bertani agar (Sigma-Aldrich) supplemented with 100 μg/ml ampicillin. After overnight incubation at 37°C, single colonies were picked up from the plates and expanded overnight under shaking at 37°C in 20 g/L Luria-Bertani broth (Sigma-Aldrich) in the presence of ampicillin. Plasmid DNA was finally purified from bacteria by PureLink^{TM}HiPure Plasmid Filter Maxiprep Kit (Invitrogen-ThermoFisher) according to the manufacturer's instructions. The quantification of plasmid DNA was assessed through a NanoVue Plus Spectrophotometer (GE Healthcare).

3.2.2 Production of retroviral vectors and infection of tumour cell lines

The production of amphotropic retrovirus vectors carrying the sequence for the IF_1-silencing was performed by transient transfection of Phoenix retroviral packaging cell line [134].

Phoenix cells were grown to 70% confluency in Petri dishes and transfected with 10 μg of either TR30013 (Scrambled) or GI325936 (shRNA) pGFP-V-RS vector (Origene Technologies) using polyethylenimine (PEI, Polysciences Inc) according to the manufacturer's instructions. After 24 hours incubation at 37°, the culture media of transfected cells were collected and centrifuged at 1500 rpm for 5 minutes. The retroviral supernatant was subsequently filtered through a 45 μm filter and frozen in aliquots.

143B and HCT116 cells at 70% confluence were subsequently infected with the retroviral supernatant containing the retroviral constructs in the presence of polybrene to increase the infection efficiency. Infected cells were incubated for 5 hours at 32°C and left overnight at 37°C. Finally, stably infected cells were selected using 1 μg/ml puromycin. Single clones were then sub-cloned by limiting dilution and assayed for IF_1-expression.

3.3 Cellular growth

Cellular growth under different experimental conditions was assessed by seeded $6x10^5$ cells in triplicate in complete medium. Cell culture media change was performed two days after seeding, which is the needed time to let cells properly adhere to the plate before exposing them to the experimental treatment (0,1% O_2, 10 μM FCCP either in the presence or absence of 80 μM 3BP).
At chosen time cells were trypsinized, collected and counted using the trypan blue dye exclusion test.

3.4 Cell viability

The viability of cells exposed to hypoxic condition (0.1% O_2) or cultured with 10 μM FCCP in either the absence or presence of 80 μM 3BP was measured by cytometry using the MUSE count and viability assay kit (Merck Millipore).
The assay distinguishes viable cells from non-viable cells on the basis of their permeability to two fluorescent dyes. The nuclear dye is membrane-permeant and stains all nucleated cells. The second dye only enters dying or dead cells with compromised membranes. The combination of two fluorescent dyes allows discrimination of nucleated cells from debris and live cells from dead or dying ones.
In detail, cells were harvested, counted and suspended at the proper concentration in the kit reagent. After 5 minutes of incubation at room temperature, cells were analysed by Muse Cell Analyzer acquiring 10 000 events, obtaining the percentages of live and dead cells.

3.5 Lowry protein quantification assay

The quantification of the protein content of examined samples was performed by the Lowry method [135]. Essentially, cell samples were lysed with 0.3 % sodium deoxycholate (Sigma Aldrich) and subsequently incubated for 10 minutes with a mixture containing three reagents in a stoichiometric ratio of 100:1:1 (reagent 1: 2 %

Na2CO3 and 0.1 M NaOH, reagent 2: 2 % Na-K tartrate, reagent 3: 1% CuSO4). Subsequently, the suspension was supplemented with the Folin-Ciocalteu's reagent to a final concentration of 3%. The last reagent reacts with aromatic aminoacid present in the sample under alkaline conditions producing a coloured compound whose absorbance was measured after 30 minutes of incubation at 750 nm in a V-450 Jasco spectrophotometer.

The sample's protein concentration (mg/ml) was then determined applying Lambert-Beer law on the basis of a standard curve, using a series of bovine serum albumin (BSA-Sigma Aldrich) standards.

3.6 SDS-PAGE and Western Blot

The evaluation of protein expression was performed by SDS-PAGE (sodium dodecyl sulphate–polyacrylamide gel electrophoresis) separation and Western blot analysis [123]. Cells were collected from the dishes, washed in Hanks' Balanced Salt Solution (HBSS) and lysed on ice in ice-cold radioimmunoprecipitation assay buffer pH 8 (50 mM Tris-HCl, 150 mM NaCl, 0.5% Na-DOC, 1% SDS) supplemented with 1 mM PMSF (phenylmethylsulfonyl fluoride), protease inhibitor cocktail (100 μg/ml) and phosphatase inhibitors (5 mM sodium fluoride and 1 mM sodium orthovanadate); all reagents were purchased from Sigma-Aldrich. The protein content of cellular lysates was quantified by the Lowry method. Subsequently, the protein lysates were diluted in Bolt LDS Sample Buffer and Bolt Sample Reducing Agent (Life Technologies) and denatured for 3 minutes at 100° C, following the manufacturer's instructions. Equal amounts of protein lysates (10, 20 or 60 μg) were then loaded into Bolt 4-12% Bis-Tris Plus gels (Invitrogen-ThermoFisher). The electrophoresis run was performed in Bolt MES SDS Running Buffer (Invitrogen- ThermoFisher) at 140 V for 90 minutes. Resolved proteins were then electroblotted onto a nitrocellulose membrane by wet transfer at 100 V for 1.15 hours at 4°C. The transfer buffer consist of 20 mM Tris-HCl pH 8.3, 150 mM glycine, 0.02 % (v/v) SDS, 20% (v/v) methanol. The protein transfer efficiency was verified by staining gels with Coomassie Brilliant Blue [136]. Following transfer, nitrocellulose membranes were blocked by incubating for 1 hour at room temperature in a blocking solution composed of 2% (w/v) not-fat dry milk

(BioRad) or 2% (w/v) BSA (Sigma-Aldrich) in phosphate-buffered saline (PBS) with 0.05% (v/v) Tween20 (Sigma-Aldrich).

Nitrocellulose membranes were then incubated with the proper diluted primary antibody, according to the manufacturer's instructions.

IF_1 (12 kDa), α-subunit (54 kDa), and d-subunit of F_1F_o-ATPase (19 kDa) primary mouse monoclonal antibodies were purchased from MitoSciences Inc., Eugene, OR.

VDAC1 (voltage dependent anion channel 1, 35 kDa) and TOMM20 (translocase of outer mitochondrial membrane 20, 16 kDa) mouse antibodies from Abcam were used to evaluate mitochondrial mass. HIF-1α was detected by a rabbit antibody from Bethyl. PINK1 (PTEN-induced kinase 1, 60 kDa) and BNIP3 (BCL2 and adenovirus E1B 19-kDa-interacting protein 3), markers of mitophagic process, were detected with a rabbit anti-PINK1 and a mouse anti-BNIP3 antibody purchased from Novus Biological and Abcam, respectively. The mitochondrial biogenesis markers SIRT1 (Sirtuin 1, 130 kDa) and PGC1α (130 kDa) were respectively revealed with a mouse and rabbit antibody from Cell Signalling Technologies.

Actin (42 kDa), used as loading control, was detected with a mouse monoclonal anti-actin primary antibody from Sigma-Aldrich.

Following the incubation of primary antibodies, membranes were washed in PBS containing 0.05% (v/v) Tween20 and subsequently incubated for 1 hour at room temperature with the proper secondary antibodies labelled with horseradish peroxidase (Life Technologies).

Protein detection was performed with the Enhanced chemiluminescence Western blotting Detection Reagent Kit (GE Healthcare) using the ChemiDoc MP system equipped with the ImageLab software (BioRad) to perform the densitometric analysis of the immunoreactive protein bands.

3.7 Brightfield and fluorescence microscopy

Brightfield and fluorescence images were acquired using a fluorescence-inverted microscope equipped with a charge-coupled device camera (Olympus IX50). High power multiple images (magnification 10x, 40x, 60x) were captured with IAS2000

software (Delta Sistemi). No less than 10 optic fields were acquired for each experimental condition.

Mitochondrial network of 143B and HCT116 cells was evaluated by incubating cells with the MitoTracker Green fluorescent probe (ThermoFisher) and acquiring fluorescence images by using the proper set of filters (excitation: 490 nm, emission: 516 nm).

Fluorescence images of mtRFP-expressing cells cultured in either presence or absence of 10 μM FCCP for 24 hours were acquired using the following set of filters: excitation 540/20 nm and emission 610/40 nm.

3.7.1 Fluorescence microscopy evaluation of mitophagy activation

The activation of the mitophagic process was assessed in IF_1-expressing and IF_1-silenced cells by fluorescence image colocalization analysis of the mitochondrial red fluorescent protein and the yellow fluorescence protein (YFP) fused to the autophagosome marker LC3 (microtubule-associated protein 1A/1B-light chain 3).

To this aim, control and IF_1-silenced cells stably expressing the mtRFP were transiently transfected with the pCMV6-LC3-YFP vector to overexpress the LC3-YFP fusion protein. In detail, cells were transfected using an 8:1 ratio of PEI to pCMV6-LC3-YFP vector (w/w). The following day, after verifying the LC3-YFP expression by fluorescence microscopy, cells were detached and seeded at the proper density for the experiment. 12 hours later, the medium was replaced with fresh media containing 25 μM chloroquine (to prevent the fusion of the autophagosomes to the lysosomes), both in the absence and presence of 10 μM FCCP. Positive controls of mitophagy activation were obtained by treating cells with chloroquine and 10 μM deferoxamine. After 24 hours of treatment, fluorescence images were acquired at magnification 40x by using the proper filters. The mtRFP signal was acquired by using the excitation and emission filters reported above.

The YFP signal was detected with the following set of filters: excitation 480/30 nm and emission 530/30 nm. Fluorescence images were then processed and merged by the AutoDeblur – Image Deconvolution Software (BioImaging Solutions Inc).

3.8 Biochemical assays

3.8.1 Lactate release

To evaluate the glycolytic flux in 143B and HCT116 cells cultured up to 72 hours in both normoxic and hypoxic conditions, the lactate released in the medium was determined every 24 hours by a colorimetric-enzymatic method. In detail, cell media were collected every 24 hours and the amount of lactate present in the medium was determined by using the Lactate PAP Fluid Kit (Centronic GmbH, Wartenberg, Germany), according to the manufacturer's instructions.

The assay consists of a two-enzyme coupled reaction performed at 37°C. In detail, lactate in the sample is first oxidized to pyruvate and hydrogen peroxide by lactate oxidase. Then, the hydrogen peroxide reacts with p-aminophenazone and p-chlorphenol in the presence of a peroxidase to form a red coloured chromogen. The absorbance of the coloured compound measured at 546 nm is proportional to the amount of lactate present in the sample, which is determined using an internal standard of known concentration.

3.8.2 Intracellular ATP content measurement

The steady-state ATP content was measured in both 143B and HCT116 cells grown under standard culture medium after short exposure (30 minutes) to metabolic inhibitors (2 mM iodoacetamide or 0.6 μM oligomycin). In addition, the intracellular ATP levels were determined in both controls and IF_1-silenced cells cultured under oxygen deprivation (0.1% O_2 and 0% O_2) and in the presence of 10 μM FCCP or FCCP plus oligomycin.

The measurements were performed by a bioluminescence method using the luciferin-luciferase system (ATP bioluminescent assay kit CLS II; Roche) [137]. In detail, the luciferin undergoes a reaction of oxidative decarboxylation at pH 7.75 in the presence of ATP, O_2 and a luciferase isolated from the firefly Photinus pyralis, yielding oxyluciferin, CO_2, adenosine monophosphate, pyrophosphate, and light emission. The

light emitted is proportional to the amount of ATP present in the sample, which is quantified by measuring the luminescence of a known amount of ATP standard.
To perform the assay, cells were detached with trypsin, washed with HBSS and suspended in a buffer solution containing 10 mM Tris-HCl, 100 mM KCl, 5 mM KH2PO4, 1 mM EGTA, 3 mM EDTA, 2 mM MgCl2 (pH 7.4). An aliquot of the cell suspension was then lysed with dimethyl sulfoxide to release the intracellular ATP and properly diluted with cold water. The luminescence of cellular extract was thus detected with the Luminoskan TL Plus luminometer (Labsystems) by adding the sample to a pH 7.75 buffer solution (0.1 M Tris/acetate, 2 mM EDTA) in the presence of luciferin-luciferase stock solution. The amount of ATP measured was finally referred to the protein content, quantified with the Lowry method and expressed as nmol/mg of protein.

3.8.3 Citrate synthase activity assay

Citrate synthase is the initial enzyme of Krebs cycle. It catalyses the reaction between acetyl coenzyme A (acetyl CoA) and oxaloacetic acid to form citric acid and reduced CoA (CoA-SH).
The activity of this enzyme is commonly used as an index of mitochondrial mass and is measured by a spectrophotometric method first described by Trounce et all. in 1992 [138]. This colorimetric assay is based on the reaction between CoA-SH, produced by citrate synthase, and the 5'-dithio-bis-2-nitrobenzoic acid (DTNB) to form the yellow-coloured 5-thio-2-nitrobenzoic acid (TNB) whose absorbance is measured at 412 nm. The rate of increase of TNB absorbance is proportional to the citrate synthase activity.
To perform the assay, both 143B and HCT116 cells grown under standard culture conditions were trypsinized, washed in HBSS and then resuspended in a buffer solution at pH 7.4 (10 mM Tris-HCl, 100 mM KCl, 5 mM KH2PO4, 1 mM EGTA, 3 mM EDTA, 2 mM MgCl2). The citrate synthase activity was assayed at 30°C suspending 20-30 μg of protein in a 125 mM Tris-HCl buffer (pH 8) continaing 0.2% Triton X-100 (a detergent allowing cellular permeabilization), 0.1 mM acetyl CoA, 0.01 mM DTNB and 0.5 mM oxaloacetate (Sigma-Aldrich) [139]. The enzymatic activity was thus assessed by monitoring the TNB absorbance at 412 nm (ε=13.6

mM^{-1} cm^{-1}) for 2 minutes. The specific activity of the enzyme, expressed as nmol/min/mg of protein, was calculated by applying the Lambert-Beer law and normalizing to the amount of protein determined by the Lowry method.

3.8.4 Mitochondrial oxygen consumption rate

Mitochondrial oxygen consumption was assessed in both intact 143B and HCT116 cells using an oxygen Clark-type electrode as previously described by Baracca et al. [140]

The measurements of endogenous respiration were performed in DMEM supplied with routine culture substrates (25 mM glucose, 4 mM glutamine and 1 mM pyruvate) at 37°C in a thermostatically controlled Stratkelvin's chamber equipped with the Clark oxygen electrode. In detail, 143B and HCT116 cells grown under standard cell culture conditions were harvested, washed, and resuspended. An aliquot of cell suspension containing 150-200 μg of protein was loaded in the electrode chamber and the oxygen consumption was then recorded for about 4-5 minutes.

The oligomycin-sensitive respiration was also evaluated monitoring the decrease in oxygen consumption rate (OCR) after the addition of oligomycin. The OCR results in the decrease of oxygen concentration in the electrode chamber over time. Data were normalized to the amount of sample protein and expressed as nmol/min/mg of protein.

3.8.5 Mitochondrial membrane potential ($\Delta\Psi_m$)

The evaluation of inner mitochondrial membrane potential ($\Delta\Psi_m$) was performed by flow cytometry staining cells with 20 nM tetramethylrhodamine methyl ester (TMRM, Molecular Probes), a lipophilic cationic probe entering mitochondria in a $\Delta\Psi_m$ – dependent manner [121]. Cells cultured under oxygen deprivation (0.1% O_2 and 0% O_2) or in the presence of 10 μM FCCP were incubated with the probe for 30 minutes at 37°C in the absence or presence of oligomycin to fully inhibits the mitochondrial ATP synthase. After incubation with TMRM, cells were trypsinized, diluted to the proper

density (250,000 cells/ml) with HBSS and analysed with MUSE cell analyser (Millipore, Billerica, MA) by acquiring 10000 events.

TMRM loaded cells were excited at 532 nm and the fluorescence emission was measured at 576/28 nm. Data were acquired and analysed by MuseSoft Analysis and Flowing software 3.1 (Cell Imaging Core, University of Turku), respectively.

3.9 Data analysis

All assays were performed at least in triplicate. All data were presented as mean ± standard deviation (SD). Statistical analyses were performed with the OriginPro 7.5 software (OriginLab Corporation) by applying analysis of variance (ANOVA) test followed by Bonferroni's post hoc test. The level of statistical significance selected was $p \leq 0.05$.

4. RESULTS

4.1 Evaluation of IF_1 expression levels and bioenergetic profile in 143B and HCT116 cell lines

IF_1, whose expression is upregulated in several solid tumours, is well reported to play as a master regulator of the hydrolytic activity of ATP synthase under ischemic condition by limiting ATP wasting and protecting ischemic cells from death. It is ubiquitously expressed in mammalian tissues; however, its expression varies greatly among different human tissues with the maximum expression levels in those tissues characterized by high energy demand and low glycolytic capacity [122,124,132].
Therefore, considering that solid tumours frequently experience low or even absent oxygen tensions and that cancer cells require a lot of energy to sustain the aggressive tumour growth, we proposed that IF_1 may play in hypoxic/anoxic cancer cells the essential role observed in ischemic non-transformed cells eventually depending on the bioenergetics profile of each tumour. In view of these considerations, we investigated the role of IF_1 in hypoxic cancer energy metabolism taking into account the bioenergetic background of both 143B and HCT116 cells, used as cellular models.

4.1.1 IF_1 expression levels

As a starting point, we compared the expression levels of IF_1 in the two cell lines chosen as models for the study. We used two cell lines derived from solid tumours, the 143B human osteosarcoma cell line, where we previously demonstrated the IF_1 capability to exclusively inhibit the reversal of ATP synthase activity without affecting the ATP synthesis [121], and the HCT116 human cell line, which is derived from colon cancer, one of those carcinomas with proved IF_1 overexpression compared to the healthy colon tissue. As reported in Fig.13, electrophoresis and immunodetection analysis of IF_1 protein levels revealed that it was significantly higher in HCT116 cells

than in osteosarcoma cells with a three-fold higher IF_1/ATP synthase ratio, as indicated by the semiquantitative analysis of IF_1 levels normalized to the ATP synthase d-subunit, thereby suggesting that the contribution of IF_1 in the bioenergetics might be different in these two tumour cell line.

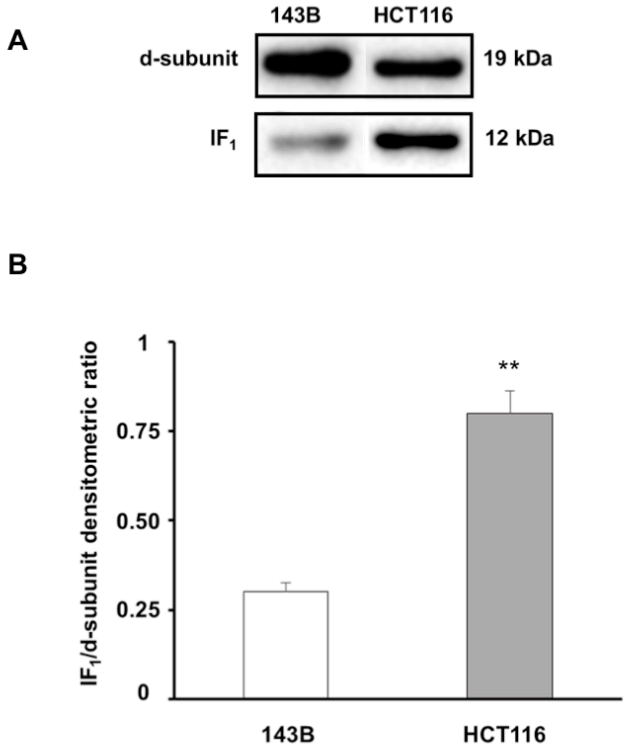

Fig. 13. The IF_1/ATP synthase ratio is significantly higher in HCT116 than in 143B cells *(A) 20 μg of 143B protein extract and 10 μg of HCT116 protein extract were analysed by SDS-PAGE followed by immunodetection of both IF_1 and ATP synthase d-subunit. (B) IF_1 to d-subunit band densitometric ratio of the two cancer cell lines. **, $p < 0.01$ indicates the statistical significance compared to 143B cells.*

4.1.2 Bioenergetic characterization of cellular models

After assessing the IF_1-expression in both 143B and HCT116 cells, we subsequently performed the bioenergetic characterization of both parental cell lines with the aim to evaluate the relationship between IF_1-expression levels and cellular energy metabolism in relation with survival of cells exposed to oxygen deprivation. Therefore, other than cell growth, we measured some metabolic parameters under standard cell culture conditions including glycolytic flux, mitochondrial mass,

endogenous respiration rate, and intracellular ATP levels in the presence of glycolysis and oxidative phosphorylation inhibitors. Then, we also evaluated the metabolic adaptation of 143B and HCT116 cells to the oxygen deprivation by exposing them to prolonged hypoxia (0.1% O_2).

4.1.2.1 Cell growth and glycolytic flux

In order to compare the proliferation rate and the glycolytic flux of 143B and HCT116 cells under optimal growth conditions, both parental cell lines were cultured up to 72 hours in normoxic conditions with saturating amounts of energy substrates (25 mM glucose, 4 mM glutamine and 1 mM pyruvate).

Cellular growth and glycolytic flux were assessed every 24 hours by counting cells and measuring lactate release in the medium, respectively. Interestingly, we observed that both parental cell lines grew similarly having the same proliferation rate, whereas

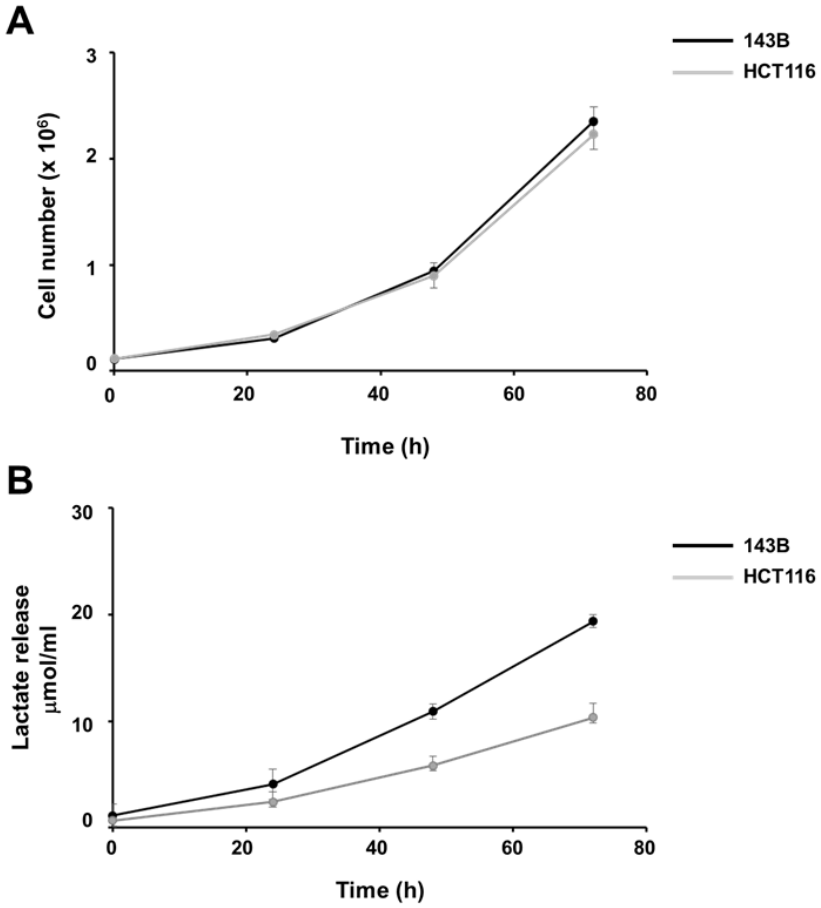

Fig.14. ***Cellular growth and glycolytic flux in 143B and HCT116 parental cell lines.*** *(A) Cell growth and (B) lactate production (micromoles of lactate per ml of growth medium) were evaluated up to 72 hours under optimal growth conditions.*

they showed differences in lactate production suggesting a different use of glucose as energy substrate. In particular, the lactate measured at each time point in the collected medium was twice higher in 143B cells than in HCT116 cells, thus indicating that the proliferation rate in 143B cells is supported by a higher glycolytic flux than in colon cancer cells (Fig. 14).

4.1.2.2 Cellular respiratory rate and mitochondrial content

Taking into account the above results that showed a similar growth in both parental cell lines and a higher glycolytic flux in 143B than in HCT116 cells, we assumed that colon cancer cells could rely more on OXPHOS than glycolysis to meet the energy demand needed to sustain the same proliferation rate of 143B cells. Therefore, to estimate the OXPHOS capacity of both parental cell lines, we subsequently assessed the oxygen consumption rate and mitochondrial content under basal conditions.
Specifically, we first evaluated through polarographic method the respiration sustained by endogenous substrates by suspending intact cells in routine basal culture medium (25 mM glucose, 4 mM glutamine and 1 mM pyruvate). As reported in Fig. 15, the HCT116 cells showed a 45% higher basal respiration compared to 143B cells. However, the OCR under basal conditions is not only controlled by energy demand and oxidative substrates availability; indeed it is also partly influenced by cellular non-mitochondrial oxygen consumption and proton leak across the mitochondrial

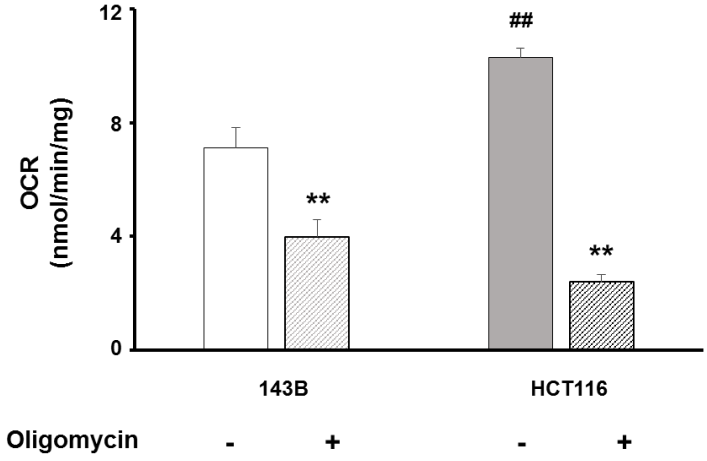

Fig. 15. Basal and oligomycin-inhibited mitochondrial respiration rate in 143B and HCT116 cells. *The oxygen consumption rate, expressed as nanomoles of O_2/min/mg of protein, was measured in intact cells in either the absence or presence of oligomycin. ## and **, $p<0.01$ indicates the statistical significance of data compared with 143B parental cells and basal OCR, respectively.*

membrane. Therefore, to estimate the OXPHOS contribution we evaluated the decrease of the OCR following the addition of oligomycin, the specific inhibitor of ATP synthase. Interestingly, the rate of oxygen consumption associated to other processes was significantly lower in HCT116 cells than 143B cells. Indeed, colon cancer cells showed a larger decrease (-75%) of OCR upon the addition of oligomycin compared to 143B cells (-40%), thus showing a larger portion of basal respiration used to drive ATP production via OXPHOS than in osteosarcoma cells. Besides, we assessed the mitochondrial content in both cell lines to evaluate whether the higher oxygen consumption rates observed in HCT116 cells compared to 143B cells were associated with a greater mitochondrial mass. A qualitative assessment of mitochondrial mass was first performed by fluorescence microscopy staining cells with MitoTracker green, a fluorescence probe specific for mitochondria. The brightfield and fluorescence microscopy images revealed that the two cell lines were different in size and mitochondrial content. In particular, HCT116 cells showed a smaller size but a higher content of mitochondria per unit cell area compared to 143B cells (Fig. 16A). Then, a quantitative estimation of mitochondrial mass was performed by assaying the enzymatic activity of the citrate synthase and the intracellular levels of two mitochondrial proteins, TOMM20 and VDAC1. In detail, citrate synthase is a Krebs cycle enzyme whose activity is widely accepted as an index of mitochondrial mass. Interestingly, the spectrophotometric evaluation of citrate synthase activity, expressed as nmol/min/mg of protein, showed a 20% increase of enzymatic activity in HCT116 cells compared to 143B cells, thus confirming the qualitative evaluation of mitochondrial content performed by fluorescence microscopy (Fig.16B). The difference in mitochondrial mass was further validated by the immunodetection of VDAC1 and TOMM20, mitochondrial proteins commonly used as mitochondrial mass markers. As we can observe in Fig. 16C, the immunoblot analysis revealed an increase of about 30% of both proteins in HCT116 cells compared to 143B cells, confirming the previous results. All the analyses thus showed a higher mitochondrial mass in colon cancer cells than in 143B cells, indicating that the higher OXPHOS capacity of HCT116 cells compared to osteosarcoma cells may be partially explained by a greater mitochondrial content. Indeed, after normalizing for the citrate synthase activity, the 45% difference observed between the non-normalized endogenous oxygen consumption rates of the two cell lines is reduced to only 15%.

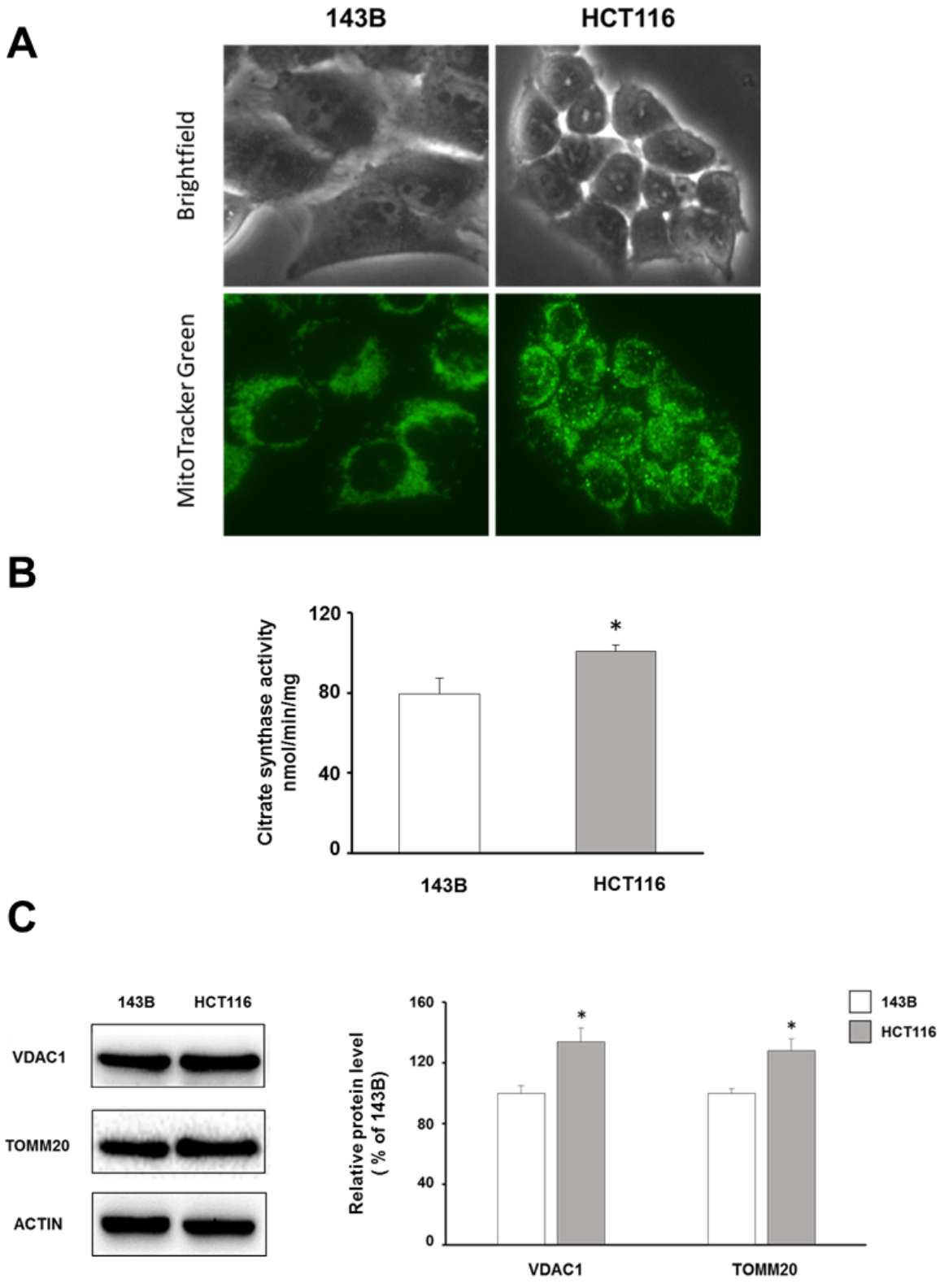

Fig. 16. Mitochondrial content in 143B and HCT116 cells. *(A) Representative brightfield and fluorescence microscopy images of both parental cell lines (magnification 60x). Cells were stained with MitoTracker green to label mitochondria. (B) Citrate synthase activity, expressed as nmol/min/ mg of protein, is used as an index of mitochondrial mass. (C) Representative immunodetection and densitometric analysis of VDAC1 and TOMM20, markers of mitochondrial mass. Histograms show VDAC1 and TOMM20 content in 15 µg of protein extract from 143B and HCT116 cells normalized to the actin content and expressed as percentage compared to 143B cells. *, $p<0.05$ indicates the statistical significance compared to 143B cells.*

4.1.2.3 Metabolic inhibitor-mediated modulation of intracellular ATP content

To estimate the contribution of each energy-producing pathway to cellular ATP production under standard culture conditions, we modulated the ATP content by alternatively inhibiting glycolysis and oxidative phosphorylation using 2 mM iodoacetamide and 0.6 μM oligomycin, respectively.

The effect of the inhibitors on steady-state intracellular ATP content was thus assessed in both parental cell lines by using a luminometric method based on the luciferin-luciferase assay. After 30 minutes of exposure to either the glycolytic inhibitor iodoacetamide or the ATP synthase inhibitor oligomycin, the 143B cells showed a 50 % decrease of ATP content compared to the basal condition in the presence of iodoacetamide and a slightly lower ATP decrease of about 30% in the presence of oligomycin, suggesting a higher contribution to ATP production from glycolysis than oxidative metabolism. Conversely, in HCT116 cells the reduction of ATP content was stronger when the ATP synthase was inhibited by oligomycin (-70%) than in the presence of iodoacetamide (-30%), thus showing that colon cancer cells rely mainly on OXPHOS for their energy production (Fig. 17).

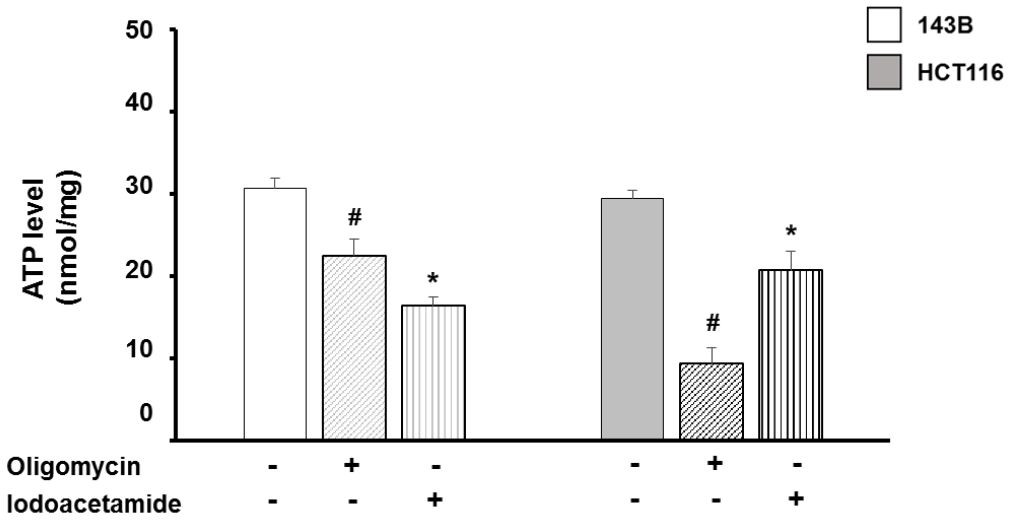

Fig. 17. Glycolysis and OXPHOS inhibition-mediated modulation of cellular ATP content. *ATP levels, expressed as nmol/mg of protein, were measured in 143B and HCT116 cells incubated for 30 minutes in the presence or absence of either iodoacetamide or oligomycin. # and *, $p<0.05$ indicates the statistical significance of date compared to controls.*

4.1.2.4 Effect of severe hypoxia on cell growth and glycolytic flux

After characterizing the bioenergetics of 143B and HCT116 cancer cells under optimal growth conditions, we exposed both cell lines to 0.1 % O_2 in order to evaluate their metabolic adaptability to severe hypoxia. To this aim, we evaluated both cell growth and glycolytic flux every 24 hours by culturing cells up to 72h at 0.1% O_2.

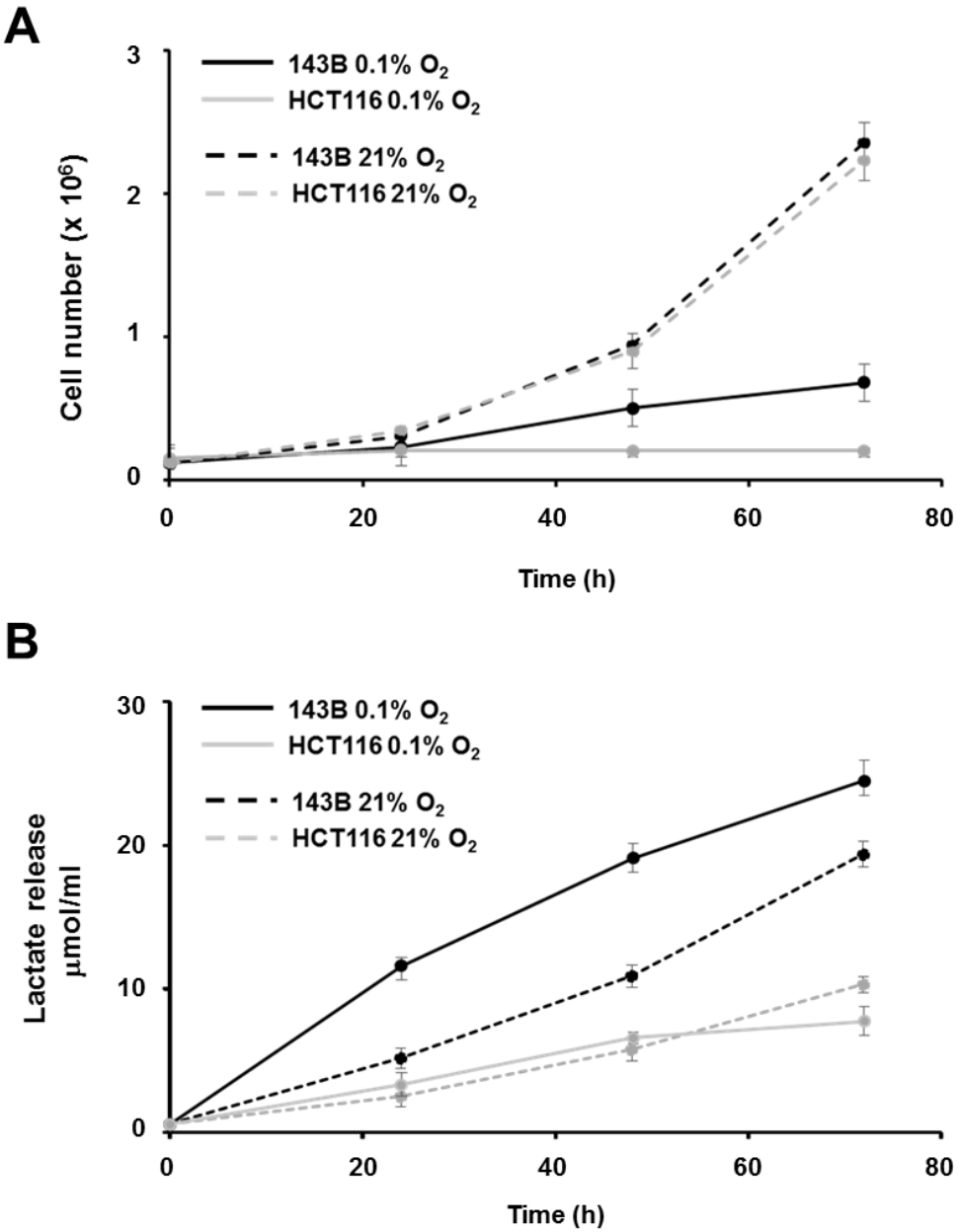

Fig. 18. Cellular growth and glycolytic flux under severe hypoxia (0.1% O_2). (A)*Cell growth and (B) lactate production (micromoles of lactate per ml of growth medium) were evaluated up to 72 hours under 0.1% O_2. The results previously obtained in normoxic conditions were also reported to be compared (dashed lines) with those observed under severe hypoxia.*

Contrary to the results obtained in normoxia, the two cell lines showed a different growth capability under limited oxygen availability. In particular, as shown in Fig. 18A, 143B cells were still able to proliferate, although they slowed down their growth compared to normoxic conditions. The proliferation of HCT116 cells was instead completely inhibited by hypoxic exposure, indicating low adaptability of colon cancer cells to hypoxia.

Consistently, the analysis of lactate production during the hypoxic exposure suggested that the inability of HCT116 cells to proliferate under oxygen deprivation was due to their low glycolytic capacity. As reported in Fig 18B, HCT116 cells showed a lower lactate production compared to 143B cells, as we previously observed in normoxic conditions. Furthermore, we noticed that the lactate release by HCT116 cells during hypoxia was quite similar to lactate produced under normoxic conditions, indicating the inability of these cells to increase their glycolytic flux and, consequently, the ATP production via glycolysis to compensate the lack of ATP production via OXPHOS.

In contrast, 143B cells showed a higher lactate release under hypoxia compared to normoxia with a 2.5 fold increase in lactate production during the first 24 hours of exposure to 0.1% O_2, thereby confirming their high glycolytic capacity and metabolic adaptation to hypoxia.

4.1.2.5 HIF-1α protein stabilization in hypoxic 143B and HCT116 cells

In light of the latter results and considering the pivotal role of HIF-1α in the adaptive regulation of energy metabolism under hypoxic conditions, we subsequently assayed the HIF-1α protein levels to assess whether the higher sensitivity to hypoxic stress observed in HCT116 cells compared to 143B cells could be related to a different

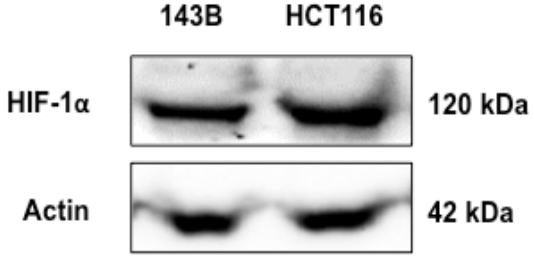

Fig. 19 Stabilization of HIF-1α under hypoxia (0.1% O_2). *HIF-1α levels were monitored after 4 hours of hypoxia exposure by analysing 60 µg of protein extract by SDS-PAGE followed by immunodetection.*

accumulation of the key modulator of the hypoxic response HIF-1α in the two cell lines.

To this aim, we evaluated the protein levels of HIF-1α after 4 hours of exposure to 0.1% O_2 in both 143B and HCT116 cells.

Unexpectedly, the immunoblot analysis revealed that HIF-1α was equally stabilized in both cell lines, suggesting that HIF-1α-independent pathways may also be involved in metabolic reprogramming and in conferring the different ability to adapt to the hypoxic environment of these two types of cells (Fig. 19).

4.1.2.6 Evaluation of mitochondrial membrane potential under severe hypoxia

In our previous studies, we demonstrated that IF_1 does not inhibit the ATP synthase activity in cancer cells unless the mitochondrial membrane potential is collapsed and the enzyme is hydrolysing ATP, as it occurs in normal ischemic cells.

Therefore, with the aim to investigate the potential protective role of IF_1 in cancer cells experiencing oxygen deprivation, we initially assessed whether the prolonged exposure to 0.1% O_2 was able to induce the mitochondrial membrane collapse required for the reversal of ATP synthase. The analysis of transmembrane potential in the two cell lines was performed after 24 and 48 hours of 0.1% O_2 exposure by loading cells with TMRM, a fluorescence probe that enters mitochondria in a $\Delta\Psi_m$-dependent manner.

As we can observe by flow cytometry analysis in Fig. 20A and B, 143B cells still maintained high levels of mitochondrial membrane potential after 48 hours of hypoxia with a slight increase in TMRM fluorescence compared to normoxia. Interestingly, the increase of $\Delta\Psi_m$ observed in 143B cells exposed to 0.1% O2 compared to normoxia confirms our previous $\Delta\Psi_m$ measurements performed in the same cell line under 0.5% O_2 [121] and may be explained by the slowdown of ETC activity due to the low oxygen availability.

Therefore, we concluded that 143B cells were able to preserve mitochondrial respiration activity and consequently the transmembrane potential even under severe and prolonged hypoxic conditions (0.1% O_2), thus excluding the activation of IF_1 inhibitory role under hypoxia.

In contrast, the severe oxygen deprivation induced in HCT116 cells a strong $\Delta\Psi_m$ reduction compared to normoxia already after 24 hours, suggesting that in colon cancer cells the hypoxic exposure inhibited the mitochondrial electron transport compromising OXPHOS activity. In conclusion, these results suggest that in HCT116, unlike in 143B cells, the hypoxic condition is able to induce the reversal of the ATP synthase, which is required to activate the IF_1 inhibitory role.

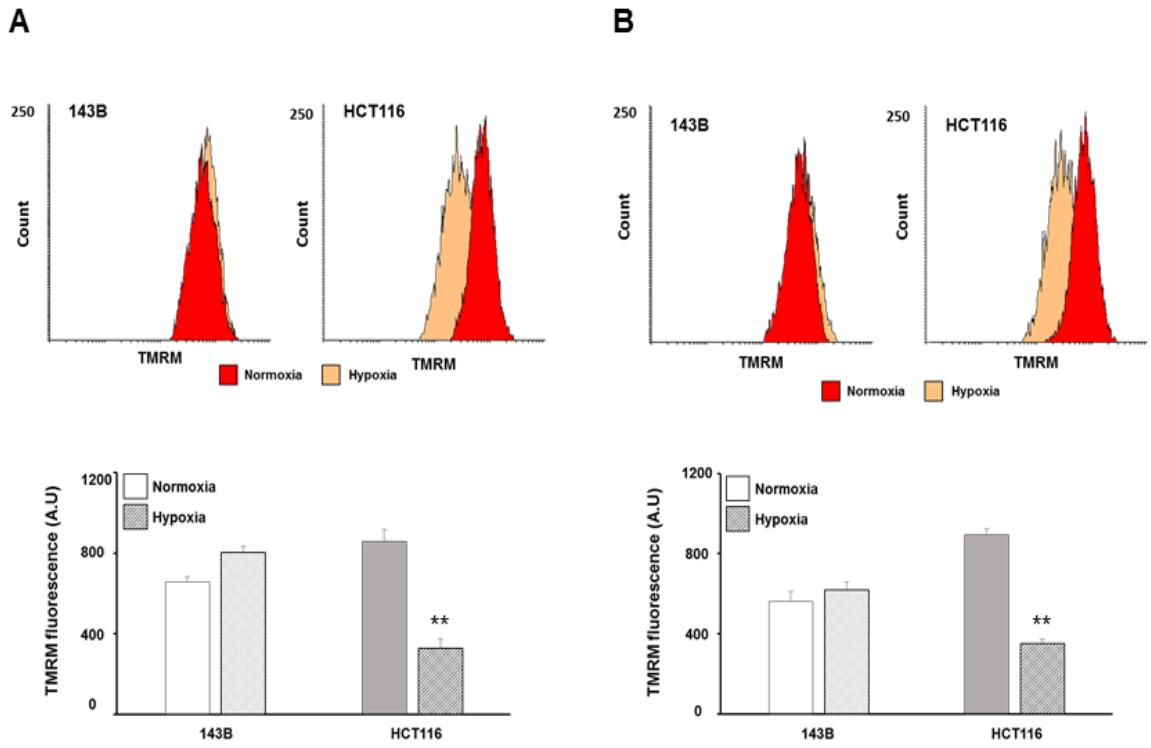

Fig. 20. Mitochondrial membrane potential under severe hypoxia exposure (0.1% O_2). *Fluorescence distribution and flow cytometry evaluation of TMRM-loaded cells cultured for 24 (A) and 48 (B) hours under normoxic and hypoxic conditions. **, $p<0.01$ indicates the statistical significance compared to normoxic data.*

4.2 Role of IF_1 in the bioenergetics of 143B and HCT116 cells experiencing oxygen deprivation

Energy supply is critical for tumour growth and the strict regulation of the ATP synthase activity by IF_1 may exert a selective advantage for cell survival and proliferation in hypoxia or anoxia, conditions frequently occurring in central zones of solid tumours.

The data so far collected showed that 143B cells with a lower IF_1/ATP synthase ratio compared to HCT116 cells have a high glycolytic capacity that allows them to increase the glycolytic flux and sustain cell proliferation under hypoxia. Furthermore, these cells can preserve their mitochondrial membrane potential even under prolonged exposure to severe hypoxia, thus excluding the activation of ATP synthase hydrolytic activity and the inhibitory function of IF_1.

In contrast, HCT116 cells, which express a significantly higher IF_1/ATP synthase ratio than 143B cells, are mainly dependent on OXPHOS for their energy production and show low adaptability to the hypoxic condition due to their limited glycolytic capacity, despite the main hypoxic factor HIF-1α being stabilized in these cells as much as in 143B cells.

Most of all, the exposure to severe hypoxia induces in HCT116 cells the collapse of mitochondrial membrane potential, which is required for the ATP hydrolytic function of the ATP synthase, thereby suggesting that in this cell line IF_1 may have a crucial role in preserving cell viability by avoiding energy depletion. Therefore, we went through these aspects by evaluating the role of IF_1 under hypoxia exposure assaying the bioenergetics changes of 143B and HCT116 cells upon stable silencing of IF_1.

4.2.1 Evaluation of IF_1 expression under oxygen deprivation (0.1% O_2)

In order to investigate the role of IF_1 in cancer cell adaptation to hypoxic condition we first assessed the protein levels under prolonged exposure to 0.1% O_2.

We therefore evaluated the IF_1 expression in both 143B and HCT116 cell lines after 48 hours of exposure to 0.1% O_2. Interestingly, the immunoblot analysis showed that the protein expression was equally increased in both cell lines, regardless of the

activation of its inhibitory effect on ATPase activity of ATP synthase, which we only observed in HCT116 cells. In particular, the semiquantitative analysis of IF_1 levels normalized to the ATP synthase d-subunit revealed an increase of about 50% of protein expression compared to the normoxic condition, thus suggesting that the overexpression of IF_1 levels may represent a common adaptive strategy of cancer cells in response to oxygen deprivation (Fig. 21).

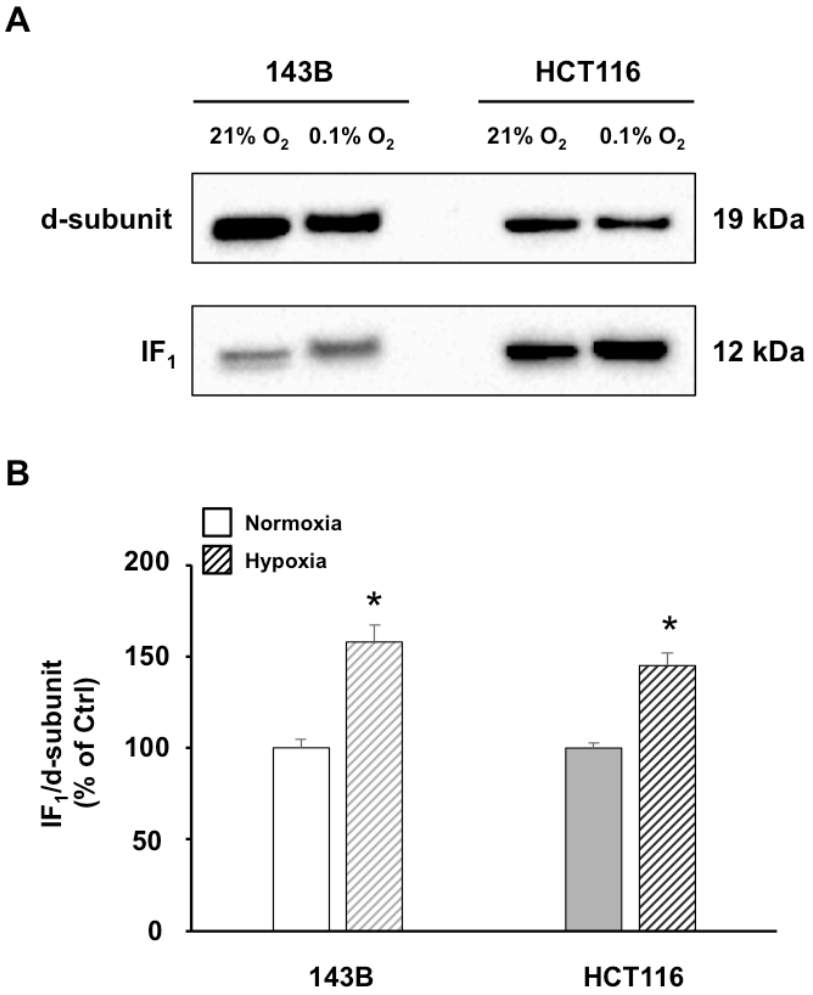

Fig. 21. ***The IF_1/ATP synthase ratio in hypoxic 143B and HCT116 cells***. *(A) 20 µg of 143B protein extract and 10 µg of HCT116 protein extract were analysed by SDS-PAGE followed by immunodetection of IF_1 and ATP synthase d-subunit in both normoxic and hypoxic conditions. (B) IF_1 to d-subunit band densitometric ratio of the two cancer cell lines after 48 hours of hypoxia exposure. *, $p < 0.05$ indicates the statistical significance compared to normoxia.*

4.2.2 Production of stable IF_1-silenced clones

To perform our investigations, we stably silenced IF_1 expression in both 143B and HCT116 cell lines.

As described in our previous study, the constitutive expression of fluorescent reporter protein negatively affects cell viability of GFP-positive clones cultured under hypoxic conditions [121]. In view of this evidence, the current study was performed by using scrambled and IF_1-silenced GFP-negative clones that were obtained transducing parental cell lines with retroviruses packaged with a pGFP-V-RS vector alternatively containing a scramble shRNA or an IF_1-shRNA. Indeed, as we can see in the map of the pGFP-V-RS vector, the GFP coding sequence is outside of the long terminal repeat regions and consequently cannot be packaged into the viral particles, thus not being expressed by the transduced cells (Fig. 22A).

Shortly, retroviruses were obtained by transfecting the Phoenix helper-free retrovirus producer cells with each vector and collecting the medium containing the assembled viral particles. Subsequently, the collected media was filtered and used to infect both 143B and HCT116 parental cell lines; 24 hours after infection, cells were observed with fluorescence microscopy to verify the absence of GFP expression. The infected cells were then split and cultured in the presence of puromycin to select cells with stable integration of the vector. Single scrambled and IF_1-silenced clones were finally obtained by limiting dilution and assayed for IF_1 expression.

In particular, the immunoblot analysis of IF_1 in both parental cells and derived clones revealed a notable reduction of expression in all the silenced clones with an average silencing efficiency of about 90%. Specifically, densitometric analysis of the bands revealed that clones E9 and C3, respectively derived from 143B and HCT116 cells, showed the best IF_1-knockdown. Furthermore, the IF_1 expression was periodically checked in selected clones by immunodetection to confirm the stable silencing of the protein over the time (Fig. 22B and C).

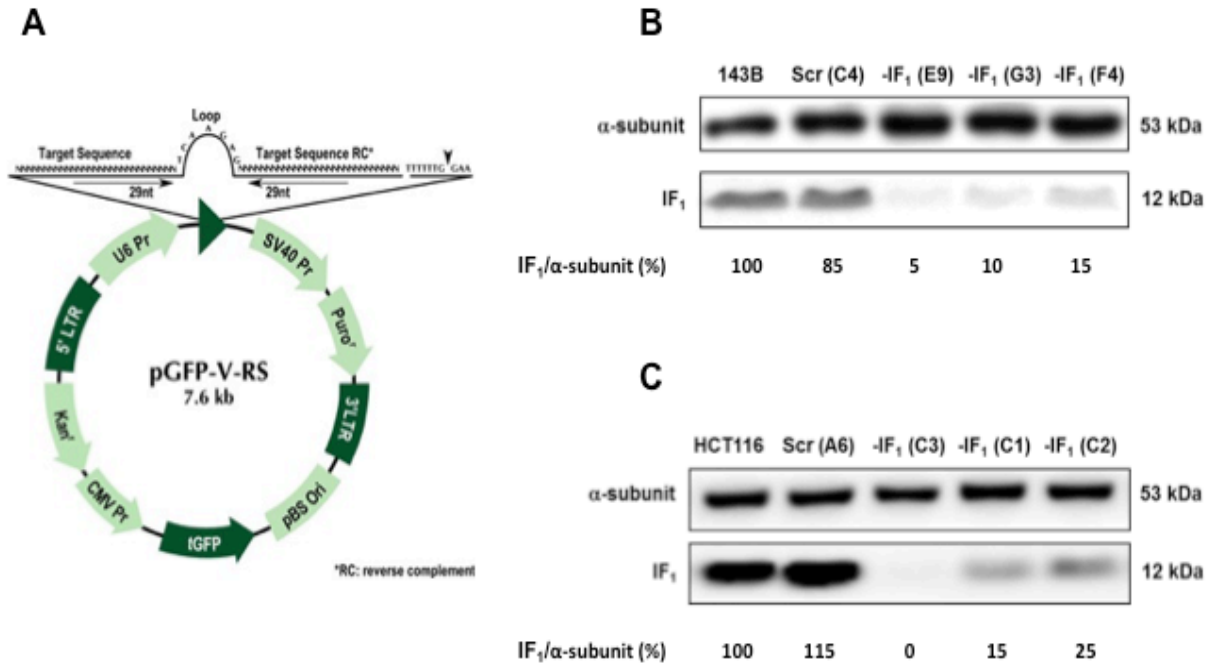

Fig. 22. Screening of GFP-negative clones stably silenced for IF_1. *(A) Map of the pGFP-VR vector. The cloning site alternatively contains the sequence for a scrambled control-shRNA or an IF_1-shRNA. (B) And (C) immunoblot analysis of IF_1 in 143B and HCT116 parental cells and in the respective derived-scrambled and IF_1-depleted clones. F_1F_0-ATPase α-subunit of each cclone was used as mitochondrial loading control. IF_1 to α-subunit band densitometric ratio was expressed as percentage of the parental cell lines ratio (bottom of the panel).*

4.2.3 Effect of IF_1 silencing on cell growth and survival under severe hypoxia (0.1% O_2)

To investigate the hypothesized protective role of IF_1 in cancer cells experiencing oxygen deprivation, the effects of severe hypoxia on growth and survival of IF_1-expressing and IF_1-silenced cells were examined in both 143B and HCT116 cell lines. Cancer cells were thus cultured in an Invivo2 hypoxic chamber with 0.1% O_2 by assessing their proliferation and viability after 24 and 48 hours of hypoxia exposure.
As previously observed, 143B cells after 48 hours of 0.1% O_2 exposure were viable and were still able to proliferate due to their adaptability to the hypoxic condition. Furthermore, as expected, no difference was observed in cellular viability and proliferation between IF_1-expressing osteosarcoma cells and IF_1-silenced cells, confirming that IF_1 does not play any role in promoting growth and survival of hypoxic cancer cells in the absence of mitochondrial membrane potential collapse (Fig. 23A and C).
In contrast, the role of IF_1 becomes crucial for HCT116 cells survival under prolonged hypoxia exposure, where we previously demonstrated that oxygen deprivation induced the mitochondrial depolarization. Indeed, as we can observe in Fig. 23 the presence of IF_1 enabled both HCT116 and scrambled cells to survive under prolonged exposure to hypoxia, whereas the IF_1-silencing induced the 65% of cellular death after 48 hours of hypoxia exposure in IF_1-depleted cells (Fig. 23C) that appear shrunk and bright under the microscope because of their release from the dish (Fig. 23B).

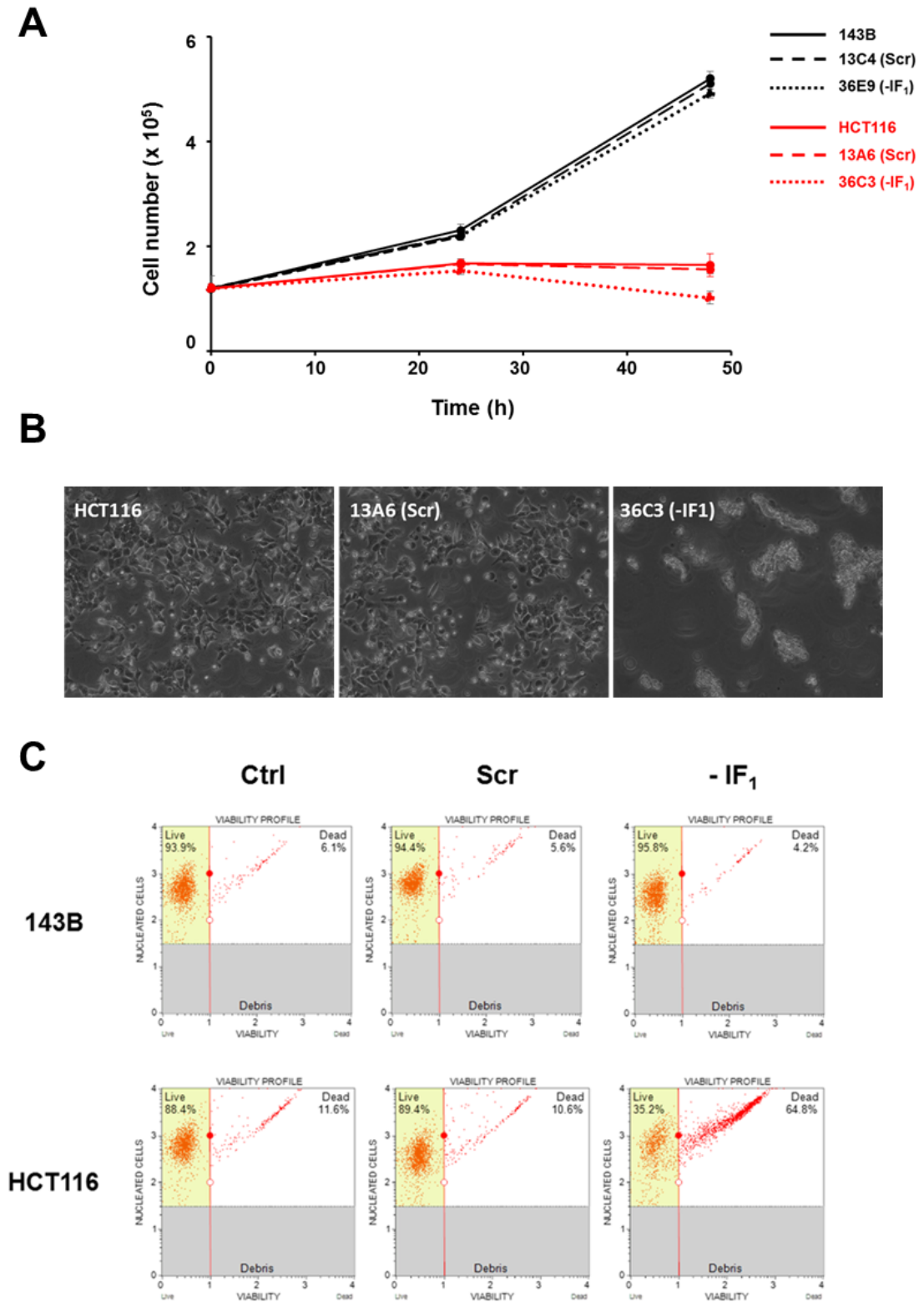

Fig. 23. Evaluation of growth and viability of both IF_1-expressing and IF_1-silenced cells up to 48 hours of hypoxia exposure. *(A) Cell growth of 143B (black) and HCT116 (red) parental cells and the respective derived-scrambled and IF_1-silenced clones under 0.1% O2. (B) Brighfield microscopy evaluation (magnification 10x) of HCT116 cells viability after 48 hours of culturing under severe hypoxia. (C) Representative cytometryc analysis of viability of both controls and IF_1-silenced cells exposed to 0.1% O_2 for 48 hours. Following the hypoxic exposure, cells were collected and viability was assayed by the MUSE count and Viability assay kit. Dot plots with red line marker providing data on live and dead cells are shown.*

4.2.4 Evaluation of mitochondrial membrane potential and ATP content in HCT116 cells and derived IF_1-silenced cells during severe hypoxia exposure (0.1% O_2)

The analyses of both transmembrane potential and ATP content were performed in HCT116 cells and IF_1-silenced derived cells to verify whether the previously observed role of IF_1 in promoting cell survival under prolonged exposure to 0.1% O_2 is due to its function of inhibitor of ATP hydrolytic activity of ATP synthase.

In detail, the evaluation of mitochondrial membrane potential was performed after 16 and 24 hours of exposure to 0.1% O_2 by staining hypoxic cells with fluorescent probe TMRM for 30 minutes at 37°C in either the absence or presence of oligomycin.

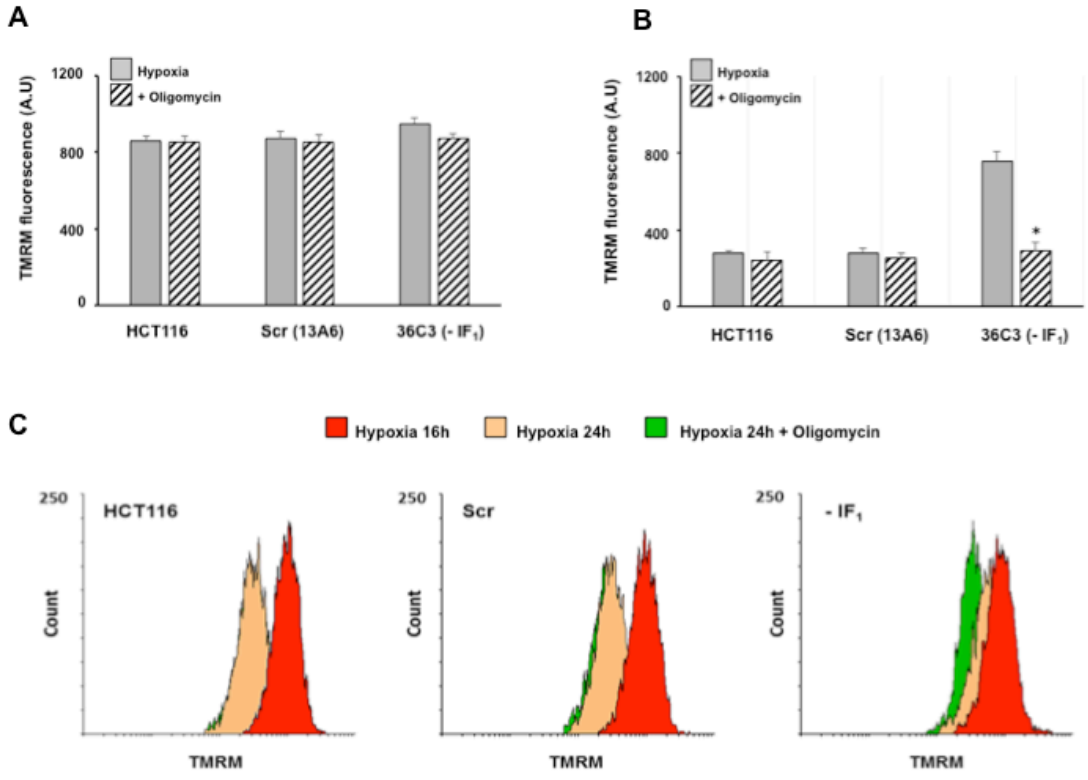

Fig. 24. Evaluation of mitochondrial membrane potential in controls and IF_1-silenced clones derived from HCT116 cells during prolonged hypoxia exposure. *Flow cytometry semiquantitative evaluation of the mitochondrial membrane potential of controls and IF_1-depleted colon cancer cells exposed to 0.1% O_2 for 16h (A) and 24h (B) in either the absence or presence of oligomycin. *, $p<0.05$ indicates the statistical significance compared to basal data. (C) Flow cytometry distribution of TMRM-loaded cells cultured for 16h and 24h under hypoxia. The distribution of TMRM loaded cells previously exposed to 24h of hypoxia upon the addition of oligomycin is also reported.*

The flow cytometry semiquantitative evaluation of $\Delta\Psi_m$ of both controls and IF_1-silenced cells showed that the collapse of mitochondrial membrane potential occurs between 16 and 24 hours of growth in the hypoxic chamber with 0.1 % O_2. Indeed, no differences were still observed in TMRM fluorescence mean values after 16 hours between controls and IF_1-silenced cells and no effect was observed on cellular $\Delta\Psi_m$ upon the addition of oligomycin (Fig. 25A and C). In contrast, prolonging the exposure to severe hypoxia up to 24 hours, we observed the $\Delta\Psi_m$ collapse in control cells, where IF_1 is reported to prevent the ATPase activity. Otherwise, IF_1-silenced cells were able to sustain the transmembrane potential due to the activation of ATP hydrolytic activity of ATP synthase. Indeed, upon the addition of oligomycin, the transmembrane potential of IF_1-silenced cells decreased to the level of controls, proving that it was previously sustained by ATPase activity at the expense of cytoplasmic ATP (Fig. 25B and C).

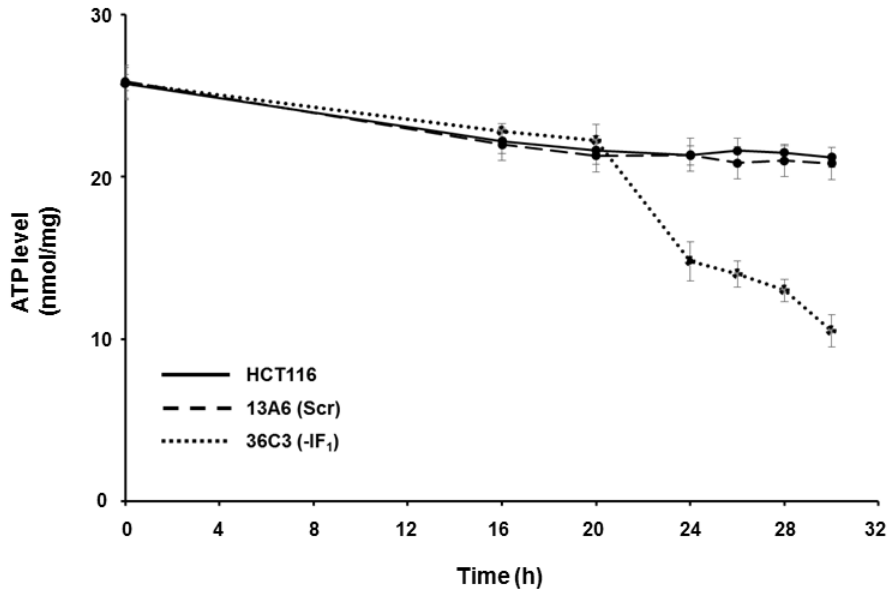

Fig.25. Cellular ATP levels during hypoxic exposure. *Intracellular ATP levels of HCT116 (solid line), along with HCT116 derived scrambled (dashed line) and IF1-silenced (dotted line) cells, was evaluated up to 30 hours of exposure to 0.1% O_2.*

To confirm this point, the analysis of intracellular ATP content of colon cancer cells and derived clones was performed over the time under hypoxia exposure.

Consistently, the evaluation of ATP levels did not highlight any difference in ATP

content between controls and IF_1-silenced cells up to 20 hours of exposure to 0.1% O_2, thus supporting our previous $\Delta\Psi_m$ data according to which no mitochondrial depolarization occurs during first 16 hours of hypoxia exposure. Subsequently, following the $\Delta\Psi_m$ collapse, a progressive decrease of ATP levels was observed only in IF_1-silenced cells due to the uncontrolled ATP hydrolysis promoted by ATP synthase (Fig. 25). Therefore, we demonstrated that cellular death observed in IF_1-silenced cells experiencing severe hypoxia was due to the progressive energy deprivation, highlighting the crucial role of IF_1 for HCT116 cell survival. Incidentally, a slight progressive decrease of ATP level was also observed in parental and scrambled hypoxic cells that reach a plateau after about 20 hours of hypoxia exposure. (Fig.25).

4.2.5 Evaluation of mitochondrial membrane potential and ATP content in 143B cells and derived IF_1-silenced cells under anoxia (0% O_2)

The analyses performed so far proved that the hypoxic condition used although severe was not sufficient to trigger the ATP hydrolytic activity of ATP synthase and activate the inhibitory function of IF_1 in osteosarcoma cells. Consequently, we could not highlight any protective role of IF_1 in 143B cells experiencing hypoxia, although we detected a significant increase of IF_1 expression in response to hypoxia exposure.
Therefore, with the aim to promote the reversal of ATP synthase and evaluate whether the IF_1 overexpression may represent a common strategy of cancer cells to protect themselves from energy wasting, we subsequently exposed 143B cells to the total oxygen deprivation, trying to reproduce the anoxic environment occurring in the most central zones of solid tumours.
The anoxic condition was generated by culturing cells in a tightly sealed glass jar in the presence of an oxygen absorber (FMT1000-ATCO). Furthermore, to avoid any possible oxygen contamination, the device was kept in the hypoxic workstation Ruskin INVIVO200 set at 0.1% oxygen tension. An oxygen sensor placed into the glass jar with cells revealed that the oxygen absorber removed all oxygen within 12-16 hours, thus establishing the anoxic condition. Therefore, the mitochondrial membrane potential and cellular ATP levels were measured in control and in IF_1-silenced cells after 20 hours of culturing in the glass jar. As shown in Fig. 26A and B, a strong decrease of $\Delta\Psi_m$ was observed in control cells (-60%) under anoxic conditions, proving that the complete absence of oxygen was needed to compromise the mitochondrial respiration in 143B cells. Otherwise, the mitochondrial membrane potential of IF_1-silenced cells appeared to be largely preserved, showing a reduction of 30% compared to the basal value. Conversely, in the presence of oligomycin the $\Delta\Psi_m$ -values were comparable in all cell analysed, suggesting that the transmembrane potential of IF_1-silenced cells was sustained by the reversal activity of ATP synthase that hydrolyses ATP. Accordingly, the analysis of ATP levels showed a larger ATP reduction of about 60% in IF_1-silenced cells than in control cells, where the ATP decrease was only 10%. Notably, when cells were cultured in presence of oligomycin, the ATP levels of both control and IF_1 silenced cells were similar, proving that the drop of ATP levels observed in the absence of oligomycin in IF_1 silenced cells was

due to the activation of the ATP hydrolytic activity of ATP synthase (Fig. 26C).

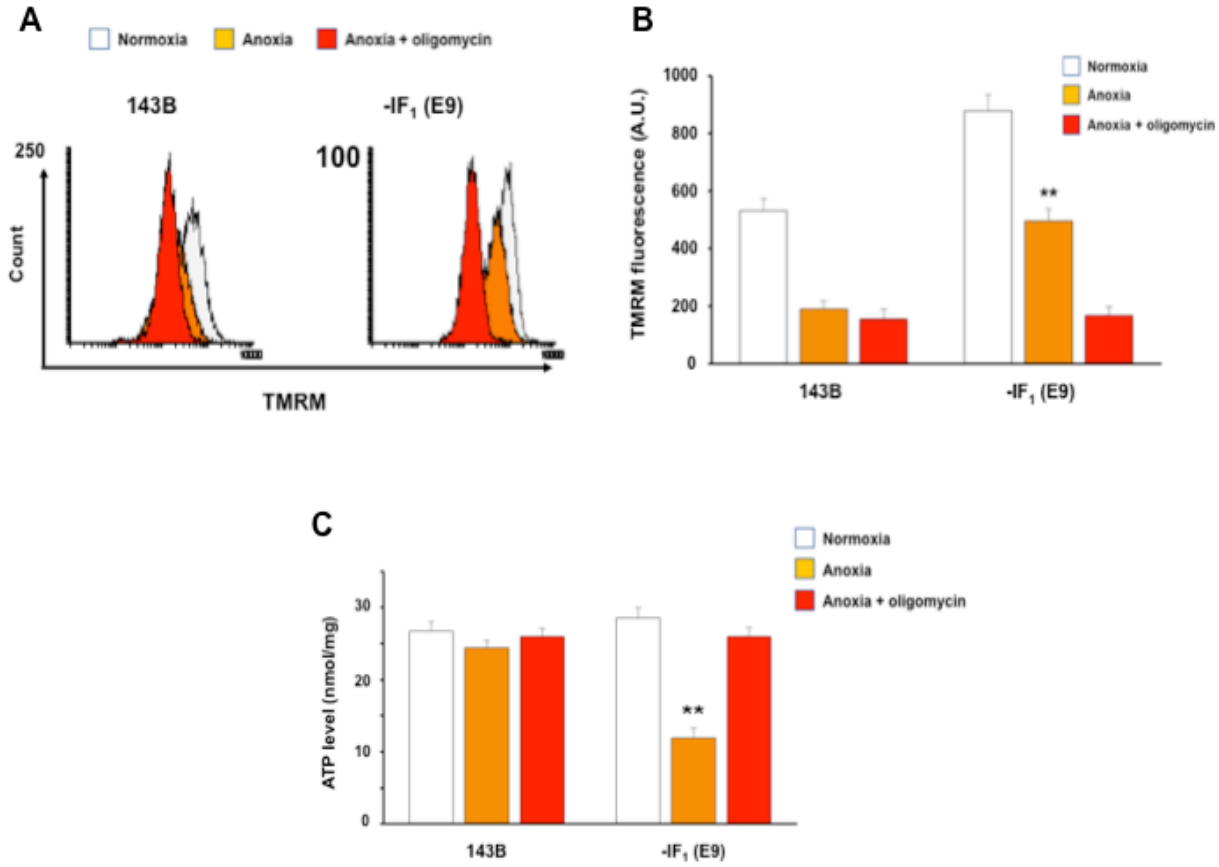

Fig.26. Mitochondrial membrane potential and intracellular ATP content measured in IF_1-expressing and IF_1-silenced osteosarcoma cells exposed to anoxia (0% O_2). *(A) Fluorescent distribution and (B) flow cytometry semiquantitative evaluation of TMRM-loaded cells upon normoxia and anoxia exposure (in the absence or presence of oligomycin). (C) Intracellular ATP levels expressed as nmol/mg of protein of both controls and IF_1-silenced osteosarcoma cells under normoxia, anoxia, and anoxia plus oligomycin addition. **, $p<0.01$ indicates the statistical significance of data compared to control.*

4.3 Comparison of IF_1 pro-survival effect in 143B and HCT116 cells with different bioenergetic phenotype

Taken together, our findings showed that the severe hypoxic condition induced mitochondrial depolarization activating the ATP hydrolytic activity of ATP synthase in HCT116 cells, thus highlighting the crucial role of IF_1 in promoting cell survival by preventing energy depletion. Therefore, we concluded that the high IF_1 expression observed in this OXPHOS-dependent tumour cell line is necessary to cope with oxygen limitation and prevent cellular death.

Otherwise, no mitochondrial depolarization occurs in the highly glycolytic 143B cells under prolonged exposure to severe hypoxia and no role of IF_1 was observed in cancer cell growth and survival. Subsequently, we demonstrated that the total absence of oxygen was required to induce the collapse of mitochondrial membrane potential in osteosarcoma cell line. Indeed, the analysis of $\Delta\Psi_m$ and ATP content upon anoxia exposure proved that IF_1 is able to modulate the ATP hydrolytic activity of ATP synthase preserving ATP level in 143B cells, as observed under hypoxic condition in HCT116 cells.

Therefore, we decided to continue our study with the aim to evaluate and compare the pro-survival effect of IF_1 in cancer cell lines characterized by different energy metabolism by exposing 143B and HCT116 cells under anoxia.

Because of technical limits previously encountered to reproduce anoxia by culturing 143B cells in glass jars, we decided to reproduce the anoxic environment by exposing both osteosarcoma and colon cancer cells to the uncoupler FCCP, able to induce the $\Delta\Psi_m$ collapse occurring in the absence of oxygen.

Consequently, we first verified the activation of the IF_1-inhibitory role under these new experimental conditions in both cell lines by measuring $\Delta\Psi_m$ and ATP levels.

The measurement of mitochondrial membrane potential was thus performed in cells exposed to 10 μM FCCP for 24 hours either in the presence or absence of oligomycin by loading cells with TMRM probe. As expected, the exposure to the uncoupler induced the $\Delta\Psi_m$ collapse in both 143B and HCT116 IF_1-expressing cells. In detail, the assessment of the fluorescence signal by flow cytometry revealed a 75 % reduction compared to normoxia in both 143B and HCT116 control cells, where IF_1 prevents the ATPase activity.

Otherwise, the reduction of TMRM fluorescence was less than 20 % in all IF_1-silenced cell types exposed to FCCP compared to the fluorescence value under basal conditions, indicating that IF_1-depleted cells were able to mainly preserve the transmembrane potential due to the activation of ATP hydrolytic activity of ATP

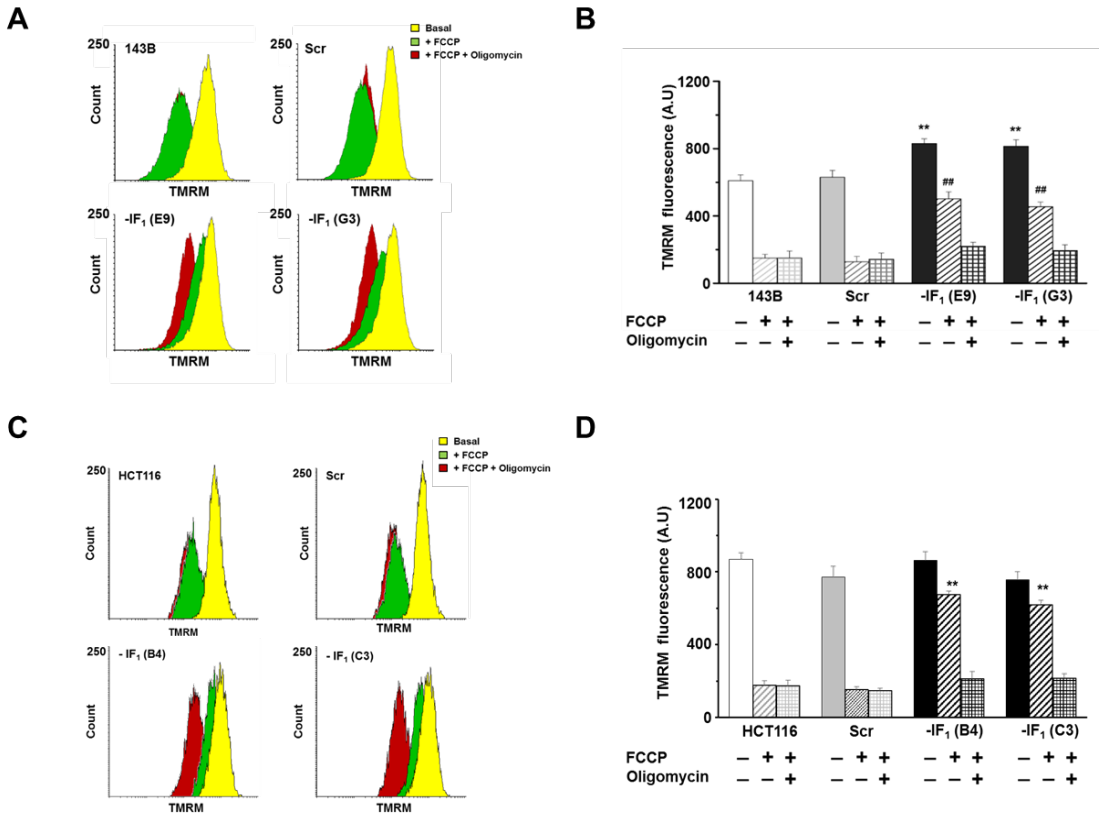

Fig. 27. Mitochondrial membrane potential in IF_1-expressing and IF_1-silenced after FCCP exposure. *Fluorescence distribution and flow cytometry semiquantitative evaluation of TMRM-loaded control and IF1-silenced cells derived from 143B (A and B) and HCT116 cells (C and D) cultured for 24h under basal conditions, in the presence of FCCP or FCCP plus oligomycin. ** and ##, $p<0.01$ indicates the statistical significance of data compared to controls.*

synthase. Indeed, when oligomycin was added with the uncoupler to inhibit the ATP synthase, the $\Delta\Psi_m$ of IF_1-silenced cells decreased reaching the value of controls (Fig.27). Accordingly, under the same experimental conditions, the steady state ATP levels were more reduced in uncoupled IF_1-silenced cells of both cell lines compared to the uncoupled controls due to the ATP consumption promoted by ATP synthase in the absence of IF_1. Consistent with these findings, the presence of oligomycin, which prevents the ATP synthase hydrolytic activity, preserved the ATP levels of both uncoupled IF_1-silenced cells that showed the same ATP content of uncoupled control

cells. Notably, the two parental cell lines showed a different percentage of ATP decrease in the presence of FCCP. Indeed, the ATP level was about 20% and 65% reduced in 143B, and HCT116 cells, respectively, confirming that the contribution of oxidative phosphorylation to total ATP production is different between the two cancer cell lines (Fig.28).

In conclusion, the analyses of $\Delta\Psi_m$ and ATP levels in both 143B and HCT116 uncoupled cells confirmed the role of IF_1 in protecting cells from ATP dissipation by the inhibition of ATP-hydrolytic activity of ATP synthase even under anoxia mimicking conditions.

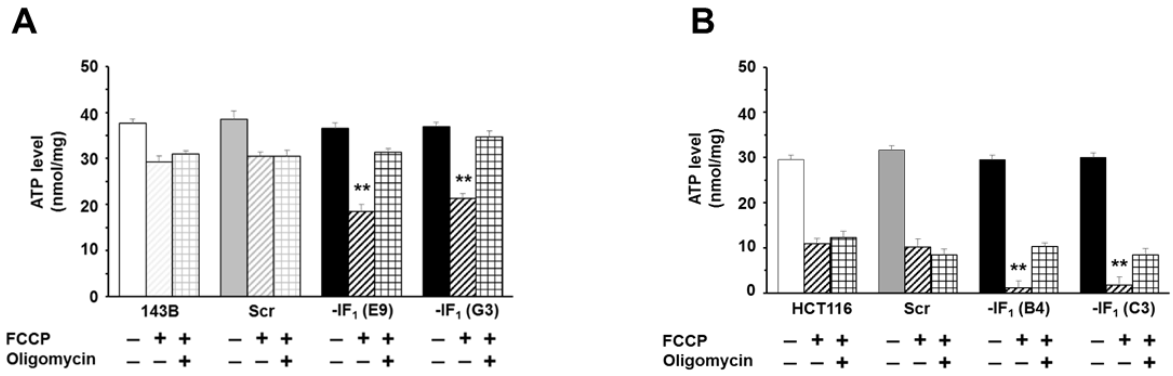

Fig. 28. Steady state ATP levels in IF_1-expressing and IF_1-silenced cells after FCCP exposure. *Intracellular ATP level, expressed as nmol/mg of protein, of both controls and IF_1-silenced cells derived from 143B (A) and HCT116 cells (B) cultured for 24h under basal conditions, in the presence of FCCP or FCCP plus oligomycin. **, $p< 0.01$ indicates the statistical significance of data upon FCCP compared to controls.*

Subsequently, to assess whether the protective role of IF_1 on growth and survival of anoxic cells depends on cancer cell energy metabolism, we evaluated the effect of IF_1 silencing on cell viability and proliferation of both 143B and HCT116 cells cultured in the presence of 10 μM FCCP for 24 hours.

Fig. 29 shows the assessment of cell growth and viability in both parental cell lines and derived clones under anoxia-mimicking conditions. In detail, as previously observed by culturing cells upon prolonged hypoxia, 143B parental cells with high glycolytic capacity were able to growth even under anoxic conditions, whereas the

HCT116 OXPHOS-dependent cells could not proliferate without OXPHOS energetic contribution due to their low glycolytic capacity (Fig.29A and B).

Interestingly, the IF_1-silencing had a different effect on survival of IF_1 silenced clones derived from 143B and HCT116 cells. In particular, the IF_1-silencing inhibited proliferation without affecting cell survival in osteosarcoma cells (Fig. 29C, top panels). Otherwise, IF_1 depletion induced 55% of cell death in HCT116 cell lines after 24 hours of anoxia exposure (Fig. 29D, top panels).

Therefore, we proposed that the energetic advantage conferred by IF_1 in preventing the ATP hydrolytic activity of ATP synthase has a different effect on cancer cell depending on the energy metabolism of each cell line. In particular, IF_1 enabled the glycolytic cell line to keep proliferating also in anoxia, while it is crucial for the survival of the OXPHOS-dependent cell line.

Furthermore, considering the promising use of glycolysis inhibitors against cancer cells under oxygen deprivation conditions, we also evaluated the combined effect of IF_1-silencing and glycolysis inhibition on cancer cell growth and survival under the above experimental conditions.

As reported in Fig. 29A and B, under normoxic conditions, the treatment with the glycolysis inhibitor 3-bromopyruvate for 24 hours induced a significant decrease of the proliferation rate in 143B cells and all derived clones (-35% compared to control condition), whereas did not significantly affect cellular growth of HCT116 cells, confirming a high dependency on glycolysis as energy supply pathway for cellular growth of 143B cells. Interestingly, we observed that in osteosarcoma cells under anoxic conditions, the energy deprivation induced by glycolysis inhibition in the presence of 80 μM 3BP repressed cell proliferation in IF_1-expressing cells and sensitized IF_1-silenced cells to death with about 45% of dead cells after 24 hours anoxic exposure (Fig. 29C, bottom panels). Conversely, in HCT116 cells, whose proliferation and energy balance were mainly affected by the exposure to the uncoupler (Fig. 29D, top panels; about 50% of cell death after 24 hours), the inhibition of glycolysis did not significantly affect cell survival neither in control cells nor in derived IF_1-silenced clones (Fig. 29D, bottom panels).

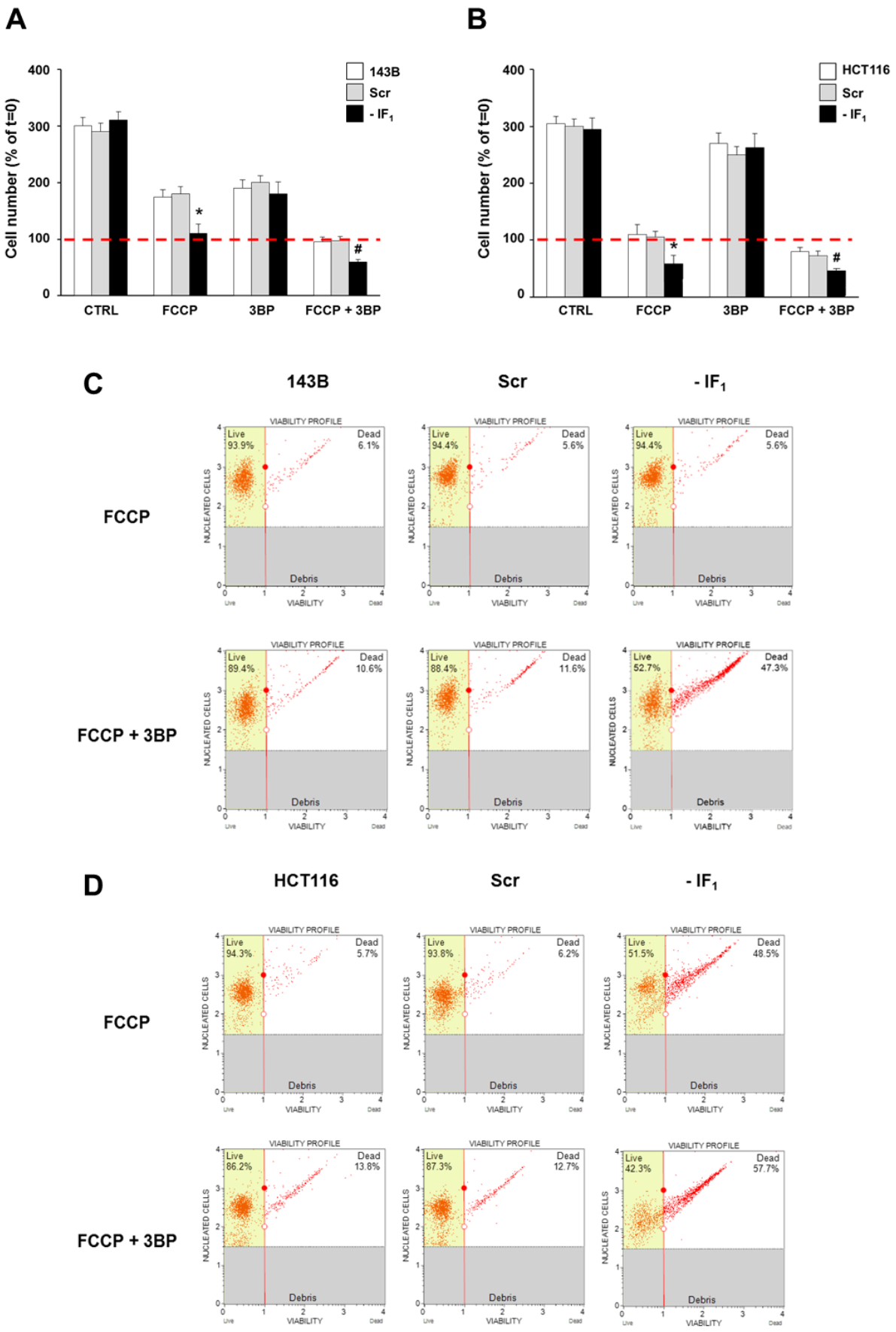

Fig. 29. Effect of IF_1-silencing on cellular growth and survival under both FCCP exposure and glycolysis inhibition in 143B and HCT116 cells. *Evaluation of cellular growth after 24 hours of exposure to 10 μM FCCP, 80 μM 3BP and 10 μM FCCP plus 80 μM 3BP in both IF1-expressing and IF1-silenced cells derived from 143B (A) and HCT116 (B) cells. * and #, $p<0.05$ indicates a statistically significant change between IF_1-silenced and controls cells. Viability profile assessed by the MUSE Count and viability assay kit of both controls and IF_1-silenced 143B (C) and HCT116 (D) cells exposed to 10 μM FCCP and 10 μM FCCP plus 80 μM 3BP for 24 hours.*

To conclude, our data indicated that reducing the overexpression of IF_1 in tumours deprives cancer cells experiencing oxygen deprivation of the energy useful for their growth or survival depending on their energy metabolism. Therefore, from a therapeutic perspective, these results may provide the basis to develop appropriate therapeutic approaches for each type of tumour based either only on IF_1-silencing or on the combined effect of IF_1-silencing and glycolysis inhibition.

4.4 Involvement of IF_1 in counteracting mitochondrial mediated-apoptotic process

The data showed so far highlighted that IF_1 overexpression in tumours is crucial when cancer cells experience oxygen deprivation, since IF_1 can promote their growth or survival limiting cellular energy waste by inhibiting the ATPase activity.

Although the inhibition of the ATPase activity by IF_1 under the above hypoxic/anoxic conditions provides an energetic advantage to cells, concurrently it leads to a prolonged collapse of mitochondrial membrane potential, a detrimental event for cellular homeostasis.

In particular, it is well known that mitochondrial depolarization may either trigger cytochrome c release-mediated apoptosis or otherwise the selective degradation of dysfunctional depolarized mitochondria by autophagy (mitophagy) to escape apoptosis. Considering that our results on 143B and HCT116 cells showed that IF_1 expressing cells can survive without showing cellular death, we supposed that the activation of mitophagy could be the mechanism used by cancer cells overexpressing IF_1 to avoid the apoptotic death. Therefore, to assess this point we continued our studies under oxygen deprivation by evaluating mitochondrial turnover and mitochondrial content in both IF_1 expressing and IF_1 silenced cells.

4.4.1 Assessment of mitophagic process

The maintenance of a healthy and functional mitochondrial network in response to stress conditions such as oxygen deprivation is critical for cellular homeostasis and

survival. Cells thus evolved a mechanism of quality control to preserve the mitochondrial system by removing damaged mitochondria and stimulating their biogenesis.

Therefore, we investigated the involvement of IF_1 in quality control mechanisms by first evaluating the activation of mitophagic process under the above anoxia-mimicking conditions. To this aim, we reproduced the mitochondrial depolarization occurring in anoxia by exposing both IF_1 expressing osteosarcoma cells and IF_1 silenced clones for 24 hours in the presence of FCCP. Hence, we assessed the protein expression of positive regulators of the mitophagic process including PINK1, whose accumulation in the outer mitochondrial membrane upon $\Delta\Psi_m$ collapse triggers mitophagy, and BNIP3, whose homodimerization is reported to drive mitochondria degradation, especially under hypoxic conditions [141].

The immunodetection and the semi-quantitative densitometric analysis reported in Fig. 30 showed that the expression of both mitophagy markers increases in IF_1 expressing cells after 24 hours of FCCP exposure, whereas PINK1 and BNIP3 levels decrease in IF_1-silenced clones compared to the basal condition, indicating that the exposure to FCCP activated mitophagy in IF_1-expressing cells and inhibited mitochondrial degradation in IF_1-silenced cells. In detail, PINK1 levels were about 50% higher in IF_1-expressing cells exposed to FCCP compared to the basal value, whereas the IF_1-silenced clones showed a 35% reduction of PINK1 expression under anoxia mimicking condition compared to the normoxic cells (Fig. 30A). Consistently, we also observed the augmented expression of BNIP3 dimeric form in uncoupled IF_1 expressing cells compared to their basal values being the percentage increase about 20% and 70% in 143B and derived scrambled cells, respectively.

Otherwise, IF_1-Knockdown cells displayed a 40% decrease of BNIP3 dimeric form compared to the basal condition (Fig. 30B).

In addition, the activation of mitophagy observed in uncoupled IF_1-expressing cells by PINK1 and BNIP3 immunodetection was also proved evaluating the sequestration of mitochondria within the autophagosome by using fluorescence microscopy. For this purpose, 143B osteosarcoma clones stably-expressing mitochondrially targeted red fluorescent probe, previously selected and characterized in our laboratory [133], were transiently transfected with a plasmid expressing a yellow fluorescent protein tagged LC3 to label the autophagomsome.

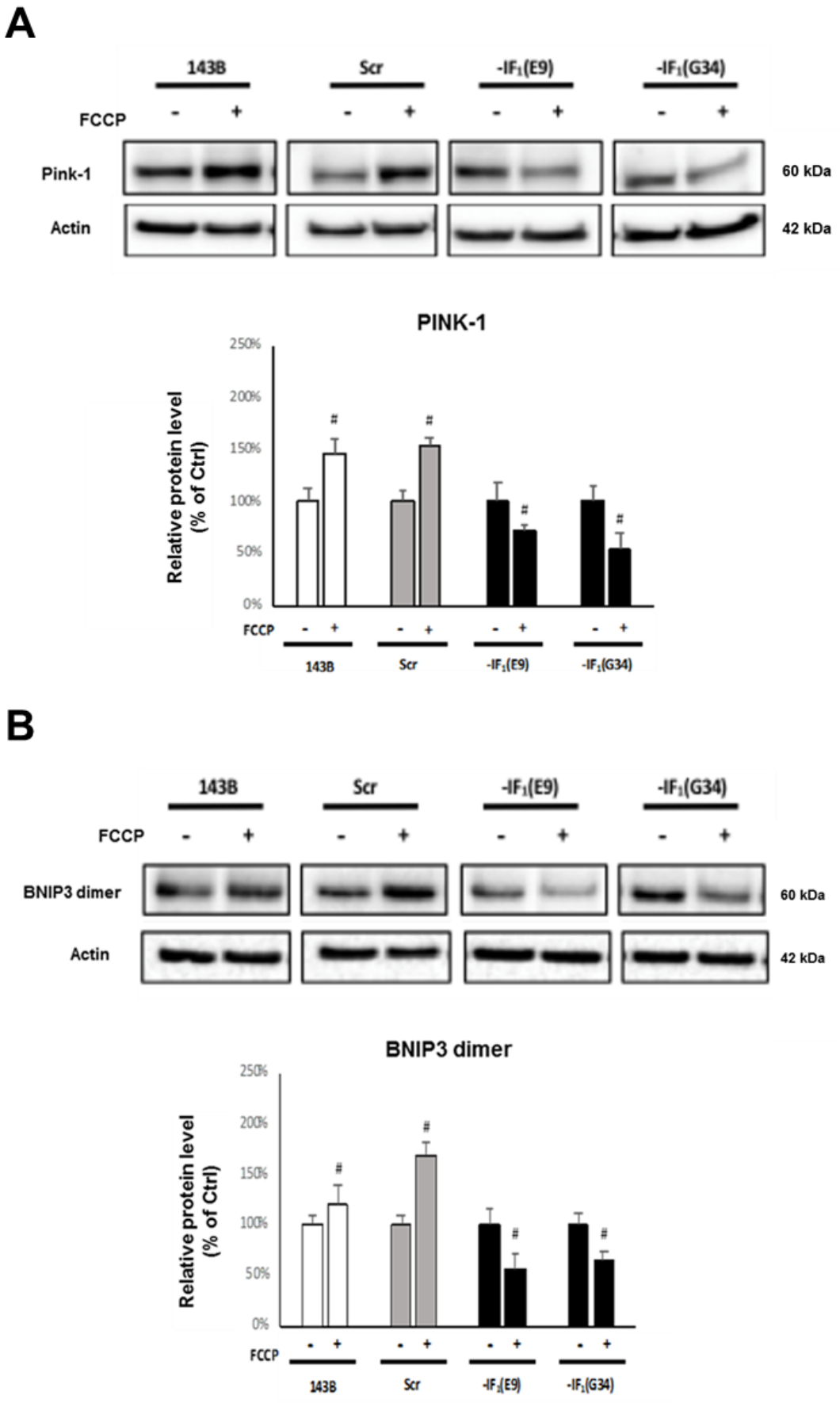

Fig. 30. Immunodetection of mitophagy markers under anoxia mimicking conditions in both IF_1-expressing and IF_1-silenced 143B cells. *Representative immunodetection and semiquantitative densitometric analysis of PINK1 (A) and BNIP3 dimer (B) in both control and FCCP-treated cells for 24h. Densitometric values were normalized to the actin content and expressed as percentage of untreated controls. #, $p<0.05$ indicates the statistical significance of data compared to controls.*

Hence, the colocalization of mitochondria and the autophagosomes was assessed under basal conditions, after 24 hours of FCCP treatment, and after 24 hours of exposure to deferoxamine, used as a positive control of mitophagy activation.

Representative fluorescence images of cells expressing mtRFP and YFP-LC3 were thus reported in Fig. 31.

In detail, Fig 31A showed that the basal rate of mtRFP:YFP-LC3 colocalization events were comparable between IF_1-expressing and IF_1-silenced cells, as demonstrated by the same colocalization signal observed by merging the mtRFP and YFP fluorescence. As observed in Fig. 31B, both controls and IF_1-silenced cells displayed a substantial increase of colocalization signal compared to the basal condition after 24 hours of deferoxamine exposure, proving that all cells were able to respond to mitophagic stimuli. Finally, Fig 31C showed that in IF_1-expressing cells the prolonged exposure to FCCP promoted the sequestration of mitochondria within autophagosomes displaying a strong increase in mtRFP:YFP-LC3 colocalization signal compared to normoxia. Conversely, in IF_1-silenced cells the LC3 signal was widespread in the cytosol without any colocalization of the two fluorescence probes, indicating the absence of mitophagic events.

Overall, these data confirmed that the prolonged exposure to anoxia mimicking conditions promoted the activation of mitophagic process in IF_1-expressing cells, while the same treatment inhibited the mitochondrial degradation in IF_1-silenced cells that showed a reduction of the basal mitophagy rate.

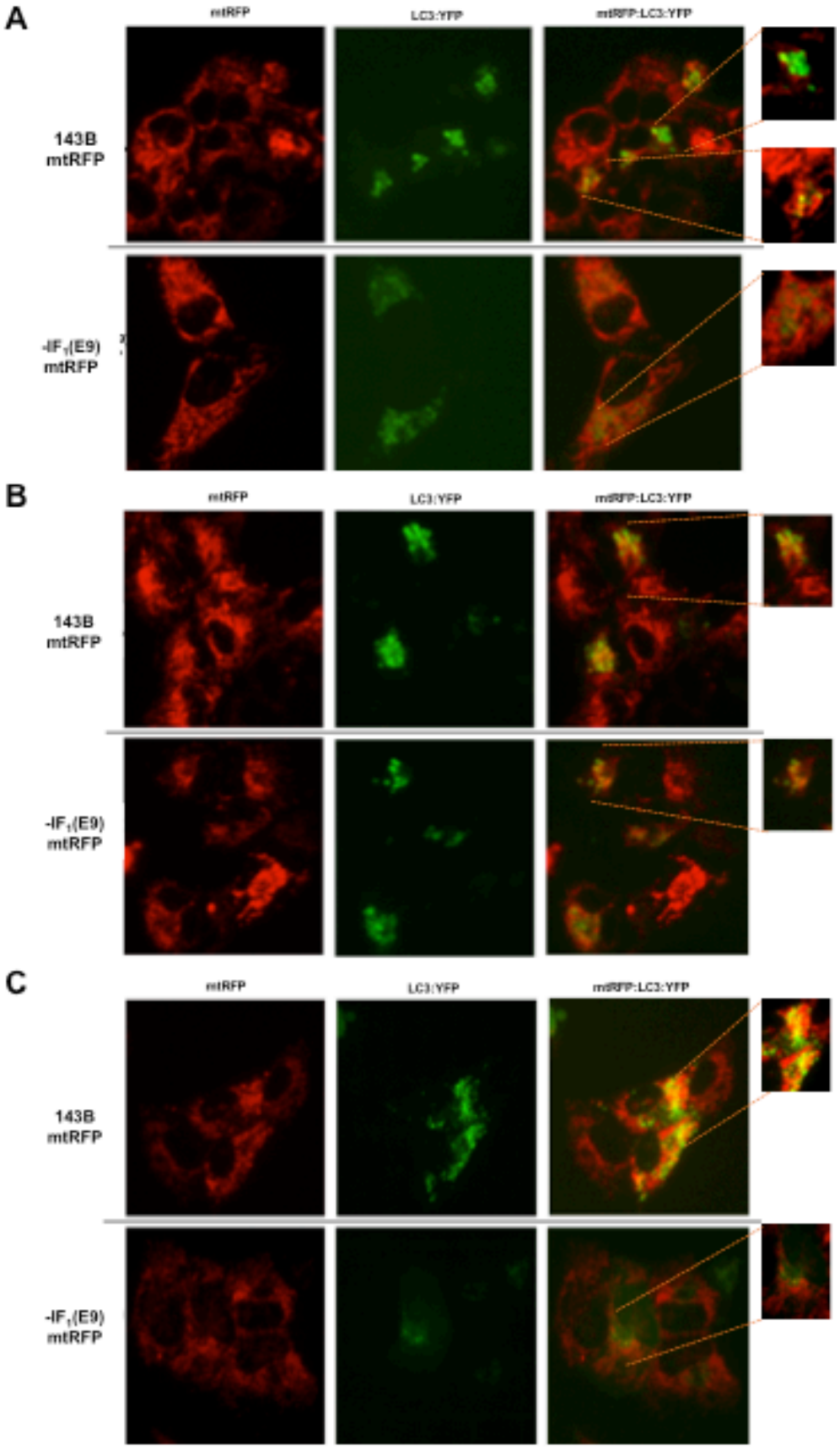

Fig. 31. Mitophagy activation assessment by evaluating the colocalization of mtRFP and LC3-YFP fluorescence in both IF_1-expressing and IF_1-silenced 143B cells under anoxia mimicking conditions. *Representative fluorescence images (Magnification 60x) under normal growing condition (A), after 24 hours of deferoxamine exposure (B) and after a 24-hour treatment with FCCP (C).*

4.4.2 Mitochondrial mass evaluation

Based on these latter results, we subsequently evaluated the impact of the different mitophagy rate observed in IF_1-expressing and IF_1-silenced cells under anoxia mimicking conditions on the mitochondrial content.

A first assessment of the mitochondrial mass was performed by analysing osteosarcoma clones stably expressing the mitochondria-targeted red fluorescence protein. After exposing cells to FCCP for 24 hours, fluorescence microscopy images were acquired and the fluorescence signal was then assessed by flow cytometry. Unexpectedly, no significant change of the fluorescence value was detected in both IF_1-expressing and IF_1-silenced cells cultured for 24 hours under uncoupling conditions compared to the basal fluorescence value, showing no change of mitochondrial mass (Fig.32).

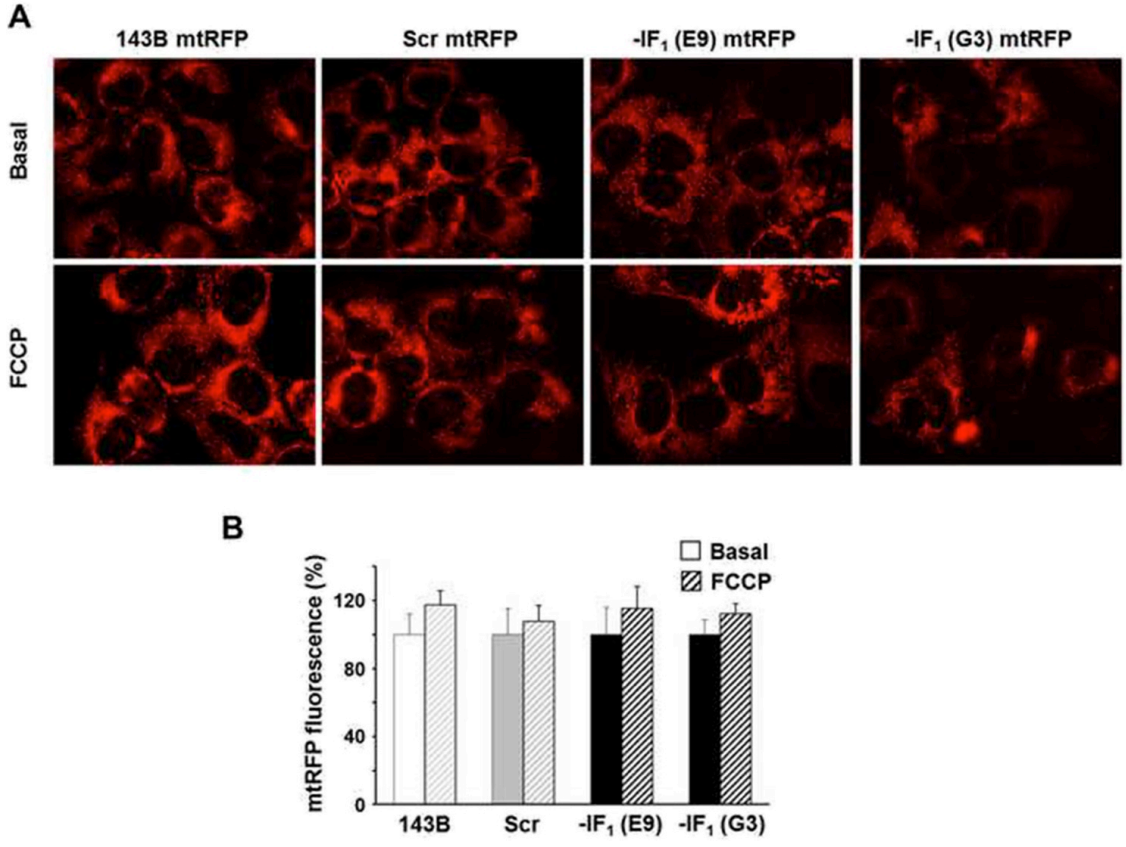

Fig. 32. Mitochondrial mass evaluation by fluorescence microscopy of mtRFP-143B cells under anoxia mimicking conditions. *Fluorescence images (magnification 40x) (A) and flow cytometry analysis (B) of both mtRFP-expressing controls and IF_1-silenced 143B-derived cells cultured for 24 hours in the absence or presence of FCCP.*

To validate this data, the mitochondrial content was also assessed through the immunodetection of TOMM20 and VDAC1 proteins, widely known as markers of mitochondrial mass. Consistent with the previous result, the immunodetection and the semiquantitative densitometric analysis confirmed that no variation of mitochondrial mass occurred after 24 hours of FCCP exposure neither in the presence nor in the absence of IF_1, indicating that both IF_1 expressing and IF_1 silenced cells were able to preserve the mitochondrial mass regardless of their different mitophagy rate (Fig. 33).

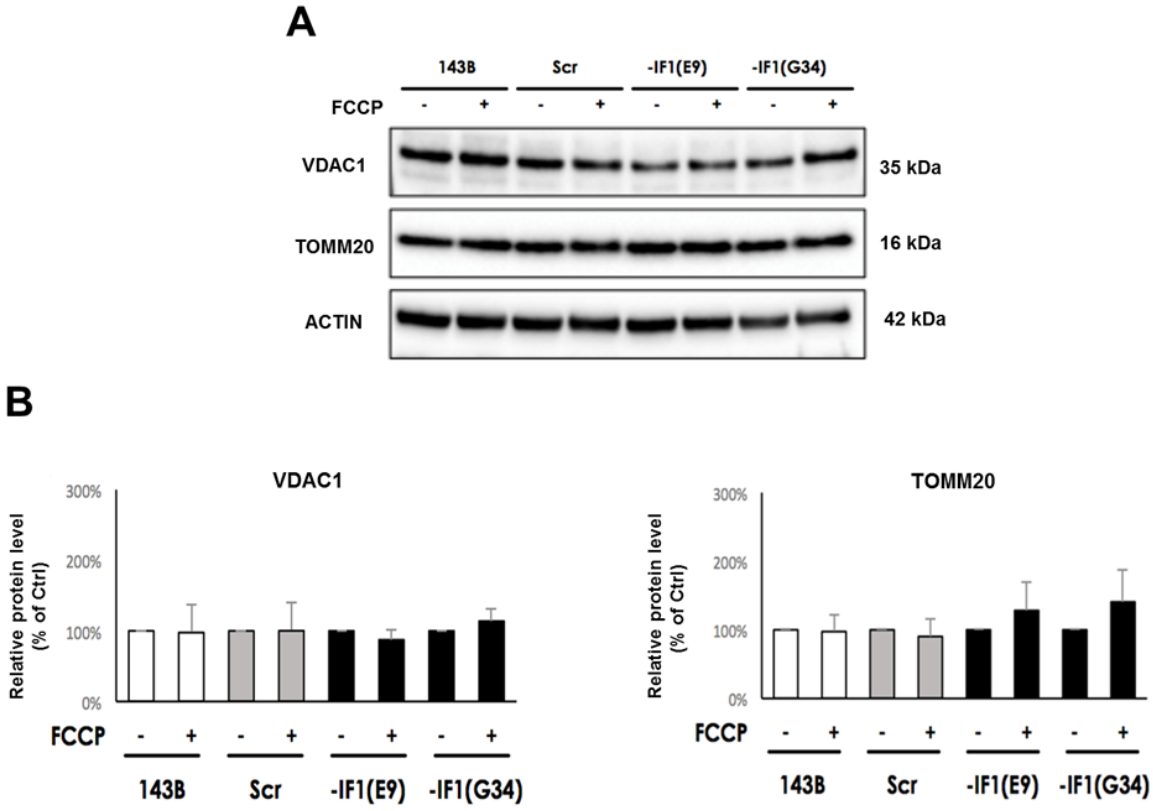

Fig. 33. Immunodetection of mitochondrial mass markers in both IF_1-expressing and IF_1-silenced 143B cells under anoxia mimicking conditions. *Representative immunodetection (A) and semiquantitative densitometric analysis of VDAC1 and TOMM20 (B) in both control and FCCP-treated cells for 24h. Densitometric values were normalized to the actin content and expressed as percentage of untreated controls.*

4.4.3 Evaluation of mitochondrial biogenesis

Considering that the mitochondrial content depends on a proper balance between mitochondrial degradation and mitochondrial biogenesis, the rate of mitochondrial biogenesis must be also taken into account to properly interpret the unexpected preservation of mitochondrial mass observed under anoxia mimicking conditions. Therefore, the assessment of mitochondrial biogenesis was performed by protein immunodetection of PGC-1α, the transcriptional co-activator of the mitochondria biogenesis genes, and its positive regulator SIRT1 in both IF_1-expressing and IF_1-silenced cells after 24 hours of FCCP exposure.

As we can observe in Fig. 34, the protein immunodetection revealed a significant increase of both biogenesis markers in IF_1-expressing cells. In particular, we observed a 30 % increase of SIRT1 expression in both control and scrambled cells compared to basal levels and an increase of PGC-1α of about 50% and 80% in control and scrambled cells, respectively. Otherwise, the expression level of both proteins upon FCCP was reduced in IF_1-knockdown clones of about 35% compared to the basal condition, suggesting the inhibition of mitochondrial biogenesis.

Therefore, taking our data into account, we concluded that IF_1-promotes mitochondrial mass preservation by the activation of both mitophagy and mitochondrial biogenesis in order to replace depolarized mitochondria. Conversely, in the absence of IF_1, the mitochondrial membrane potential preservation by ATP hydrolysis may act as a signal for mitochondrial mass maintenance and thus neither mitophagy nor biogenesis is stimulated.

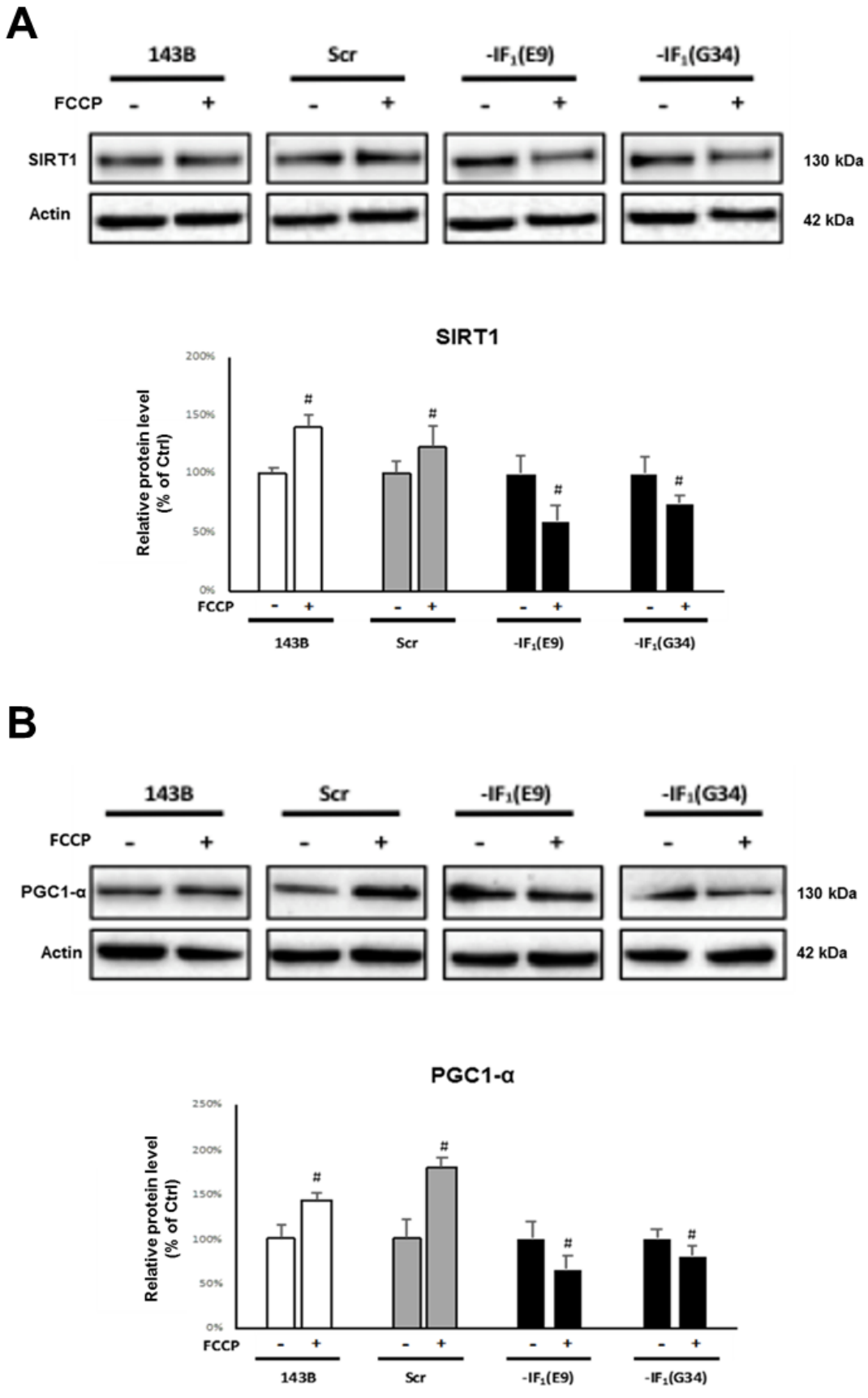

Fig. 34 ***Immunodetection of mitophagy markers under anoxia mimicking conditions in both IF$_1$-expressing and IF$_1$-silenced 143B cells.*** *Representative immunodetection and semiquantitative densitometric analysis of SIRT1 (A) and PGC1-α (B) in both control and FCCP-treated cells for 24h. Densitometric values were normalized to the actin content and expressed as percentage of untreated controls. #, $p<0.05$ indicates the statistical significance of data compared to controls.*

5. DISCUSSION AND CONCLUSIONS

Cancer tissues show great heterogeneity of energy metabolism that is the result of metabolic reprogramming strategies occurring during tumorigenesis. Cancer metabolic reprogramming is very extensive and it depends on the metabolic features of tissues of origin and tumour microenvironment. This reprogramming process provides tumours with an increased metabolic flexibility that allows them to meet the high energy demand needed to survive and proliferate even under environmental stress conditions, such as lack of nutrients or oxygen deprivation. Therefore, targeting energy metabolism of tumours has become an important area of research in cancer biology.

Exploiting the differences between normal and cancer cell metabolism has thus turned out to be an intriguing strategy to identify molecular targets for cancer therapy. In this context, among proteins involved in the energy metabolism, the endogenous inhibitor protein of the mitochondrial F_1F_o-ATPase, IF_1, has raised interest in oncology research as an upregulated protein in solid tumours compared to normal tissues.

Physiologically, IF_1 is ubiquitously expressed in mammalian tissues where it preserves cellular energy when the mitochondrial function is compromised by inhibiting the ATP hydrolytic activity of ATP synthase triggered by the collapse of mitochondrial membrane potential.

The most common injury leading to respiration impairment and the consequent collapse of transmembrane potential is the oxygen deprivation. Indeed, normal cells may experience lack of oxygen both under pathological conditions (e.g. ischemia) and physiologically due to transient episodes of compromised O_2 availability. Under these conditions, the ATP synthase, as a reversible nanomotor, works in reverse hydrolysing ATP to obtain the energy needed to restore the $\Delta\Psi_m$, whose preservation is essential for all cellular functions. Nevertheless, the uncontrolled ATP hydrolysis would be deleterious to the cells and is tightly regulated by IF_1, which limits energy dissipation and protects cells from death. Accordingly, IF_1 has been widely reported to be essential to prevent the irreversible necrotic damage in myocardial tissue where the ATP synthase contributes 90% of total ATP, whereas glycolysis is unable to satisfy

the high energy demand. Interestingly, myocardium is one of the most highly IF_1-expressing tissues. Indeed, despite its ubiquitous expression, IF_1 levels widely vary in human tissues, with the highest expression in high-energy-demanding tissues (e.g. heart, liver, and kidney) and a negligible expression in other ones including breast, colon, ovary, and lung. High levels of IF_1 are also reported in several solid tumours derived from tissues with negligible IF_1 expression. Notably, the overexpression of IF_1 in these tumours, such as gliomas and lung, liver, bladder, and stomach carcinomas, has also been correlated with advanced clinical stage and poor prognosis, thus pointing out the potential of the protein both as a prognostic marker and a therapeutic target [73-77].

In view of the above, an increasing number of studies attempts to understand the reasons for IF_1 overexpression in tumours mainly investigating the mechanisms by which IF_1 regulates the activity of its physiological target, the ATP synthase, and the energy metabolism in cancer cells.

In this regard, we previously demonstrated that IF_1 exerts its regulatory function against the ATP synthase activity in cancer cells only when the enzyme hydrolyses ATP following mitochondrial depolarization. Indeed, we proved that in uncoupled osteosarcoma cells the ATPase-inhibitory function of IF_1 modulates cancer bioenergetics allowing a total preservation of the cellular energy, thus suggesting that IF_1 overexpression might exert a selective advantage for tumour cell survival and proliferation [121]. Consequently, we asked ourselves whether IF_1 exerted the same action in all the tumour cells, whatever their bioenergetics. Hence, these questions prompted us to deeply study the involvement of this protein in the regulation of tumour energy metabolism when oxygen supply declines, as it occurs in solid tumours where oxygen levels vary from the perivascular regions to the anoxic necrotic areas.

In particular, the study presented herein was addressed to investigate the role of IF_1 in cancer cell survival and proliferation under oxygen deprivation in relation to the bioenergetic profile of each tumour and the level of IF_1 expression.

To this aim, the investigations were conducted in two cell lines derived from solid tumours, the osteosarcoma 143B and the colon carcinoma HCT116 cell lines expressing different levels of IF_1 and displaying different bioenergetic phenotypes.

Specifically, our analyses of IF_1 expression and bioenergetic profile characterization revealed that osteosarcoma cells, showing a lower IF_1/ATP synthase ratio compared to

HCT116 cells, are characterized by a high glycolytic capacity and are capable to further increase their glycolytic flux and sustain cell proliferation under prolonged exposure to hypoxic conditions (0.1 % O_2). In contrast, colon cancer cells expressing a 3-fold higher IF_1/ATP synthase ratio than 143B cells mainly rely on OXPHOS for energy production. Furthermore, although the master regulator of adaptive response to hypoxia, HIF-1α, is equally stabilized in both cell lines, HCT116 cells display low adaptability to severe hypoxic conditions due to their limited glycolytic capacity that makes them unable to grow under hypoxia, suggesting that these cells might be lacking in other factors mediating the hypoxic response.

The differences just described suggest that the impact of IF_1 in cellular bioenergetics may vary between cancer cells depending on their energy metabolism, as also proposed by Campanella and co-workers, who reported significant differences in the relative IF_1 expression levels in different populations of primary mammalian cells with distinct metabolic phenotypes [96, 124].

In particular, considering that highly oxidative cells are more vulnerable to mitochondrial dysfunction due to hypoxic/anoxic exposure than glycolytic ones, it can be assumed that the observed high IF_1/ATP synthase ratio represents a crucial defence mechanism to prevent rapid ATP consumption during respiratory inhibition. Consistently, IF_1 was also referred to as a hypoxia-related protein. Indeed, a report supports the role of IF_1 in protecting rat liver cells exposed to oxygen deprivation and related its expression to the action of HIF-1α [142]. According to these findings, our analysis under hypoxic conditions revealed a significant increase of IF_1 levels of about 50% after 48 hours of exposure to 0.1% O_2 in both cell lines compared to their basal normoxic levels (Fig. 21), indicating that IF_1 overexpression may represent a common adaptive strategy of cancer cells to cope with hypoxic/anoxic stress.

Therefore, we went through these aspects by assaying the bioenergetics of 143B and HCT116 cells following stable silencing of IF_1 under limited oxygen availability. For this purpose, we first identified in both cell lines the oxygen deprivation conditions needed to induce the reversal of ATP synthase and activate the IF_1 inhibitory role.

According to our findings the prolonged exposure to 0.1% O_2 was able to inhibit the mitochondrial respiration in HCT116 cells, inducing mitochondrial depolarization. Essentially, we observed that the collapse of the mitochondrial membrane potential occurs between 16 and 24 hours of hypoxia exposure. Indeed, after 16 hours no

differences were still observed in $\Delta\Psi_m$ either between controls and IF_1-silenced cells or upon addition of oligomycin. In contrast, a longer exposure to hypoxia up to 24 hours induced the loss of transmembrane potential in controls cells, where IF_1 is reported to inhibit the ATP hydrolytic activity of ATP synthase. Conversely, $\Delta\Psi_m$ was still preserved in IF_1-silenced cells even after 24 hours of hypoxia exposure due to the activation of ATPase activity of the ATP synthase. Indeed, upon oligomycin addition, the transmembrane potential decreased to the level of controls, confirming that it was previously sustained by the ATP synthase activity at the expense of glycolytic ATP. Accordingly, the analysis of intracellular ATP content showed a progressive decrease of ATP levels during hypoxia exposure only in IF_1-silenced cells following the $\Delta\Psi_m$ collapse, whereas the ATP levels were preserved in controls cells due to the presence of IF_1. All these analyses for the first time proved the role of IF_1 in preventing energy deprivation in HCT116 cells experiencing severe hypoxia, highlighting its function as a modulator of cancer cell bioenergetics. Noteworthy, we subsequently demonstrated that the energetic advantage conferred by IF_1 to HCT116 cells is crucial for their survival. Indeed, we observed that the presence of IF_1 enables HCT116 control cells to survive under prolonged exposure to hypoxia, while the IF_1-silencing induces about 65% of cellular death after 48 hours of severe hypoxia exposure in IF_1-depleted clones.

Contrary to the above data on HCT116 cells, the analyses carried out in the highly glycolytic 143B cells under prolonged exposure to 0.1% O_2 revealed that the hypoxic condition, although severe, was not sufficient to inhibit the electron transport chain and consequently to induce mitochondrial depolarization, confirming our previous analyses conducted in the same cell line under less severe hypoxic conditions (24 hours at 0.5% O_2) [121]. Specifically, we herein observed that 143B cells maintain high transmembrane potential levels even after 48 hours of exposure to severe hypoxia (0.1% O_2) also showing a slight increase in $\Delta\Psi_m$ value compared to normoxia due to the slowdown of the electron transport across the inner membrane under limited availability of oxygen. The preservation of respiratory chain activity observed in hypoxic 143B cells might be explained by a high oxygen affinity of cytochrome c oxidase of these cells. Indeed, it has been reported that in certain solid tumours the HIF-1α stabilization induces the expression of COX subunit isoforms able to optimize the electron transfer chain activity under hypoxic conditions [55].

Therefore, considering that osteosarcoma cells preserve the mitochondrial respiration activity and the trasnmembrane potential even upon severe hypoxia, we excluded a regulatory contribution of IF_1 under these experimental conditions. Accordingly, we did not observed any protective function of IF_1 by evaluating cancer cell growth and viability of both hypoxic control and IF_1-silenced cells.

Afterwards, the analysis of $\Delta\Psi_m$ and ATP content upon anoxia exposure proved that the total absence of oxygen was needed to induce the $\Delta\Psi_m$ collapse in 143B cells and highlight the function of IF_1 in cellular bioenergetics. We thus demonstrated that in anoxic osteosarcoma cells, cultured in tightly sealed glass jars in the presence of oxygen absorbers, IF_1 is able to modulate the ATP hydrolytic activity of ATP synthase preserving ATP level, as observed under severe hypoxia in HCT116 cells.

Consequently, in order to compare the role of IF_1 in promoting survival/growth of cancer cells with different bioenergetic phenotypes under oxygen deprivation conditions, we reproduced the $\Delta\Psi_m$ collapse occurring in the absence of oxygen by exposing both 143B and HCT116 cells and their derived IF_1-silenced clones to FCCP uncoupler. Under these conditions, we observed that IF_1 silencing inhibited proliferation without inducing cell death in 143B cells, whereas it induced 55% of cellular death in IF_1-silenced cells after 24 hours of anoxia exposure. Therefore, we concluded that the energetic advantage conferred by IF_1 to cancer cells experiencing oxygen deprivation allowed the glycolytic cell lines to keep proliferating, while it is crucial for the OXPHOS-dependent cell line survival.

Furthermore, considering the widespread use of glycolytic inhibitors to target energy metabolism of hypoxic/anoxic cancer cells, we exposed both control and IF_1-silenced cells to the glycolytic inhibitor 3-brmopyruvate. Interestingly, our findings showed that the combined effect of both IF_1-silencing and glycolysis inhibition under anoxic conditions sensitized 143B cells to 40% of cellular death after 24 hours, thus resulting as a promising approach against glycolytic cancer cells. Conversely, the inhibition of glycolysis did not further affect cell survival of anoxic HCT116 cells, whose viability was mainly compromised by IF_1-silencing. Overall, these novel concepts could intriguingly find application analysing the potential of metabolic drugs against individual cancers.

Based on our results, IF_1 overexpression is crucial when cancer cells experience oxygen deprivation, since it can promote tumour growth or survival preserving cellular

energy. Nevertheless, under these conditions, the IF_1 expression also leads to the collapse of mitochondrial membrane potential, which constitutes a damaging event for cellular homeostasis being a signal for the activation of mitochondrial dependent apoptotic death. Alternatively, it is well known that cells also evolved mechanisms to escape apoptosis including the selective degradation of dysfunctional mitochondria. Hence, taking into account that both 143B and HCT116 cells were still viable despite the prolonged exposure to mitochondrial depolarization, we proposed that the activation of mitophagic process would represent a mechanism used by cancer cells overexpressing IF_1 to escape apoptosis in the presence of depolarized mitochondria.

Accordingly, the evaluation of both mitophagy and mitochondrial biogenesis along with the mitochondrial content in IF_1-expressing and IF_1-depleted 143B cells exposed to the FCCP uncoupler revealed that the presence of IF_1 promotes the mitochondrial mass renewal to replace damaged mitochondria.

Indeed, fluorescence images of 143B cells exposed to the uncoupler clearly showed the increase of mitochondria sequestration within the autophagosome compared to the basal conditions, indicating the activation of mitophagic process. Furthermore, we observed in IF_1-expressing cells an increase of positive regulators of both mitophagy (PINK1 and BNIP3) and mitochondrial biogenesis (PGC-1α and SIRT1), indicating the increase of mitochondrial turnover in these cells.

Conversely, in IF_1-silenced cells the maintenance of $\Delta\Psi_m$ by ATP hydrolysis acts as a signal for mitochondrial mass preservation and thus neither mitophagy nor biogenesis was stimulated. Indeed, we observed that the expression of both mitophagic and biogenesis markers was downregulated in IF_1-silenced clones under these experimental conditions. This may also be explained considering that mitochondrial turnover is a high energy-demanding process that could not be sustained by IF_1-silenced cells, whose energy content is hugely decreased under mitochondrial depolarization conditions. Interestingly, further analyses on the effects of the prolonged $\Delta\Psi_m$ collapse on both mitochondrial content and mitochondrial turnover processes are currently ongoing in the highly oxidative HCT116 cells in order to assess the impact of the different energy metabolism in promoting the mitochondrial mass renewal.

In the light of all data collected so far, we thus concluded that IF_1 overexpression represents a common strategy of cancer cells experiencing oxygen deprivation to

protect themselves from energy depletion, conferring an energetic advantage to sustain their growth or survival. It is also noteworthy that the energetic advantage conferred by IF_1 has a different effect on cancer cell survival depending on the energy metabolism of each cell line. In particular, the presence of IF_1 enabled the highly glycolytic cell line to keep proliferating, while it is crucial for the survival of OXPHOS-dependent cells, which notably express a higher IF_1/ATP synthase ratio compared to the glycolytic ones. However, more work will be necessary to establish the generality of these observations and further investigations are currently ongoing in other cancer cell lines for this purpose.

In addition, data obtained in 143B cells indicate that the presence of IF_1 also promotes a continuous renewal of the mitochondrial mass by enhancing both mitophagy and mitochondrial biogenesis to replace dysfunctional mitochondria, a mechanism that may protect depolarized IF_1-expressing cells from mitochondria-mediated apoptosis and promptly provide functional mitochondria in case of reoxygenation.

Therefore, based on our findings, reducing the overexpression of IF_1 in cancer cells experiencing oxygen deprivation may represent a promising strategy to deprive solid tumours of the energy required for their growth or survival. From a therapeutic perspective, these results thus provide interesting basis to develop appropriate therapeutic approach targeting energy metabolism based on IF_1 silencing, possibly in combination with glycolysis inhibitors.

Interestingly, additional studies in collaboration with Professor Walker from Cambridge University are ongoing to further explore the role of IF_1 as a therapeutic target by deepening the mechanism by which IF_1 regulates the activity of ATP synthase, the master regulator of energy metabolism. This project includes the evaluation of the effects of mutant forms of IF_1 on the ATP synthase activity by producing cancer cell lines expressing different altered forms of the protein through genome editing. Hopefully, the identification of forms able to inhibit the OXPHOS activity by blocking the ATP synthase under normoxic conditions might have interesting effects on cancer growth and survival, providing useful information for developing possible antitumor strategies.

6. IMAGES SOURCES

Figure 1: Cannino, G., Ciscato, F., Masgras, I., Sánchez-Martín, C., & Rasola, A. (2018). Metabolic plasticity of tumor cell mitochondria. *Frontiers in oncology*, *8*, 333.

Figure 2: Biner, O., Schick, T., Ganguin, A. A., & von Ballmoos, C. (2018). Towards a synthetic mitochondrion. *CHIMIA International Journal for Chemistry*, *72*(5), 291-296.

Figure 3: Tatiparti, K., Gawde, K. A., & Alasab, H. (2017). Pancreatic Cancer-The Role of Hypoxia. *Scientific Pages Pancreat Cancer*, *1*(1), 1-5.

Figure 4: He, J., Ford, H. C., Carroll, J., Douglas, C., Gonzales, E., Ding, S., ... & Walker, J. E. (2018). Assembly of the membrane domain of ATP synthase in human mitochondria. *Proceedings of the National Academy of Sciences*, *115*(12), 2988-2993.

Figure 5: Leslie, A. G., & Walker, J. E. (2000). Structural model of F1–ATPase and the implications for rotary catalysis. *Philosophical Transactions of the Royal Society of London. Series B: Biological Sciences*, *355*(1396), 465-471.

Figure 6: Walker, J. E. (2013). The ATP synthase: the understood, the uncertain and the unknown.

Figure 7: Alberts, B., Bray, D., Hopkin, K., Johnson, A. D., Lewis, J., Raff, M., ... & Walter, P. (2013). *Essential cell biology*. Garland Science.

Figure 8: Faccenda, D., & Campanella, M. (2012). Molecular Regulation of the Mitochondrial F1Fo-ATPsynthase: Physiological and Pathological Significance of the Inhibitory Factor 1 (IF 1). *International journal of cell biology*, *2012*.

Figure 9: Cabezón, E., Montgomery, M. G., Leslie, A. G., & Walker, J. E. (2003). The structure of bovine F 1-ATPase in complex with its regulatory protein IF1. *Nature Structural & Molecular Biology*, *10*(9), 744-750.

Figure 10: Faccenda, D., & Campanella, M. (2012). Molecular Regulation of the Mitochondrial F1Fo-ATPsynthase: Physiological and Pathological Significance of the Inhibitory Factor 1 (IF 1). *International journal of cell biology*, *2012*.

Figure 11: Gledhill, J. R., Montgomery, M. G., Leslie, A. G., & Walker, J. E. (2007). How the regulatory protein, IF1, inhibits F1-ATPase from bovine mitochondria. *Proceedings of the National Academy of Sciences*, *104*(40), 15671-15676.

Figure 22A: Available at https://www.origene.com/catalog/vectors/shrna-vectors/tr30007/pgfp-v-rs-shrna-vector.

7. BIBLIOGRAPHY

1 HANAHAN, Douglas; WEINBERG, Robert A. The hallmarks of cancer. *cell*, 2000, vol. 100, no 1, p. 57-70.

2 HANAHAN, Douglas; WEINBERG, Robert A. Hallmarks of cancer: the next generation. *cell*, 2011, vol. 144, no 5, p. 646-674.

3 KREUZALER, Peter, et al. Adapt and conquer: Metabolic flexibility in cancer growth, invasion and evasion. *Molecular metabolism*, 2020, vol. 33, p. 83-101.

4 SUN, Linchong, et al. Metabolic reprogramming for cancer cells and their microenvironment: Beyond the Warburg Effect. *Biochimica et Biophysica Acta (BBA)-Reviews on Cancer*, 2018, vol. 1870, no 1, p. 51-66.

5 YANG, Dongki; KIM, Jaehong. Mitochondrial Retrograde Signalling and Metabolic Alterations in the Tumour Microenvironment. *Cells*, 2019, vol. 8, no 3, p. 275.

6 GOUIRAND, Victoire; GUILLAUMOND, Fabienne; VASSEUR, Sophie. Influence of the tumor microenvironment on cancer cells metabolic reprogramming. *Frontiers in oncology*, 2018, vol. 8, p. 117.

7 Warburg, O. H. (1926). über den Stoffwechsel der Tumoren. J. Springer.

8 DANHIER, Pierre, et al. Cancer metabolism in space and time: beyond the Warburg effect. *Biochimica et Biophysica Acta (BBA)-Bioenergetics*, 2017, vol. 1858, no 8, p. 556-572.

9 KOPPENOL, Willem H.; BOUNDS, Patricia L.; DANG, Chi V. Otto Warburg's contributions to current concepts of cancer metabolism. *Nature Reviews Cancer*, 2011, vol. 11, no 5, p. 325-337.

10 PHAN, Liem Minh; YEUNG, Sai-Ching Jim; LEE, Mong-Hong. Cancer metabolic reprogramming: importance, main features, and potentials for precise targeted anti-cancer therapies. *Cancer biology & medicine*, 2014, vol. 11, no 1, p. 1.

11 DEBERARDINIS, Ralph J.; CHANDEL, Navdeep S. Fundamentals of cancer metabolism. *Science advances*, 2016, vol. 2, no 5, p. e1600200.

12 SCHOONJANS, Céline A.; GALLEZ, Bernard. Metabolic Plasticity of Tumor Cells: How They Do Adapt to Food Deprivation. En *Tumor Microenvironment*. Springer, Cham, 2020. p. 109-123.

13 VANDER HEIDEN, Matthew G.; CANTLEY, Lewis C.; THOMPSON, Craig B. Understanding the arburg effect: the metabolic requirements of cell proliferation. *science*, 2009, vol. 324, no 5930, p. 1029-1033.

14 WARBURG, Otto. On the origin of cancer cells. *Science*, 1956, vol. 123, no 3191, p. 309-314.

15 Warburg O. On respiratory impairment in cancer cells. Science 1956; 124:269-270

16 ZU, Xin Lin; GUPPY, Michael. Cancer metabolism: facts, fantasy, and fiction. *Biochemical and biophysical research communications*, 2004, vol. 313, no 3, p. 459-465.

17 RODRÍGUEZ-ENRÍQUEZ, Sara, et al. Transcriptional Regulation of Energy Metabolism in Cancer Cells. *Cells*, 2019, vol. 8, no 10, p. 1225.

18 CORBET, Cyril; FERON, Olivier. Tumour acidosis: from the passenger to the driver's seat. *Nature Reviews Cancer*, 2017, vol. 17, no 10, p. 577.

19 CANNINO, Giuseppe, et al. Metabolic plasticity of tumor cell mitochondria. *Frontiers in oncology*, 2018, vol. 8, p. 333.

20 VYAS, Sejal; ZAGANJOR, Elma; HAIGIS, Marcia C. Mitochondria and cancer. *Cell*, 2016, vol. 166, no 3, p. 555-566.

21 PORPORATO, Paolo Ettore, et al. Mitochondrial metabolism and cancer. *Cell research*, 2018, vol. 28, no 3, p. 265-280.

22 SOLAINI, Giancarlo; SGARBI, Gianluca; BARACCA, Alessandra. Oxidative phosphorylation in cancer cells. *Biochimica et Biophysica Acta (BBA)-Bioenergetics*, 2011, vol. 1807, no 6, p. 534-542.

23 CORBET, Cyril; FERON, Olivier. Cancer cell metabolism and mitochondria: nutrient plasticity for TCA cycle fueling. *Biochimica et Biophysica Acta (BBA)-Reviews on Cancer*, 2017, vol. 1868, no 1, p. 7-15.

24 CAZZANIGA, Massimiliano; BONANNI, Bernardo. Relationship between metabolic reprogramming and mitochondrial activity in cancer cells. Understanding the effect of metformin and its clinical implications. *Anticancer research*, 2015, vol. 35, no 11, p. 5789-5796.

25 PENTA, John S., et al. Mitochondrial DNA in human malignancy. *Mutation Research/Reviews in Mutation Research*, 2001, vol. 488, no 2, p. 119-133.

26 HOCHHAUSER, Daniel. Relevance of mitochondrial DNA in cancer. *The Lancet*, 2000, vol. 356, no 9225, p. 181-182.

27 LU, Jianxin; SHARMA, Lokendra Kumar; BAI, Yidong. Implications of mitochondrial DNA mutations and mitochondrial dysfunction in tumorigenesis. *Cell research*, 2009, vol. 19, no 7, p. 802-815.

28 HERTWECK, Kate L.; DASGUPTA, Santanu. The landscape of mtDNA modifications in cancer: a tale of two cities. *Frontiers in oncology*, 2017, vol. 7, p. 262.

29 SABHARWAL, Simran S.; SCHUMACKER, Paul T. Mitochondrial ROS in cancer: initiators, amplifiers or an Achilles' heel?. *Nature Reviews Cancer*, 2014, vol. 14, no 11, p. 709-721.

30 BURKE, Peter J. Mitochondria, bioenergetics and apoptosis in cancer. *Trends in cancer*, 2017, vol. 3, no 12, p. 857-870.

31 IZZO, Valentina, et al. Mitochondrial permeability transition: new findings and persisting uncertainties. *Trends in cell biology*, 2016, vol. 26, no 9, p. 655-667.

32 WANG, Chunxin; YOULE, Richard J. The role of mitochondria in apoptosis. *Annual review of genetics*, 2009, vol. 43, p. 95-118.

33 UM, Hong-Duck. Bcl-2 family proteins as regulators of cancer cell invasion and metastasis: a review focusing on mitochondrial respiration and reactive oxygen species. *Oncotarget*, 2016, vol. 7, no 5, p. 5193.

34 WARREN, Chloe FA; WONG-BROWN, Michelle W.; BOWDEN, Nikola A. BCL-2 family isoforms in apoptosis and cancer. *Cell death & disease*, 2019, vol. 10, no 3, p. 1-12.

35 SICA, Valentina, et al. Oxidative phosphorylation as a potential therapeutic target for cancer therapy. *International Journal of Cancer*, 2020, vol. 146, no 1, p. 10-17.

36 KÜHLBRANDT, Werner. Structure and function of mitochondrial membrane protein complexes. *BMC biology*, 2015, vol. 13, no 1, p. 89.

37 GU, Jinke, et al. The architecture of the mammalian respirasome. *Nature*, 2016, vol. 537, no 7622, p. 639-643.

38 GENOVA, M. L., et al. Is supercomplex organization of the respiratory chain required for optimal electron transfer activity?. *Biochimica et Biophysica Acta (BBA)-Bioenergetics*, 2008, vol. 1777, no 7-8, p. 740-746.

39 CHABAN, Yuriy; BOEKEMA, Egbert J.; DUDKINA, Natalya V. Structures of mitochondrial oxidative phosphorylation supercomplexes and mechanisms for their stabilisation. *Biochimica et Biophysica Acta (BBA)-Bioenergetics*, 2014, vol. 1837, no 4, p. 418-426.

40 HATEFI, Youssef. The mitochondrial electron transport and oxidative phosphorylation system. *Annual review of biochemistry*, 1985, vol. 54, no 1, p. 1015-1069.

41 MITCHELL, Peter. Coupling of phosphorylation to electron and hydrogen transfer by a chemi-osmotic type of mechanism. *Nature*, 1961, vol. 191, no 4784, p. 144-148.

42 ASHTON, Thomas M., et al. Oxidative phosphorylation as an emerging target in cancer therapy. *Clinical Cancer Research*, 2018, vol. 24, no 11, p. 2482-2490.

43 WHITAKER-MENEZES, Diana, et al. Hyperactivation of oxidative mitochondrial metabolism in epithelial cancer cells in situ: visualizing the therapeutic effects of metformin in tumor tissue. *Cell cycle*, 2011, vol. 10, no 23, p. 4047-4064.

44 SHIN, Min-Kyue; CHEONG, Jae-Ho. Mitochondria-centric bioenergetic characteristics in cancer stem-like cells. *Archives of pharmacal research*, 2019, vol. 42, no 2, p. 113-127.

45 TAN, An S., et al. Mitochondrial genome acquisition restores respiratory function and tumorigenic potential of cancer cells without mitochondrial DNA. *Cell metabolism*, 2015, vol. 21, no 1, p. 81-94.

46 BAJZIKOVA, Martina, et al. Reactivation of dihydroorotate dehydrogenase-driven pyrimidine biosynthesis restores tumor growth of respiration-deficient cancer cells. *Cell metabolism*, 2019, vol. 29, no 2, p. 399-416. e10.

47 SULLIVAN, Lucas B., et al. Supporting aspartate biosynthesis is an essential function of respiration in proliferating cells. *Cell*, 2015, vol. 162, no 3, p. 552-563.

48 ZHENG, J. I. E. Energy metabolism of cancer: Glycolysis versus oxidative phosphorylation. *Oncology letters*, 2012, vol. 4, no 6, p. 1151-1157.

49 SMOLKOVÁ, Katarína, et al. Waves of gene regulation suppress and then restore oxidative phosphorylation in cancer cells. *The international journal of biochemistry & cell biology*, 2011, vol. 43, no 7, p. 950-968.

50 JIA, Dongya, et al. Elucidating the metabolic plasticity of cancer: mitochondrial reprogramming and hybrid metabolic states. *Cells*, 2018, vol. 7, no 3, p. 21.

51 YU, Linglin, et al. Modeling the genetic regulation of cancer metabolism: interplay between glycolysis and oxidative phosphorylation. *Cancer research*, 2017, vol. 77, no 7, p. 1564-1574.

52 JIA, Dongya, et al. Elucidating cancer metabolic plasticity by coupling gene regulation with metabolic pathways. *Proceedings of the National Academy of Sciences*, 2019, vol. 116, no 9, p. 3909-3918.

53 MILOTTI, Edoardo; STELLA, Sabrina; CHIGNOLA, Roberto. Pulsation-limited oxygen diffusion in the tumour microenvironment. *Scientific reports*, 2017, vol. 7, p. 39762.

54 VAUPEL, Peter; MAYER, Arnulf. Availability, not respiratory capacity governs oxygen consumption of solid tumors. *The international journal of biochemistry & cell biology*, 2012, vol. 44, no 9, p. 1477-1481.

55 SEMENZA, Gregg L. Oxygen-dependent regulation of mitochondrial respiration by hypoxia-inducible factor 1. *Biochemical Journal*, 2007, vol. 405, no 1, p. 1-9.

56 SOLAINI, Giancarlo, et al. Hypoxia and mitochondrial oxidative metabolism. *Biochimica et Biophysica Acta (BBA)-Bioenergetics*, 2010, vol. 1797, no 6-7, p. 1171-1177.

57 SCHULZE, Almut; HARRIS, Adrian L. How cancer metabolism is tuned for proliferation and vulnerable to disruption. *Nature*, 2012, vol. 491, no 7424, p. 364-373.

58 KIM, Soo-Youl. Cancer energy metabolism: shutting power off cancer factory. *Biomolecules & therapeutics*, 2018, vol. 26, no 1, p. 39.

59 SHAHRUZAMAN, Shazwin Hani; FAKURAZI, Sharida; MANIAM, Sandra. Targeting energy metabolism to eliminate cancer cells. *Cancer management and research*, 2018, vol. 10, p. 2325.

60 MORENO-SÁNCHEZ, Rafael, et al. Energy metabolism in tumor cells. *The FEBS journal*, 2007, vol. 274, no 6, p. 1393-1418.

61 AZEVEDO-SILVA, J., et al. The anticancer agent 3-bromopyruvate: a simple but powerful molecule taken from the lab to the bedside. *Journal of bioenergetics and biomembranes*, 2016, vol. 48, no 4, p. 349-362.

62 FAN, Tengjiao, et al. Tumor energy metabolism and potential of 3-bromopyruvate as an inhibitor of aerobic glycolysis: Implications in tumor treatment. *Cancers*, 2019, vol. 11, no 3, p. 317.

63 WHEATON, William W., et al. Metformin inhibits mitochondrial complex I of cancer cells to reduce tumorigenesis. *elife*, 2014, vol. 3, p. e02242.

64 SCHÖCKEL, Laura, et al. Targeting mitochondrial complex I using BAY 87-2243 reduces melanoma tumor growth. *Cancer & metabolism*, 2015, vol. 3, no 1, p. 11.

65 ZHANG, Xiaonan, et al. Induction of mitochondrial dysfunction as a strategy for targeting tumour cells in metabolically compromised microenvironments. *Nature communications*, 2014, vol. 5, no 1, p. 1-14.

66 KENWOOD, Brandon M., et al. Identification of a novel mitochondrial uncoupler that does not depolarize the plasma membrane. *Molecular metabolism*, 2014, vol. 3, no 2, p. 114-123.

67 CHEONG, Jae-Ho, et al. Dual inhibition of tumor energy pathway by 2-deoxyglucose and metformin is effective against a broad spectrum of preclinical cancer models. *Molecular cancer therapeutics*, 2011, vol. 10, no 12, p. 2350-2362.

68 CINTRON, N. M.; PEDERSEN, Peter L. A protein inhibitor of the mitochondrial adenosine triphosphatase complex of rat liver. Purification and characterization. *Journal of Biological Chemistry*, 1979, vol. 254, no 9, p. 3439-3443.

69 BOSETTI, Francesca, et al. Myocardial ischemic preconditioning and mitochondrial F1F0-ATPase activity. *Molecular and cellular biochemistry*, 2000, vol. 215, no 1-2, p. 31-38.

70 SÁNCHEZ-ARAGÓ, María, et al. Expression, regulation and clinical relevance of the ATPase inhibitory factor 1 in human cancers. *Oncogenesis*, 2013, vol. 2, no 4, p. e46-e46.

71 GARCÍA-AGUILAR, Ana; CUEZVA, José M. A review of the inhibition of the mitochondrial ATP synthase by IF1 in vivo: reprogramming energy metabolism and inducing mitohormesis. *Frontiers in Physiology*, 2018, vol. 9, p. 1322.

72 RHODES, Daniel R., et al. Oncomine 3.0: genes, pathways, and networks in a collection of 18,000 cancer gene expression profiles. *Neoplasia (New York, NY)*, 2007, vol. 9, no 2, p. 166.

73 SONG, Ruipeng, et al. Reciprocal activation between ATPase inhibitory factor 1 and NF-κB drives hepatocellular carcinoma angiogenesis and metastasis. *Hepatology*, 2014, vol. 60, no 5, p. 1659-1673.

74 GAO, Yi-Xing, et al. ATPase inhibitory factor 1 expression is an independent prognostic factor in non-small cell lung cancer. *American journal of cancer research*, 2016, vol. 6, no 5, p. 1141.

75 WEI, Shihu, et al. Silencing of ATPase inhibitory factor 1 inhibits cell growth via cell cycle arrest in bladder cancer. *Pathobiology*, 2015, vol. 82, no 5, p. 224-232.

76 YIN, Tao, et al. ATPase inhibitory factor 1 is a prognostic marker and contributes to proliferation and invasion of human gastric cancer cells. *Biomedicine & Pharmacotherapy*, 2015, vol. 70, p. 90-96.

77 WU, Jianheng, et al. ATPase inhibitory factor 1 is a potential prognostic marker for the migration and invasion of glioma. *Oncology letters*, 2015, vol. 10, no 4, p. 2075-2080.

78 PAUMARD, Patrick, et al. The ATP synthase is involved in generating mitochondrial cristae morphology. *The EMBO journal*, 2002, vol. 21, no 3, p. 221-230.

79 WALKER, John E., et al. Primary structure and subunit stoichiometry of F1-ATPase from bovine mitochondria. *Journal of molecular biology*, 1985, vol. 184, no 4, p. 677-701.

80 MEYER, Björn, et al. Identification of two proteins associated with mammalian ATP synthase. *Molecular & Cellular Proteomics*, 2007, vol. 6, no 10, p. 1690-1699.

81 WALKER, John E. The ATP synthase: the understood, the uncertain and the unknown. 2013.

82 BOYER, Paul D. Coupling mechanisms in capture, transmission and use of energy. *Annual Review of Biochemistry*, 1977, vol. 46, p. 955-1026.

83 BOYER, P. D. Toward an adequate scheme for the ATP synthase catalysis. *Biochemistry (Moscow)*, 2001, vol. 66, no 10, p. 1058-1066.

84 LESLIE, Andrew GW; WALKER, John E. Structural model of F1–ATPase and the implications for rotary catalysis. *Philosophical Transactions of the Royal Society of London. Series B: Biological Sciences*, 2000, vol. 355, no 1396, p. 465-471.

85 FILLINGAME, Robert H.; ANGEVINE, Christine M.; DMITRIEV, Oleg Y. Mechanics of coupling proton movements to c-ring rotation in ATP synthase. *FEBS letters*, 2003, vol. 555, no 1, p. 29-34.

86 CHINOPOULOS, Christos; ADAM-VIZI, Vera. Mitochondria as ATP consumers in cellular pathology. *Biochimica et Biophysica Acta (BBA)-Molecular Basis of Disease*, 2010, vol. 1802, no 1, p. 221-227.

87 REES, David M., et al. Structural evidence of a new catalytic intermediate in the pathway of ATP hydrolysis by F1–ATPase from bovine heart mitochondria. *Proceedings of the National Academy of Sciences*, 2012, vol. 109, no 28, p. 11139-11143.

88 MARTÍNEZ-REYES, Inmaculada, et al. TCA cycle and mitochondrial membrane potential are necessary for diverse biological functions. *Molecular cell*, 2016, vol. 61, no 2, p. 199-209.

89 ZOROVA, Ljubava D., et al. Mitochondrial membrane potential. *Analytical biochemistry*, 2018, vol. 552, p. 50-59.

90 GUNTER, Karlene K.; GUNTER, Thomas E. Transport of calcium by mitochondria. *Journal of bioenergetics and biomembranes*, 1994, vol. 26, no 5, p. 471-485.

91 MARTIN, Jörg; MAHLKE, Kerstin; PFANNER, Nikolaus. Role of an energized inner membrane in mitochondrial protein import. Delta psi drives the movement of

presequences. *Journal of Biological Chemistry*, 1991, vol. 266, no 27, p. 18051-18057.

92 ADAM-VIZI, Vera; CHINOPOULOS, Christos. Bioenergetics and the formation of mitochondrial reactive oxygen species. *Trends in pharmacological sciences*, 2006, vol. 27, no 12, p. 639-645.

93 ZAMZAMI, Naoufal, et al. Sequential reduction of mitochondrial transmembrane potential and generation of reactive oxygen species in early programmed cell death. *The Journal of experimental medicine*, 1995, vol. 182, no 2, p. 367-377.

94 KUBLI, Dieter A.; GUSTAFSSON, Åsa B. Mitochondria and mitophagy: the yin and yang of cell death control. *Circulation research*, 2012, vol. 111, no 9, p. 1208-1221.

95 ATAULLAKHANOV, Fazoil I.; VITVITSKY, Victor M. What determines the intracellular ATP concentration. *Bioscience reports*, 2002, vol. 22, no 5-6, p. 501-511.

96 CAMPANELLA, Michelangelo, et al. IF1: setting the pace of the F1Fo-ATP synthase. *Trends in biochemical sciences*, 2009, vol. 34, no 7, p. 343-350.

97 PULLMAN, Maynard E.; MONROY, Gladys C. A naturally occurring inhibitor of mitochondrial adenosine triphosphatase. *Journal of biological chemistry*, 1963, vol. 238, no 11, p. 3762-3769.

98 CORTÉS-HERNÁNDEZ, Paulina, et al. The inhibitor protein of the F1F0-ATP synthase is associated to the external surface of endothelial cells. *Biochemical and biophysical research communications*, 2005, vol. 330, no 3, p. 844-849.

99 ICHIKAWA, Naoki, et al. Nucleotide sequence of cDNA coding the mitochondrial precursor protein of the ATPase inhibitor from humans. *Bioscience, biotechnology, and biochemistry*, 1999, vol. 63, no 12, p. 2225-2227.

100 FACCENDA, Danilo; CAMPANELLA, Michelangelo. Molecular Regulation of the Mitochondrial F1Fo-ATPsynthase: Physiological and Pathological Significance of the Inhibitory Factor 1 (IF 1). *International journal of cell biology*, 2012, vol. 2012.

101 CONTESSI, Stefania, et al. Identification of a Conserved Calmodulin-Binding Motif∈ the Sequence of F 0 F 1 ATPsynthase Inhibitor Protein. *Journal of bioenergetics and biomembranes*, 2005, vol. 37, no 5, p. 317-327.

102 CABEZON, E., et al. The structure of bovine IF1, the regulatory subunit of mitochondrial F-ATPase. *The EMBO journal*, 2001, vol. 20, no 24, p. 6990-6996.

103 CABEZON, Elena, et al. Modulation of the oligomerization state of the bovine F1-ATPase inhibitor protein, IF1, by pH. *Journal of Biological Chemistry*, 2000, vol. 275, no 33, p. 25460-25464.

104 SCHNIZER, Richard, et al. Histidine-49 is necessary for the pH-dependent transition between active and inactive states of the bovine F1-ATPase inhibitor protein. *Biochimica et Biophysica Acta (BBA)-Protein Structure and Molecular Enzymology*, 1996, vol. 1292, no 2, p. 241-248.

105 GREEN, David W.; GROVER, Gary J. The IF1 inhibitor protein of the mitochondrial F1F0-ATPase. *Biochimica et Biophysica Acta (BBA)-Bioenergetics*, 2000, vol. 1458, no 2-3, p. 343-355.

106 ROUSLIN, William. Protonic inhibition of the mitochondrial oligomycin-sensitive adenosine 5'-triphosphatase in ischemic and autolyzing cardiac muscle. Possible mechanism for the mitigation of ATP hydrolysis under nonenergizing conditions. *Journal of Biological Chemistry*, 1983, vol. 258, no 16, p. 9657-9661.

107 WALKER, John E. The regulation of catalysis in ATP synthase. *Current opinion in structural biology*, 1994, vol. 4, no 6, p. 912-918.

108 BASON, John V., et al. Pathway of binding of the intrinsically disordered mitochondrial inhibitor protein to F1-ATPase. *Proceedings of the National Academy of Sciences*, 2014, vol. 111, no 31, p. 11305-11310.

109 CABEZÓN, Elena, et al. The structure of bovine F 1-ATPase in complex with its regulatory protein IF 1. *Nature Structural & Molecular Biology*, 2003, vol. 10, no 9, p. 744-750.

110 GLEDHILL, Jonathan R., et al. How the regulatory protein, IF1, inhibits F1-ATPase from bovine mitochondria. *Proceedings of the National Academy of Sciences*, 2007, vol. 104, no 40, p. 15671-15676.

111 BASON, John V., et al. Binding of the inhibitor protein IF1 to bovine F1-ATPase. *Journal of molecular biology*, 2011, vol. 406, no 3, p. 443-453.

112 ROUSLIN, William; PULLMAN, Maynard E. Protonic inhibition of the mitochondrial adenosine 5′-triphosphatase in ischemic cardiac muscle. Reversible binding of the ATPase inhibitor protein to the mitochondrial ATPase during ischemia. *Journal of molecular and cellular cardiology*, 1987, vol. 19, no 7, p. 661-668.

113 SOLAINI, Giancarlo; HARRIS, David A. Biochemical dysfunction in heart mitochondria exposed to ischaemia and reperfusion. *Biochemical Journal*, 2005, vol. 390, no 2, p. 377-394.

114 GARCÍA-BERMÚDEZ, Javier; CUEZVA, Jose M. The ATPase Inhibitory Factor 1 (IF1): A master regulator of energy metabolism and of cell survival. *Biochimica et Biophysica Acta (BBA)-Bioenergetics*, 2016, vol. 1857, no 8, p. 1167-1182.

115 GARCÍA-BERMÚDEZ, Javier, et al. PKA phosphorylates the ATPase inhibitory factor 1 and inactivates its capacity to bind and inhibit the mitochondrial H+-ATP synthase. *Cell reports*, 2015, vol. 12, no 12, p. 2143-2155.

116 ACIN-PEREZ, Rebeca, et al. Cyclic AMP produced inside mitochondria regulates oxidative phosphorylation. *Cell metabolism*, 2009, vol. 9, no 3, p. 265-276.

117 SÁNCHEZ-CENIZO, Laura, et al. Up-regulation of the ATPase inhibitory factor 1 (IF1) of the mitochondrial H+-ATP synthase in human tumors mediates the metabolic shift of cancer cells to a Warburg phenotype. *Journal of Biological Chemistry*, 2010, vol. 285, no 33, p. 25308-25313.

118 ESPARZA-MOLTÓ, Pau B.; NUEVO-TAPIOLES, Cristina; CUEZVA, José M. Regulation of the H+-ATP synthase by IF1: a role in mitohormesis. *Cellular and Molecular Life Sciences*, 2017, vol. 74, no 12, p. 2151-2166.

119 FORMENTINI, Laura, et al. The mitochondrial ATPase inhibitory factor 1 triggers a ROS-mediated retrograde prosurvival and proliferative response. *Molecular cell*, 2012, vol. 45, no 6, p. 731-742.

120 FUJIKAWA, Makoto, et al. Assessing actual contribution of IF1, inhibitor of mitochondrial FoF1, to ATP homeostasis, cell growth, mitochondrial morphology, and cell viability. *Journal of Biological Chemistry*, 2012, vol. 287, no 22, p. 18781-18787.

121 SGARBI, G., et al. The role of the ATPase inhibitor factor 1 (IF1) in cancer cells adaptation to hypoxia and anoxia. *Biochimica et Biophysica Acta (BBA)-Bioenergetics*, 2018, vol. 1859, no 2, p. 99-109.

122 TANTON, Helen, et al. F1F0-ATP synthase inhibitory factor 1 in the normal pancreas and in pancreatic ductal adenocarcinoma: effects on bioenergetics, invasion and proliferation. *Frontiers in Physiology*, 2018, vol. 9, p. 833.

123 BARBATO, Simona, et al. The inhibitor protein (IF1) of the F1F0-ATPase modulates human osteosarcoma cell bioenergetics. *Journal of Biological Chemistry*, 2015, vol. 290, no 10, p. 6338-6348.

124 CAMPANELLA, Michelangelo, et al. Regulation of mitochondrial structure and function by the F1Fo-ATPase inhibitor protein, IF1. *Cell metabolism*, 2008, vol. 8, no 1, p. 13-25.

125 STRAUSS, Mike, et al. Dimer ribbons of ATP synthase shape the inner mitochondrial membrane. *The EMBO journal*, 2008, vol. 27, no 7, p. 1154-1160.

126 GARCÍA, José J., et al. The inhibitor protein (IF1) promotes dimerization of the mitochondrial F1F0-ATP synthase. *Biochemistry*, 2006, vol. 45, no 42, p. 12695-12703.

127 TOMASETIG, Lara, et al. Dimerization of F0F1ATP synthase from bovine heart is independent from the binding of the inhibitor protein IF1. *Biochimica et Biophysica Acta (BBA)-Bioenergetics*, 2002, vol. 1556, no 2-3, p. 133-141.

128 SGARBI, Gianluca, et al. Hypoxia and IF1 expression promote ROS decrease in cancer cells. *Cells*, 2018, vol. 7, no 7, p. 64.

129 CAMPANELLA, Michelangelo, et al. IF1, the endogenous regulator of the F1Fo-ATPsynthase, defines mitochondrial volume fraction in HeLa cells by regulating autophagy. *Biochimica Et Biophysica Acta (BBA)-Bioenergetics*, 2009, vol. 1787, no 5, p. 393-401.

130 FACCENDA, Danilo, et al. Control of mitochondrial remodeling by the ATPase inhibitory factor 1 unveils a pro-survival relay via OPA1. *Cell reports*, 2017, vol. 18, no 8, p. 1869-1883.

131 FACCENDA, D., et al. IF 1 limits the apoptotic-signalling cascade by preventing mitochondrial remodelling. *Cell Death & Differentiation*, 2013, vol. 20, no 5, p. 686-697.

132 ESPARZA -MOLTÓ, Pau B., et al. Tissue-specific expression and post-transcriptional regulation of the ATPase inhibitory factor 1 (IF1) in human and mouse tissues. *The FASEB Journal*, 2019, vol. 33, no 2, p. 1836-1851.

133 COSTANZINI, Anna, et al. Mitochondrial Mass Assessment in a Selected Cell Line under Different Metabolic Conditions. *Cells*, 2019, vol. 8, no 11, p. 1454.

134 PEAR, Warren S., et al. Production of high-titer helper-free retroviruses by transient transfection. *Proceedings of the National Academy of Sciences*, 1993, vol. 90, no 18, p. 8392-8396.

135 LOWRY, Oliver H., et al. Protein measurement with the Folin phenol reagent. *Journal of biological chemistry*, 1951, vol. 193, p. 265-275.

136 Brunelle, J. L., & Green, R. (2014). Coomassie blue staining. In *Methods in enzymology* (Vol. 541, pp. 161-167). Academic Press.

137 BARACCA, Alessandra, et al. Glucose plays a main role in human fibroblasts adaptation to hypoxia. *The international journal of biochemistry & cell biology*, 2013, vol. 45, no 7, p. 1356-1365.

138 TROUNCE, Ian A., et al. [42] Assessment of mitochondrial oxidative phosphorylation in patient muscle biopsies, lymphoblasts, and transmitochondrial cell lines. En *Methods in enzymology*. Academic press, 1996. p. 484-509.

139 SGARBI, Gianluca, et al. Resveratrol preserves mitochondrial function in a human post-mitotic cell model. *The Journal of nutritional biochemistry*, 2018,

140 BARACCA, Alessandra, et al. Mitochondrial Complex I decrease is responsible for bioenergetic dysfunction in K-ras transformed cells. *Biochimica et Biophysica Acta (BBA)-Bioenergetics*, 2010, vol. 1797, no 2, p. 314-323.

141 CHOURASIA, Aparajita H.; BOLAND, Michelle L.; MACLEOD, Kay F. Mitophagy and cancer. *Cancer & metabolism*, 2015, vol. 3, no 1, p. 4.

142 HUANG, Li-Ju, et al. Hypoxia-inducible factor 1α regulates the expression of the mitochondrial ATPase inhibitor protein (IF1) in rat liver. *Shock*, 2011, vol. 36, no 1, p. 90-96.